DEVELOPMENT OF A STRUCTURAL INTERACTION ASSESSMENT CRITERIA USING PROGRESSIVE DEFORMABLE BARRIER DATA

Eduardo del Pozo de Dios
Ignacio Lázaro
Applus IDIADA
Spain
Pascal Delannoy
Safran Engineering - SAFRAN Group, CERAM Passive Dpt
France
Robert Thomson
VTI
Sweden
Ton Versmissen
Ellen van Nunen
TNO
The Netherlands
Paper Number 13-0421

ABSTRACT

Structural interaction has been one of the critical issues for improved frontal impact protection. An evaluation procedure for structural interaction has been difficult to develop using objective test data procedures. While previous research with the PDB barrier has been promising based on subjective evaluations, an objective assessment criteria has been elusive. Part of the EU project FIMCAR focused on the development of an assessment procedure to assess important frontal impact characteristics like load spreading.

Test and simulation data from vehicle impacts with the PDB or MPDB were collected for different vehicle models, spanning a range of vehicle masses and vehicle classes. Available car-to-car crash tests were also collected for reference. The main information analyzed w.r.t. the assessment of load spreading was the deformation pattern of the PDB barrier after a test. These deformation plots were reviewed and subjectively assessed by experts. The subjective assessments were used to develop key characteristics that should be detected by a numerical assessment of the 3D data. These subjective assessments were then compared to different objective (numerical) assessments for the barriers to ensure correlation of the results and then validated with available car-car data. Assessment of the influence of assessment area and scanning resolution were also performed.

The deformation profiles could be grouped into three main groups where the horizontal and vertical load spreading distinguished vehicles with good or poor performance. The main focus was the development of an assessment of the horizontal load spreading between the longitudinals. A metric based on the slope or gradient, of barrier deformations in the lateral or vehicle Y axis proved to be the best candidate. A horizontal assessment area based on 60% of the overall vehicle width and a vertical area between 330 and 580mm from ground was used. The 99%ile value for the Digital Derivative in Y (DDY) with a threshold value of 3.5 could discriminate between vehicle with an even (homogeneous) deformation pattern or a vehicle with localized structures.

The candidate for an (M)PDB metric that assesses horizontal load spreading provides an objective method to assess structural interaction. The assessment has been validated for the vehicles that can be clearly grouped into a good or poor performance category. There are a number of vehicles that are in a borderline area that require further evaluation. The cases where vehicle-to-vehicle crash data is available have validated the performance of those vehicles. Further validation using field data and car-to-car test or simulation results can finalize the metric development.

The paper addresses a central issue for frontal impact performance. While structural alignment and occupant compartment stability issues can be addressed by adding the FWDB test procedure as proposed by the FIMCAR project to the current ODB procedure, there is no test procedure available that reliably assesses horizontal load spreading. The proposed DDY metric for the PDB test procedure allows the front structure for

vehicles to be assessed and be updated to also assess vertical load spreading.

INTRODUCTION

Crash compatibility, defined as the level of self and partner protection, between the two vehicles involved in a collision is a key factor in the assessment of vehicle safety performance in frontal impacts. Compatibility has been considered a crucial concept for frontal impact safety for many years, but no final assessment approach has been defined. There are several test procedures that have been classically considered for the assessment of crash compatibility. Two tests approaches come from previous research activities (EEVC WG15 and FP5 VC-COMPAT), and both are composed of an offset and a full-width test procedure. However, in both cases there was no final decision in the assessment methodology. A third test procedure, based on a moving deformable barrier, has been investigated in the latest research activities regarding compatibility.

The FIMCAR (Frontal Impact and Compatibility Assessment Research) research project was co-founded by the European Commission within the 7th Framework Programme to address the compatibility issue and aim to provide answer to questions identified in previous research projects. Previous research projects identified some frontal crash incompatibilities between vehicles, due to the differences in front stiffness, bad structural interaction, insufficient compartment strength and mass differences. One of the goals of FIMCAR was to develop and proposed a compatibility assessment methodology that would be accepted by the majority of the involved industry and research organizations. For that purpose, different off-set, full-width and mobile deformable barrier (MDB) procedures were analyzed during the project and their capabilities for the assessment of frontal compatibility were investigated.

In this paper, the activities performed within the FIMCAR project using the Progressive Deformable Barrier, PDB, and the Mobile Progressive Deformable Barrier MPDB to develop and propose a structural interaction assessment criteria are described.

Off-set existing procedures

Three off-set procedures are currently used in regulations, research and consumer testing activities:

- Off-set Deformable Barrier Procedure (ODB)
- Progressive Deformable Barrier Procedure (PDB)
- Small Overlap Procedure

The ODB frontal crash test was developed by the Enhanced European Vehicle-Safety Committee (EEVC) between 1989 and 1995 and simulates the collision of the tested vehicle against another vehicle of similar mass [1]. The test consists in a frontal crash where the car impacts a kinetic energy absorber (a deformable barrier also developed by the EEVC and based on aluminum honeycomb technology) with an off-set of 40% on the driver side. This crash test is currently used in the European regulation and Directive at a speed of 56 km/h. The European Consumer Testing Program Euro NCAP adopted this same procedure in 1996 increasing the test speed to 64km/h [2]. A Hybrid III Anthropomorphic Test Device (ATD) is used to evaluate the self-protection of the vehicle measuring parameters such as forces, deflections or accelerations that are related with the probability of sustaining an injury of a determined severity during the crash. This EEVC barrier is used by car manufacturers and crash test laboratories all over the world for off-set frontal passenger vehicle's protection assessment according with the following standards:

- Regulatory : UN ECE R94, European Directive 96/79/CE, FMVSS 208, ARD 73/00
- Consumer testing: Euro NCAP, IIHS, USNCAP, C-NCAP, A-NCAP, J-NCAP, etc…

However, there are no current activities that investigate the use of this procedure for measuring structural interaction, although for some studies a wall of load cells was mounted behind the deformable barrier to measure the force levels during the frontal impact [3].

The PDB procedure is performed at 60km/h and 50% overlap on the driver side and simulates a frontal collision of the tested vehicle against other vehicle. The stiffness of the PDB is significantly higher than the ODB and is in line with the current vehicle fleet in Europe. The barrier was proposed in previous research projects by France, is also

based on aluminum honeycomb technology and is only used for research activities.

Figure 1. (PDB 60 km/h crash test).

The small overlap procedure consists in a frontal impact against a rigid obstacle with 25% overlap on the driver side, leading to higher intrusions than the larger overlaps. In 2012 the Insurance Institute for Highway Safety introduced the small overlap tests in its assessment of frontal impact protection, after some research programs highlighted that narrow objects are still one of the sources of severe injuries [4]. The test is performed at 64km/h and the assessment of self-protection is performed trough the measurements of a Hybrid III dummy seated in the driver position.

Limitations of ODB procedure assessing compatibility and advantages of PDB

The requirements currently set for self-protection lead to the design of large vehicles with a stiffer front end (compared to small vehicles) in order to compensate for their mass because the ODB test is more severe for heavy vehicles than the lighter ones. These tests also lead to higher compartment strength, since the solutions have been optimized against ODB or rigid wall but not car-to-car configurations. The current ODB procedure was developed being adapted to the geometry and force deformation of vehicles from the 1990's, but both the geometry and stiffness have changed a lot in the current vehicle's front design. This makes compatibility requirements more and more difficult to achieve, but the fact is that improving partner-protection while keeping the current levels of self-protection is needed for future vehicles.

The EEVC WG15 provided some issues of the ODB barrier such as barrier instability for the new generation of cars due to the low stiffness of the barrier, test severity has increased with the increased of car mass and keeping constant speed, self-protection is depending on vehicle size and mass, it is difficult to assess force levels with constant speed (bottoming out of barriers causes undesired inertial loads) and the assessment of structural interaction is not possible because of load spreading and subsequent barrier bottoming out.

To overcome these issues, the new PDB was developed to harmonize the test severity among vehicles of different masses, encouraging the light vehicles to improve the passenger compartment stiffness without increasing the force levels of the heavy vehicle's front end, and leading to a better force matching between vehicles. Its stiffness increases with the crush depth and provides different characteristic in the vertical axis. The dimensions and the stiffness make the bottoming-out very unlikely in the PDB and the barrier face is capable of generating sufficient differential deformation of both the weak and stiff parts of the car's front structure to replicate what happens in most accidents. The PDB barrier represents the opponent vehicle and the fact that it does not bottom-out allows the analysis of the opponent vehicle deformations. The assessment of load spreading is impossible with the ODB while the PDB is designed to assess the load spreading based on barrier face deformation.

The design of this barrier has the intention of encouraging future car designs to incorporate structures that distribute the force on a large surface better for structural interaction and partner-protection. The 60 km/h test speed of the PDB procedure will increase the test severity for light vehicles which will lead to an increase of the front structure stiffness. The severity for heavy vehicles is expected to be unchanged, so the frontal stiffness of heavy vehicles should not be modified. In conclusion, test severity for all vehicle mass range will be harmonized. This speed will also ensure that the level of EES is comparable to current levels (ECE R94).

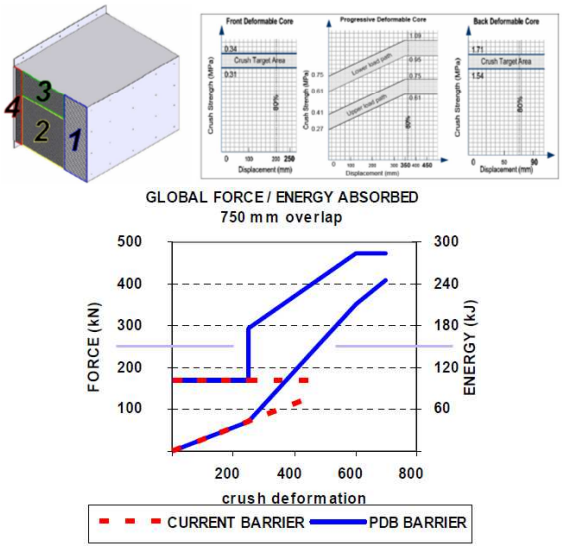

Figure 2. PDB characteristics (top) and comparison of ODB and PDB in terms of global force and energy

FIMCAR APPROACH

Based on previous work and the accident analysis performed during the FIMCAR project, the Consortium established a list of the critical compatibility requirements [5]. A total of 8 main priorities were identified, but the ones that need to be evaluated in the off-set procedure are:

- Load spreading
- Structural alignment: over-ride/under-ride, small overlap and fork effect were found predominant in cases with injuries and fatalities
- Single vehicle collision compartment strength evaluation
- Evaluate restraint systems for different pulses (combined with full width FW procedure)

FIMCAR has analyzed existing crash compatibility data from previous research projects, Euro NCAP and ECE R94 tests. Previous research projects indicated that load cell measurements in off-set procedures are not appropriated to assess load distribution, so FIMCAR decision was to concentrate in PDB procedure and assess the barrier face deformation. This cannot be done in the ODB because the barrier is normally overcrushed and the vehicle contacts the rigid barrier face.

The PDB barrier was divided in three areas for evaluation (Figure 3):

- Upper area: This area is above Primary Energy Absorbing Structures (PEAS) and secondary Energy Absorbing Structures (SEAS) for most of the vehicles.
- Middle area: Includes the Common Interaction Zone (CIZ). For most vehicles is where the PEAS are located.
- Lower area: This area is below PEAS for most of the vehicles, but in some cases is where SEAS are located.

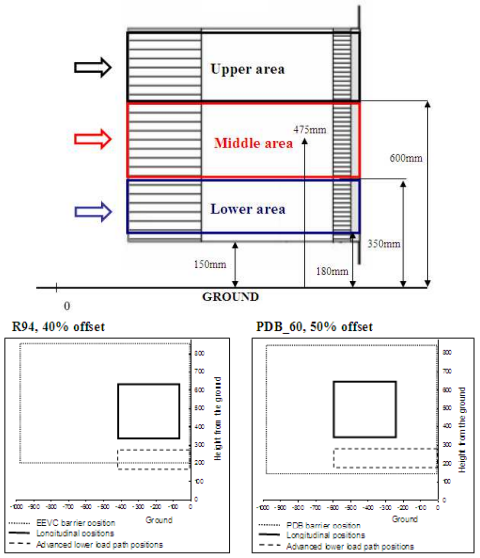

Figure 3. Areas of assessment of the PDB Barrier and differences in ODB and PDB structures location

Significant longitudinal deformations in the upper area will increase the risk of over-ride/under-ride issues. Homogeneous deformations in the middle area are promoted to improve partner-protection issues such as “fork effect” and the small overlap. Deformations in the lower area are also promoted to improve compatibility issues as well.

During the initial development phase of the PDB metric, the development was supported by a database of 37 PDB tests at 60 km/h performed in previous research projects (e.g. VC-COMPAT). FIMCAR contributed to this database with 7 additional tests to develop the new metric. Therefore, a total of 44 cases were available to develop this metric.

In a first phase, the barriers were classified following a subjective approach, only considering the barrier deformation and not the vehicle data. This subjective classification is shown in Figure 4.

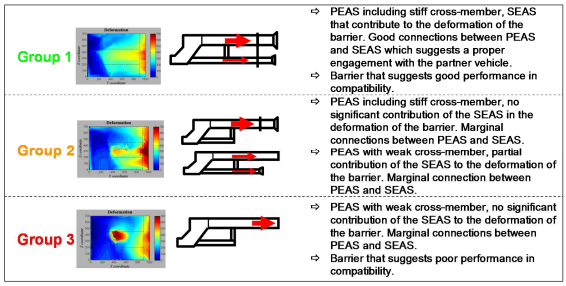

Figure 4: Subjective classification by groups

In the second phase the classification of the barriers based on the subjective evaluation was modified to focus in the main objectives defined by the FIMCAR Consortium:

- Relevant crash loads to be in the common interaction zone (406 to 508 mm) and distributed horizontally across the CIZ
- Vertical load distribution assessed inside and below the CIZ.

The proposed metric was based on the PASS/FAIL approach shown in Figure 5. In a first phase the presence of a load path is analyzed, and then the characteristics of the load path in terms of spreading loads through the barrier are considered.

The aim of the criteria is to identify the structures capable to significantly deform the barrier. The 3D measurements of the barrier allow the identification of the vehicle load paths that will be detected if certain quantile values are above certain limits. Regarding the load spreading, different criteria were considered: Total Variation criteria (TV), Smooth Deformation Index (SDI), Area of significant deformations and Horizontal Load Spreading. For its simplicity and some promising correlation results, the horizontal load spreading was considered the best option for evaluating the load spreading of a detected PEAS and SEAS.

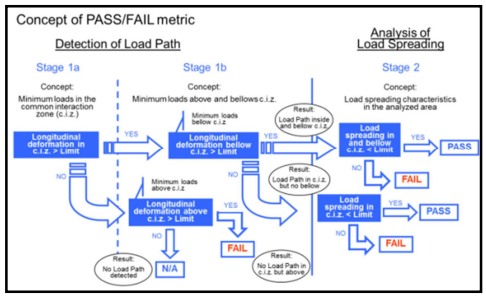

Figure 5. Proposal for metric.

RESULTS

PDB metric description

A total of 44 cases were considered to develop the PDB metric, including 37 cases from previous research projects and 7 cases conducted within the FIMCAR project. The PDB barrier deformation was taken as a reference for the metric development. In a first phase a subjective classification described in Figure 4 was considered and then a criterion based on load path detection and load spreading characteristics was defined.

The PDB was vertically divided in two main zones, the area for assessing PEAS and the area for assessing SEAS. The area for assessing the PEAS was identified as the priority for evaluating the load spreading and it was decided that should include the CIZ of Part 581 (406 to 508 mm from ground) for harmonization purposes with the FW procedure. Finally an area from 330 to 580 mm from ground was selected (Figure 6).

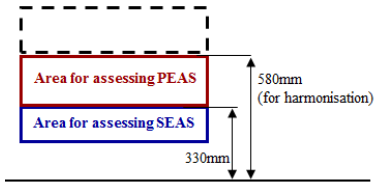

Figure 6. PDB areas of assessment.

For the calculation of the PDB metric calculation the following steps need to be follow:

- Scan the PDB
- Pre-process the PDB scanning
- Criteria calculation: Load path detection and Load Spreading characteristics
- Metric calculation: PASS/FAIL threshold definition

Both the PDB definition and certificate and the PDB scan procedures are detailed in the FIMCAR

Deliverable D2.2 [6]. Different pre-processing methods were investigated: Ray Tracing method and Deformation Projection method. Although both methods presented reasonably consistent results, VTI method was adopted for further PDB analysis due to the most consistent filtering of the data and having deformation gradient less susceptible to small tears or folds.

Then, the load path was evaluated by the deformations based on the 3D measurements of the barrier, which allow the identification of the vehicle's load paths. The load path detection was assessed by the Longitudinal Deformation of the barrier using the developed (d) criterion. This criterion is based on statistics characteristics of the deformation at a defined zone, taking coefficients of the barrier longitudinal deformations. Figure 7 shows an example of limits for detecting load paths. The stiffness of the vehicle is also evaluated, limiting the maximal longitudinal deformation.

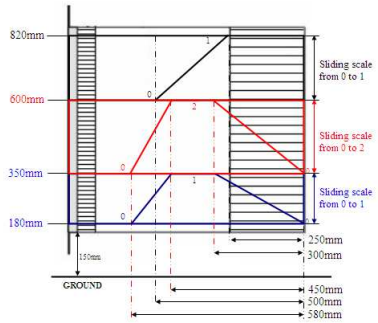

Figure 7: Load path detection, longitudinal deformation

The area of the barrier considered for horizontal load spreading could be divided in N equal sub-zones. Vertical limits were set from 330 to 580mm from ground while the horizontal limits will vary depending on the vehicle's width.

The differences of longitudinal deformations and relative distances between them are analyzed using different parameters:

- D is the average of longitudinal deformation of the complete area
- Di (i=1 to N) is the average of longitudinal deformation for the i sub-zone
- q%i (i=1 to N) is the q% of longitudinal deformation for the i sub-zone
- DDY, Digital Derivative in Y direction, based on change of slope or gradient

And some criteria have been developed using these parameters:

- D/Di esimates of the horizontal variation of the i sub-zone compare to the total average
- ei=D-Di is the deviation of a sub-zone from the overall average of deformation
- Statistics of DDY (i.e. max DDY, 99%ile DDY and STD DDY)

The DDY calculation on the entire longitudinal area was the best candidate to evaluate the load spreading.

$$\text{For } y=1 \text{ to } Ny,\ z=1 \text{ to } Nz \quad DDY(y,z) = \frac{|X(y,z)-X(y-1,z)|}{\text{mesh size}}$$

Figure 8. DDY equation

Different options for the metric development were considered:

- Lateral limit: (W/2-100mm), 80%, 70% and 60% of vehicle width
- Vertical definition: CIZ of Part 581 and Row 3&4
- DDY criteria: max DDY, 99%ile DDY and standard deviation of DDY
- Mesh dimensions: 1,3,5,10 mm

The 99%ile DDY calculated in the defined area gives an estimation of the homogeneity of the barrier. Lower values correspond to small variations in the analyzed area, therefore more homogeneous vehicle deformation.

The horizontal limits of investigation are fixed at 150 mm from the center of the vehicle and extend laterally to the side of the tested vehicle. A limit of 60% of the vehicle width was proposed.

The assessment area that provided best correlation with the subjective classification and showed acceptable repeatability and reproducibility results consisted of:

- 330-580 mm (row 3 and 4 in the full width (FW) tests
- 60% of the vehicle width
- 99% DDY with a threshold of 3.5

In Figure 9 the subjective classification against the 99%ile DDY in the previously described evaluation area is shown. Using a threshold value of 3.5, the 99%ile DDY discriminated between vehicles with an even (homogeneous) deformation pattern, G1, and barrier with localized holes, G3.

The criterion had a good sensitivity to discriminate vehicles according to the subjective rating although there were some borderline cases that request further review. It can be seen that the criterion showed good repeatability for the different Supermini 2 tests with all the values around 0.6. Acceptable R&R in terms of PASS/FAIL assessment was found for the cases studied in previous projects, except the left and right hand versions (cases 9 and 19 in Figure 9). Differences are due to the asymmetric powertrain structures and should be considered in a "worst case" condition for testing. The metric was also consistent with the modification of vehicles for compatibility. Vehicle 56 was modified to create vehicle 54 for compatibility and the metric result changed accordingly and correlated with the PASS/FAIL results.

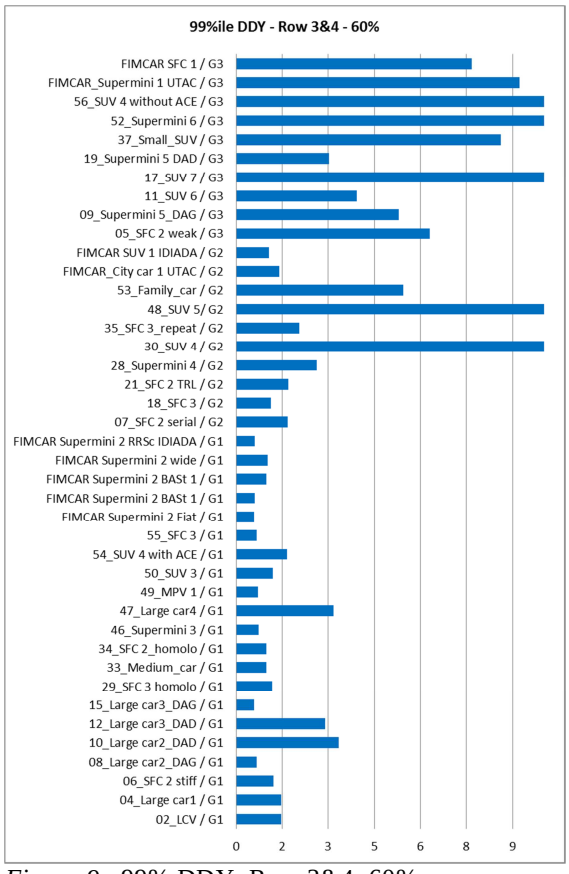

Figure 9. 99% DDY, Row 3&4, 60%.

Simulations

In order to investigate the robustness of the metric and assessment criteria and to identify potential for misuse in vehicle design some simulations using generic car models (GCM).

GCM models with and without sub-frame load path were used to simulate PDB tests at 60 km/h and with 50% offset according to PDB test protocol.

- GCM1_A: Supermini without sub-frame load path
- GCM1_B: Supermini with sub-frame load path
- GCM2_A: Small Family Car with sub-frame load path
- GCM2_B: Small Family Car without sub-frame load path
- GCM3_A: Large/Executive Car with sub-frame load path

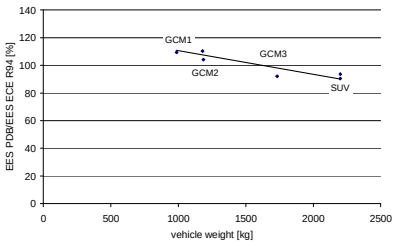

Figure 10. EES dependency on vehicle weight

The models were tested following the PDB 60 km/h and the ODB 56 km/h configurations. Vehicles from different sizes and front-end structures were simulated in equal test conditions. Output parameters like maximal intrusions, EES and accelerations can be used to estimate the test severity for the different models. Simulation results showed a clear tendency of decreasing requirements for the PDB tests when increasing the vehicle weight (Figure 10).

PDB tests

A total of 7 tests were performed using the PDB procedures. Figure 11 shows the complete test matrix and the main objective of each test. This testing program support the final development of the assessment procedure and support the repeatability and reproducibility (R&R) evaluation of the PDB approach. A detail description of these tests can be found in D2.2 of the FIMCAR Project [6].

Vehicle to test	Laboratory	Test Date	Test configuration	Objective	Partner-protection
Supermini 2	FIAT	Jun 2011	PDB60	Test severity validation (self-protection) and comparison with other test modes (FWRB and MPDB)	Good performance expected
City Car 1	UTAC	Sep 2011	PDB60	Comparison with Supermini 2 in terms of the vehicle performance	Good performance expected
Supermini 1	PSA	Nov 2011	PDB60	Test severity validation (self-protection) and validation of the compatibility assessment	Marginal performance expected
Supermini 2	BASt	Jan 2012	PDB60	Repeatability issues	Good performance expected
Supermini 2	BASt	Apr 2012	PDB60	Repeatability issues	Good performance expected
SUV 1	IDIADA	May 2012	PDB60	Test severity validation (self-protection) and validation of the compatibility assessment	Good performance expected
Small family Car 1 (SFC 1)	IDADA	Jun 2012	PDB60	Test severity validation (self-protection) and validation of the compatibility assessment	PASS/FAIL limit investigation

Figure11: PDB test matrix

In order to address the compartment strength, the pulse, intrusion and dummy readings were considered. The PDB scanning was also analyzed in order to evaluate the Structural interaction of the vehicle (load spreading).

Pulse The vehicle pulse gives an estimation of test severity in terms of deceleration (higher pulse indicates higher severity and shorter duration also suggests higher severity). This pulse was measured at the B-pillar base of the vehicle. The pulses for all the PDB tests are shown in figure 12. This figure shows that small vehicles reach higher deceleration peaks than heavy vehicles.

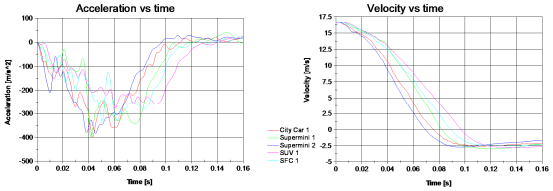

Figure 12: Tested vehicles pulses

The maximum mean acceleration (maximum Delta V divided by the time to reach this maximum Delta V) was used to compare the level of severity between the vehicles. The Supermini 2 test was more severe in terms of deceleration pulse compared to the others and the lowest values were reached by the SUV1 and the SFC.

Intrusion The residual displacement of structural components in the passenger compartment (intrusion) provides an indication of the level of self-protection offered by the tested vehicle. For instance, the presence or not of rearward displacement of the A-Pillar will indicate a level of self-protection of the tested vehicle. European vehicles produce a very low A-pillar rearward displacement in off-set test (R94, Euro NCAP or PDB) and the same behavior was observed in the FIMCAR tested vehicles, where the A-pillar intrusions were always below 30mm.

Dummy readings Dummy measurements are a direct indicator of vehicle's self-protection. This measurements were performed using a Hybrid III 50%tile male dummy (ECE R94) and the injury parameters obtained were compared to Euro NCAP rating to provide an estimation of the level of protection provided by the vehicle and compare PDB and Euro NCAP rating.

Figure 13: PDB vs Euro NCAP ODB dummy readings for Sumpermini 2 test

As the PDB test represents a more severe test for the Supermini 2 compared to the Euro NCAP one, higher injury values were obtained in the PDB compared to the test performed by Euro NCAP.

PDB Scanning PDB procedure serves to investigate the level of partner-protection provided by the tested vehicle and in particular, the PDB assessment is focus on load spreading issues, measured through the scans of the tested barriers. The PDB scans obtained in the 7 tests performed were included in the development of the PDB metrics as explained in the PDB metric description.

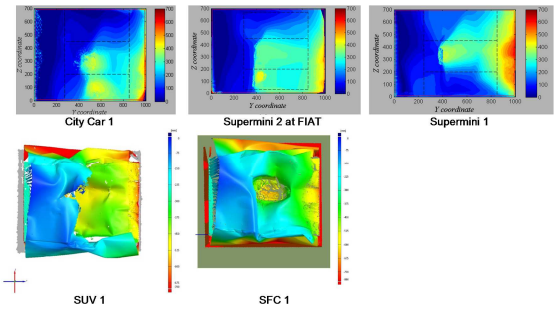

Figure 14: PDB scans

Validation of the PDB metric

The validation of the PDB metric involved PDB and the associated car-to-car tests to show that the vehicles that showed "compatibility" problems failed the metric and those without these issues were addressed appropriately by the PDB metric.

Three series of car-to-car crashes were used to support the off-set assessment proposal, the PDB metric (PASS/FAIL definition) and the final validation of the PDB metric:

- Supermini 2, aligned and misaligned
- Supermini 1, aligned and misaligned
- SUV 1 vs. SFC 1, aligned and misaligned and SUV 2 vs. SFC 1 aligned

In these tests the main issues addressed were the under-ride/over-ride and also the "fork effect" in the aligned conditions, where no under-ride was present. The reference test used for FIMCAR was the Euro NCAP test.

In the car-to-car tests, the Supermini 2 in both the aligned and misaligned crash tests was OK in the load spreading. Therefore, the Supermini 2 test series suggests that the tested vehicle should be a clear PASS the load spreading metric. In the Supermini 1 case, the aligned car-to-car test presented acceptable results for both tested cars, but the misaligned situation showed a bad performance in the lowered car compared to the other vehicles (aligned and raised), which was identified as an "incompatible" situation (under-ride of the raised vehicle) probably due to the absence of SEAS, or other structures to support vertical load spreading. High injuries for the driver and high vehicle intrusions were measured. The PEAS of the Supermini 1 worked well in alignment conditions so should PASS the metric.

Finally, the last car-to-car test series showed better results in the SUV 1 vs. SFC 1 (aligned and misaligned) compared to the SUV 2 vs. SFC 1 (aligned), this last test was classified as an "incompatible" situation due to a fork effect. As conclusion, the SUV 1 will be a clear PASS vehicle, while the SUV 2 and SFC 1 need to be further evaluated in order to understand the final reason of the fork effect and the main responsible of the "incompatible" situation.

Repeatability and reproducibility

In order to study the repeatability and reproducibility of the procedure, it was decided by the FIMCAR Consortium to perform three tests of the Supermini 2 in two different laboratories (FIAT and BAST). The results of the acceleration vs time and velocity vs time are shown in figure 15.

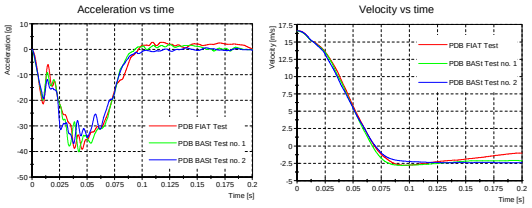

Figure 15. Supermini 2 test pulses.

A barrier separation at the outer part of the PDB was observed in the FIAT test. The issue seemed to be caused during the vehicle rebound phase (Figure 14, time 150ms). It affected the PDB analysis when extended to 70% or 80%, so a limit of 60% was proposed. In terms of dummy readings, comparable results were obtained in FIAT and BAST test 2 (BAST test 1 was not compared since the restrain systems was not fired).

MPDB tests

The Mobile Progressive Deformable Barrier (MPDB) procedure consists in the assessment of the vehicle with a moving trolley equipped with a deformable barrier in a frontal configuration. The same barrier used in the PDB was used for the MPDB tests as the development of a new barrier was out of the scope of FIMCAR.

The two parameters used in the tests to define the test severity were:

- Test speed: 50 km/h (test were also conducted at 45 and 56km/h)
- Trolley mass: 1500 kg (simulations were also performed with 1300 and 2200 kg of trolley mass)

All tests were conducted using Hybrid III 50%tile except that a Hybrid III 5%tile female was used on the passenger seat to investigate the protection level for these type of occupant. Figure 16 shows the test matrix for the MPDB tests.

Lab	Number	Vehicle	Vehicle mass [kg]	Trolley mass [kg]	Vehicle speed [km/h]	Trolley speed [km/h]	Offset [%]	Driver	Passenger
Reference tests: Velocity 50 km/h / Trolley mass 1500 kg / Offset 50%									
TTAI	F114204	Supermini 3	1136	1503	50.4	50.4	50	50th	5th
TTAI	F112902	Citycar 1	1159	1503	50.1	50.1	50	50th	5th
Fiat	17204A	Supermini 2	1225	1512	50	50	50	50th	50th
BAST	FM06C3MB	Supermini 1	1301	1500	50.1	50.1	50	50th	5th
IDIADA	111410CF	Small Family Car 2	1482	1500	50.4	50.1	50	50th	5th
TTAI	F103904	Small Family Car 2	1484	1512	49.8	49.4	50	50th	50th
IDIADA	122701CF	SUV 1	1907	1500	50.4	50.4	51	50th	50th
UTAC	AFFSEP1202056	SUV 2	1912	1500	50.5	50.5	50	50th	50th
TTAI	F105005	SUV 4	2440	1510	49.8	49.4	50	50th	5th
Low speed tests: Velocity 45 km/h / Trolley mass 1500 kg / Offset 50%									
TTAI	F114303	Supermini 3	1136	1503	44.7	44.8	50	50th	5th
TTAI	F114203	Citycar 1	1156	1503	45.1	44.9	55	50th	5th
TNO	F054801	Small Family Car 2	1403	1500	45.1	45.1	50	50th	50th
TNO	F055001	Small Family Car 2	1405	1500	45.2	45.1	50	50th	50th
High speed tests: Velocity 56 km/h / Trolley mass 1500 kg / Offset 50%									
TNO	F084003	Supermini 2	1161	1514	56.1	55.8	50	50th	50th
BAST	FM01OPMB	Small Family Car 2	1446	1533	56	56	56	50th	50th

Figure 16. MPDB test matrix.

For all the vehicles a baseline test was carried out at a speed of 50km/h and a trolley mass of 1500kg, showing, in some cases an acceleration range slightly higher than the current Euro NCAP tests. The duration of the pulses is significant shorter than UN-ECE Regulation 94 or Euro NCAP tests, as trolley and vehicle are both moving. To study effect of velocity, tests at different speeds (45, 50 and 56 km/h) were carried out using the Small Family Car 2.

To compare all the results for all vehicles, the maximum mean B-pillar acceleration of the MPDB tests are presented in Figure 17. The maximum mean acceleration has been defined as:

$$\max mean\ acc = \frac{\max Delta - v}{time\ to \max Delta - v}$$

In general, lower B-pillar accelerations are measured in heavier vehicles. However for all vehicles with a reference test, the MPDB B-pillar acceleration is higher than in Euro NCAP tests. For the Small Family Car 2 and SUV 4, the MPDB is more severe than the fixed offset test. For the delta-v and due to the test configuration, it can be observed that the delta-v of the MPDB is depending of the mass of the tested vehicle. In the case of the static tests, the delta-v is higher due to the vehicle rebound.

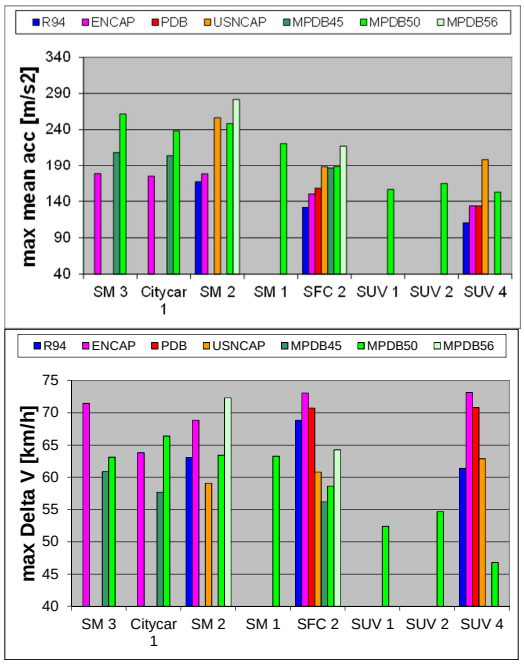

Figure 17. MPDB tests - maximum mean acceleration and delta-V results.

After the tests, vehicle deformations were measured. For small and average size vehicle the A-Pillar deformations were higher in the baseline MPDB that the reference tests, being the MPDB more severe for the compartment strength than the R94 and the Euro NCAP. However, all vehicles except the Citycar 1 were below 50mm of A-Pillar intrusion.

For the dummy readings in the MPDB tests, it needs to be taken into account that the restraint systems are not yet designed/optimized for this test mode (airbags are triggered earlier than in PDB or Euro NCAP tests), so better dummy results than the obtained in the FIMCAR tests are expected in the future. In general dummy results are worse than Euro NCAP results for light vehicle and comparable to Euro NCAP scores the heavy ones.

One of the main results of the tests was the deformation of the PDB. The details of the scanned barriers can be found in D4.2 of the FIMCAR Project [7]. Based on PDB assessment metric, the metric for the MPDB was developed. The metric based on the slope, or gradient, of barrier deformations in the lateral or vehicle Y axis proved to be the best candidate. A horizontal assessment area based on 60% of the overall vehicle width and a vertical area between 305 and 555 mm (row 3 and row 4 of the Full width load cell) was used. The 99%ile value for the Digital

Derivative in Y (DDY) with a threshold value of 3.5 (higher results are worse than lower ones) could discriminate between vehicle with an even (homogeneous) deformation pattern or a barrier with localized holes. The assessment results are shown in Figure 18.

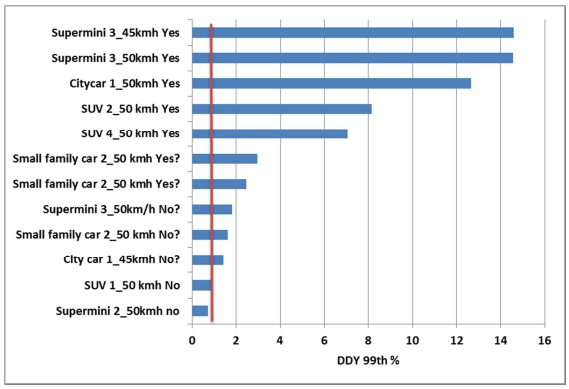

Figure 18. MPDB assessment results.

The remarks "yes / no" refer to whether or not a good spreading of the load was obtained during the test based on the judgment of an expert of the PDB deformation. The results presented in Figure 18 show a good correlation between the expert view during the development phase and DDY 99th% values. The question marks referred to situations where the expert has no clear view about the required results. For the metrics these unclear observations are located between real "yes" and "no" observations. The red line shows the proposed target value of 3.5 based on the PDB results analysis.

CONCLUSIONS

Two off-set candidates were evaluated during the FIMCAR project, the ODB and PDB test procedures. The PDB procedure was identified at the start of the project as the one with more potential to evaluate the issues and priorities defined in FIMCAR, but still some open issues need be addressed in order to be considered for the assessing of frontal impact crash compatibility.

	Structural Interaction		Front End Force / Deformation		Compartment Integrity		Restraint System	
	Alignment	Load Spreading	Deforma-tion force	Energy Absorption	Sufficient for self-protection	Enhanced for light vehicles	Different pulses	Restraint Capacity
Priority	1	1	2	1	1	2	1	1
Can be addressed by? (FIMCAR conclusions)								
ODB	N	N	N	-	Y	N	-	-
PDB	Y	?	Y	-	?	Y	-	-
	Metric development		Test procedure characteristics					

Figure 19. ODB and PDB compatibility assessment comparison.

Activities carried out during the project to develop the structural interaction assessment criteria using PDB data included 7 PDB tests, 15 MPDB tests and car-to-car tests. A new assessment metric for assessing compatibility using PDB tests was proposed. In addition, the PDB definition and certification and PDB scan procedures were developed in order to harmonize the analysis of the test procedure.

Different metrics have been investigated for assessing compatibility issues using the PDB procedure. The proposed metric is based on the DDY criterion, a vehicle mass independent criterion calculated from the PDB barrier's deformations. More specifically, it calculates the barrier's slope in the lateral (Y) direction and penalizes vehicles producing high slopes such as those occurring at the edges of holes. However, the metric still needs to be developed further and validated. Finally, R&R issues have been analysed for the PDB test procedure using the FIMCAR Supermini 2 PDB data. Three different tests were performed in two different FIMCAR laboratories showing repeatable results.

A draft protocol for the MPDB test has been set up. Tests were conducted in various laboratories showing the feasibility of reproducing the test configuration. A trolley mass of 1500 kg and test speed of 50 kg/h is proposed to define the required test severity. For vehicles outside the range between 1000 kg to 2200 kg, for example light electrical vehicles or heavy SUV's, an update of these specifications must be considered in the future. The metric for horizontal load spreading based on the deformation of the PDB barrier is also suitable for MPDB tests

The full scale tests performed showed that the PDB represents a reasonable severe test compared to the Euro NCAP test, which is considered the reference today in Europe. The vehicle pulse and dummy values measured in the PDB tests showed comparable results to the Euro NCAP reference.

Further validation is needed for vehicles with masses over 2000 kg.

The PDB and MPDB tests are currently the only configurations that can potentially assess horizontal load spreading. Candidates for assessing load spreading have been identified but there is still validation and repeatability issues that must be resolved before the candidates can be forwarded to rule makers.

ACKNOWLEDGEMENTS

The authors would like to acknowledge the European Commission that co-funded this project through the FP7 programme (Grant Agreement no. 234216). The authors wish to acknowledge the Partners of the FIMCAR Consortium for their contributions.

The members of the FIMCAR consortium are: Technische Universität Berlin, Bundesanstalt für Straßenwesen. Chalmers tekniska hoegskola AB, Centro Recerche Fiat S.C.p.A., Daimler AG, FIAT Group Automobiles Spa, Humanetics GmbH, IAT Ingenieurgesellschaft für Automobiltechnik mbH, IDIADA Automotive Technology SA, Adam Opel GmbH, Peugeot Citroën Automobiles SA, Renault s.a.s, TNO, TRL Limited, UTAC, Volvo Car Corporation, Volkswagen AG, TÜV Rheinland TNO Automotive International BV.

REFERENCES

[1]. EEVC, Enhanced European Vehicle-safety Committee, www.eevc.org

[2]. Euro NCAP, European New Car Assessment Programme, www.eurocap.com

[3]. Edwards, M., de Coo, P., van der Zweep, C., Thomson, R., Damm, R., Martin, T., Delannoy, P., Davies, H., Wrige, A., Malczyk, A., Jongerius, C., Stubenböck, H., Knight, I., Sjöberg, M., Ait-Salem Duque, O., Hashemi, R., ”Improvement of Vehicle Crash Compatibility through the Development of Crash Test Procedures (VC-COMPAT) - Final Report”, GRD2/2001/50083, 2007

[4]. IIHS STATUS REPORT Vol. 44, No.2, March 2009

[5]. Johannsen H., Edwards M., Lazaro I., Versmissen T., Thomson R., "Proposal for a frontal impact and compatibility assessment approach based on the European FIMCAR project", ESV Conference 2013, Seoul

[6]. Lazaro, I, Adolph, T., Vie, N., Thomson, R., “Updated off-set test protocol”, Frontal Impact and Compatibility Assessment Research (FIMCAR), Deliverable D2.2, European Commission Grant Agreement: 234216, 2012

[7]. Versmissen, T., “Final development of MPDB”, Frontal Impact and Compatibility Assessment Research (FIMCAR), Deliverable D4.2, European Commission Grant Agreement: 234216, 2012

[8]. UN-ECE document, ECE/TRANS/WP.29/GRSP/2007/17

[9]. Delannoy, P., Martin, T., Castaing, P.: Comparative evaluation of frontal off-set test to control self and partner-protection, Paper number 05-0010, ESV Conference 2005

[10]. IIHS Frontal Small Overlap Crashworthiness Evaluation. Crash Test Protocol (Version I) February 2012

[11]. Chauvel C., Faverjon G, Bertholon N., Cuny S., Delannoy P.: Self-protection and Partner-protection for new vehicles (UNECE R 94 Amendment), Paper number 11.0209

[12]. Delannoy, P., Martin, T.; Meyerson, S., Summers, L.; Wiacek, C.: PDB Barrier Face Evaluation by DSCR and NHTSA’s Joint Research Program, ESV Conference 2007

[13]. VC-Compat Abstract of Report D27: Crash test results and analyses performed for initial validation of proposed compatibility test procedures, November 2006

[14]. Delannoy, P., Faure, J.: Compatibility assessment proposal close to real life accidents, Paper number 94, ESV Conference 2003

[15]. PDB information, www.pdb-barrier.com

[16]. Sandqvist, P. “Car-to-car Test Results”, Frontal Impact and Compatibility Assessment Research (FIMCAR), Deliverable D2.1, European Commission Grant Agreement: 234216, 2012

[17]. Lazaro, I., Vie, N., Thomson, R., Schwedhelm, H., “Final development of Off-Set Test”, Frontal Impact and Compatibility Assessment

Research (FIMCAR), Deliverable D2.1, European Commission Grant Agreement: 234216, 2012

[18]. Adolph, T., Edwards, M., Thomson, R., Vie, N., "Final development of Full Width Test", Frontal Impact and Compatibility Assessment Research (FIMCAR), Deliverable D3.2, European Commission Grant Agreement: 234216, 2012

[19]. Versmissen, T., "Final development of MPDB", Frontal Impact and Compatibility Assessment Research (FIMCAR), Deliverable D4.1, European Commission Grant Agreement: 234216, 2012

[20]. Versmissen, T., van der Zweep, C., Mooi, H., McEvoy, S., Bosch-Rekveldt, M., "The Development of a Load Sensing Trolley for Frontal Off-set Testing" , ICRASH Conference, Paper 71, 2006

[21]. Hynd, M., Pichter, M., Hynd, D., Robinson, B., Carroll, J.A., "Analysis for the development of legislation on child occupant protection.", TRL report, 2010

[22]. Pascal Delannoy Jacques Faure, "compatibility assessment proposal close to real life accidents" ESV -2003 conference, paper 94.

[23]. UPDATED REVIEW OF POTENTIAL TEST PROCEDURES FOR FMVSS NO. 208 Prepared By The OFFICE OF VEHICLE SAFETY RESEARCH William T. Hollowell, Hampton C. Gabler, Sheldon L. Stucki, Stephen Summers, James R. Hackney

SMALL-OVERLAP FRONTAL IMPACTS INVOLVING PASSENGER CARS IN GERMANY

Matthias Kuehn
Thomas Hummel
Jenoe Bende
German Insurers Accident Research
Germany

Paper Number 13-0370

ABSTRACT

Small-overlap frontal impacts involving passenger cars have again become a topic of discussion among specialists, and more recently among the public at large. The publication of relevant test results by the Insurance Institute for Highway Safety (IIHS) [1] has triggered questions with respect to the relevance of these collisions to accident situations and with respect to the conclusions that can be drawn and any measures to be implemented. And yet this type of collision is not something that is unknown. On the contrary, among experts, it has been a matter for discussion for decades. You will, for instance, find information and the findings from investigations at the NHTSA [2], Steyr-Daimler-Puch [3] and Autoliv [4].

In Germany also, the question of how relevant small-overlap frontal impact collisions are and what the consequences of this type of collision are is currently being raised. In an attempt to clarify this, the UDV (German Insurers Accident Research) has carried out a comprehensive set of analyses using its accident database (UDB). The UDB contains a representative sample of all damage claims in Germany (all types of road users) and currently covers more than 5,000 third-party motor insurance claims from the years 2002 through 2009. All the accidents in this database involve personal injury and damage costs of €15,000 or more. The objective of the current data analysis was to place small-overlap frontal impacts in the context of all collisions involving passenger cars and to derive the characteristics of such collisions on the basis of detailed accident parameters. In addition, the patterns of injury were analyzed and compared with those resulting from other collision scenarios.

The findings described in this paper are based on the retrospective analysis of 3,242 accidents involving passenger cars. 60% of these accidents (n=1,930) were frontal impacts and 15% (n=485) involved at least one passenger car with a small overlap at the front of the car.

The present paper provides evidence of the relevance of small-overlap frontal impacts to the accident situation in Germany and, in the opinion of the authors, justifies efforts to implement counter-measures. In this context, active systems should also play a greater role in the future.

DATABASE

The German Insurers Accident Research (UDV) is a department of the German Insurance Association (Gesamtverband der Deutschen Versicherungswirtschaft e.V. – GDV) and has access to all the third-party vehicle insurance claims reported to the GDV. For 2011, these amounted to 3.5 million claims, of which 2.7 million were claims involving cars. For the purposes of accident research, the UDV set up a database (referred to as the UDB), taking a representative cross-section (years 2002-2009) from this large data pool. The data collected is conditioned for interdisciplinary purposes for the fields of vehicle safety, transport infrastructure and traffic behavior. The contents of the claim files from the insurers form the basis of the UDB. Around 700 to 1,000 new cases are added to the UDB each year.

STRUCTURE OF THE CAR ACCIDENTS AND RELEVANCE OF A SMALL OVERLAP

In this paper – both in the body of the text and in the graphics and tables – the terms "frontal collision", "small overlap", "large overlap" and "case car" are used. These terms are defined as follows:

- Frontal collision: The front of the car sustains the initial and most serious impact of the collision.
- Small overlap: The front of the car sustains the initial and most serious impact of the

collision with an overlap of not more than 25% (on the right or left).

- Large overlap: The front of the car sustains the initial and most serious impact of the collision with an overlap of more than 25% (on the right or left or in the center).
- Case car: This is the car that sustains a small-overlap impact in a frontal collision. (Note: There may be **more than one** case cars involved in **the same** accident.)
- Note that the figures presented in the paper apply in some cases to the accidents (when the analysis is at the accident level) and in some cases to the cars involved (when the analysis is at the level of those involved). These figures are highlighted for emphasis in the text.

Relevance of small overlap

The German insurers' accident database (UDB) contains 3,242 accidents involving at least one car (not including vans/light commercial vehicles) (figure 1). The analysis of these cases showed that, in around 60% of these accidents (n=1,930), at least one car sustained a frontal impact. In this group of car frontal collisions, there are n=485 cases in which at least one of the cars involved was a case car with a small overlap. These accidents thus account for around 15% of all car accidents and 25% of all car accidents with a frontal collision. In addition to head-on frontal collisions between two vehicles, the 485 accidents also include cases in which the case car collided frontally with the rear end or side of another vehicle, against a rigid obstacle or an unprotected road user.

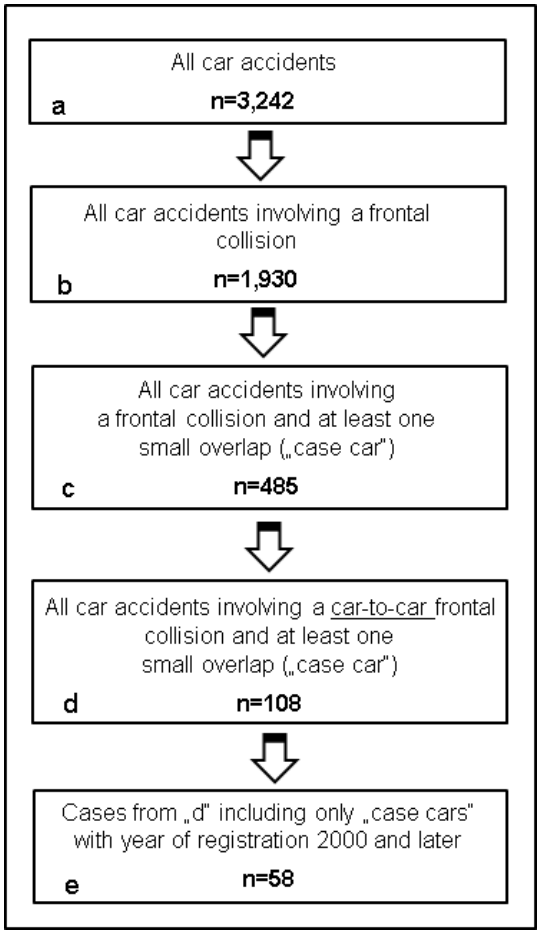

Figure 1. Classification of the car accidents in the UDB by data pools

Collision opponents of the cars that had a "small overlap"

The 485 car accidents with at least one "small overlap" account for a total of 551 involved case cars (see figure 1, "c"). These 551 case cars make up 24% of all the cars (n=2,267) which were involved in a frontal collision in n=1,930 accidents. The cars with a small overlap most frequently collided with other cars (in 52% of cases, as shown in figure 2), followed by motorized two-wheel vehicles (17%) and vulnerable road users (12%).

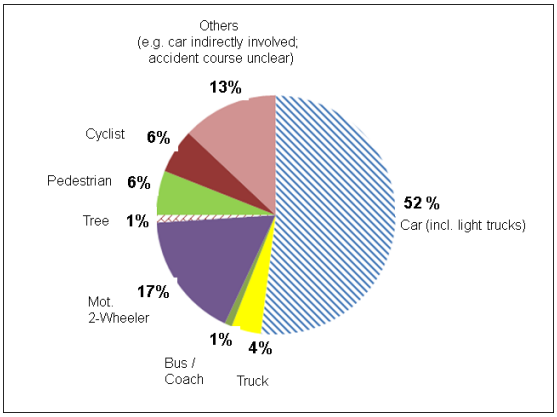

Figure 2. Car frontal collisions involving at least one small overlap, subdivided by the collision opponent of the case car (n=485 accidents)

Car-to-car frontal collisions with a small overlap

In order to get the clearest possible picture of the frontal collisions with a small overlap, the analyses in this section are limited to accidents involving car-to-car frontal collisions (n=108 cases). In these accidents both cars sustained an impact at the front, at least one of them with a small overlap.

Car-to-car frontal collisions with a small overlap characterized by light conditions, road conditions and by accident location Around 70% of the 108 accidents involving car-to-car frontal collisions with a small overlap took place in daylight, and around 60% took place on a dry road surface. In more than a third of the cases, the road surface was wet or slippery.

As far as the accident location is concerned, the analyses revealed that almost two-thirds of the accidents occurred on rural roads (figure 3), with 37% of these occurring in the vicinity of a bend. This gives reason to believe that a collision with a small overlap often happens because the party responsible for the accident gets into the oncoming lane unintentionally as a result of a driving error or due to inappropriate speed.

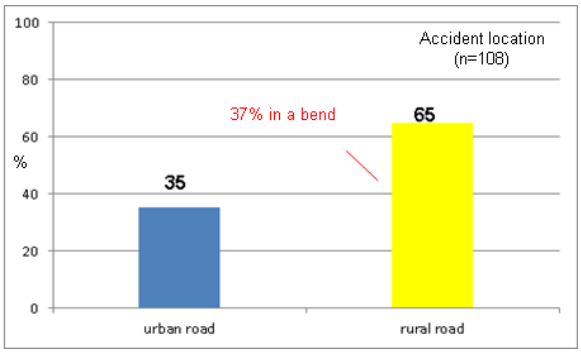

Figure 3. Car-to-car frontal collisions with a small overlap, broken down by accident location (n=108 accidents)

Accident types in car-to-car frontal collisions with a small overlap The accident type "driving accident" makes up 29% and has the highest share within the n=108 accidents involving car-to-car frontal collisions and a small overlap. 74% of these driving accidents took place in the vicinity of a bend (figure 4). These figures strengthen the suspicion that departing from your own lane and the subsequent frontal collision with a small overlap can often be attributed to driving errors or driving at inappropriate speeds. It was also possible to establish that the case-car driver in driving accidents was the main party responsible for the accident in around two-thirds of the cases. Accidents caused by "turning off the road" also account for a high percentage of these accidents (27%) and are the second most frequent accident type. These mostly involved a driver violating the right of way of the oncoming traffic when turning to the left and colliding with the oncoming car (86%). In around half of these cases, the case-car driver was the main party responsible for the accident. The third most frequent accident type is the "accident in longitudinal traffic" (24%). A considerable proportion of these are overtaking accidents (43%), around half of which were caused by the case-car driver.

It is worth pointing out here that figure 4 also provides key information indicating which accidents, in particular, could be addressed by advanced driver assistance systems in order to improve safety as much as possible. For example, an advanced driver assistance system that handled both "turning off the road" accidents and "turning-into or crossing a road" accidents would address around 40% of the accidents examined here.

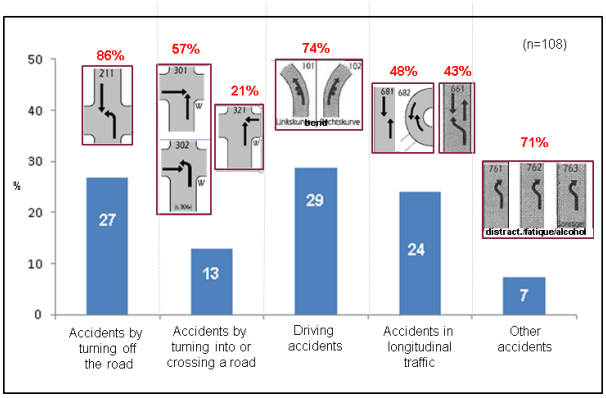

Figure 4. Car-to-car frontal collisions with a small overlap, subdivided by three-digit accident type and showing the percentage of case cars that were the main party responsible for the accident (n=108 accidents)

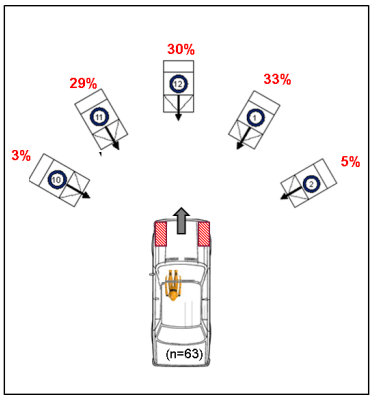

Figure 5. Direction of the impact from the viewpoint of the case car in car-to-car frontal collisions with a small overlap (n=63 case cars involved)

DETAILED ANALYSES FOR SELECTED CASE CARS IN CAR-TO-CAR FRONTAL COLLISIONS

The only accidents described in this section are the 58 accidents involving car-to-car frontal collisions with a small overlap in which the case car was registered in the year 2000 or later (see also figure 1) in order to be sure that the vehicles involved were designed to meet EuroNCAP requirements and thus have a certain level of passive safety. This selection criterion (car-to-car frontal collision, small overlap, registered in the year 2000 or later) was met by a total of 68 cars involved.

Direction and location of the impact

Of the 68 case cars with a small overlap thus selected, there was information on the direction of the impact for a total of 63 of them (figure 5). The direction of the impact refers to the direction of the force to which the vehicle is subjected during the initial collision. The analyses revealed that the impact was sustained at an angle in a clear majority of the cases (i.e. in the case of 70% of the 63 case cars involved). In addition, it was possible to ascertain the location of the impact on the case car for the three most common directions of impact, which were 11, 12 and 1 o'clock (figure 6). In most of the cases, the impact was sustained on the left-hand side of the front of the vehicle (the driver's side). In collisions with impact direction 12 o'clock (which is often the scenario in crash tests), the impact was sustained by the left-hand side of the front of the vehicle in 100% of the cases.

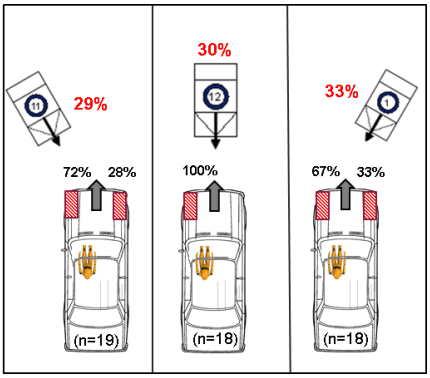

Figure 6. Location of the impact on the case car for the three most common directions of impact in car-to-car frontal collisions with a small overlap (n=18, respectively n=19 case cars involved)

Airbag equipment, airbag deployment and degree of damage

All of the considered 68 case cars with year of registration 2000 or later were equipped with a driver's airbag. It was possible to ascertain whether the airbag was deployed in the case of 55 of the case cars involved: The driver's airbag was deployed in 38 cars (69%); in the other 17 cars, the airbag had not deployed.
For the case cars with a deployed airbag and an impact on the driver's side (n=28), it was possible to determine the degree of damage at the front of the case car in accordance with the UDV definition (figure 7). It emerged that in the most cases the degree of the damage was slight or moderate (degrees of damage 2 and 3). However, 21% of the case cars

involved sustained a strong damage at the front (degree of damage 4), which amounts, according to the definition, to deformations of the passenger compartment and restriction of the survival space (figure 8). No extreme damage (degree of damage 5) occurred in this case material.

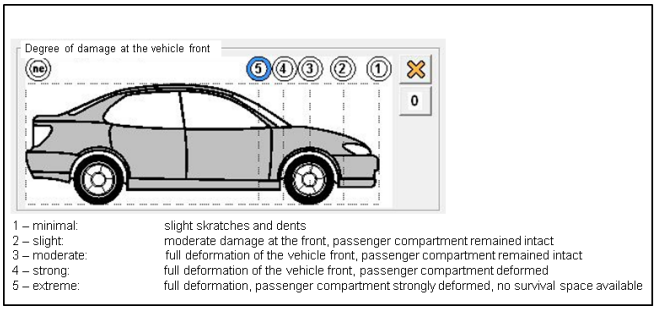

Figure 7. Degrees of damage at the front for cars in accordance with the UDV definition

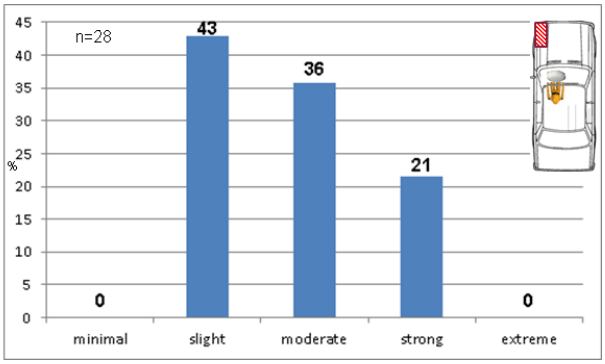

Figure 8. Relative distribution of the degrees of damage at the front for case cars with deployed driver's airbag and with an impact on the driver's side (n=28 case cars)

Technical rescue of the drivers

For 59 of the total of 68 case cars examined here, there was information available about the technical rescue of the driver (figure 9). In most cases (85%) the drivers were able to free themselves. However, in 15% of the cases professional rescue services had to free them using light or heavy equipment. The use of rescue equipment indicates that it is highly likely that the driver was trapped in the car.

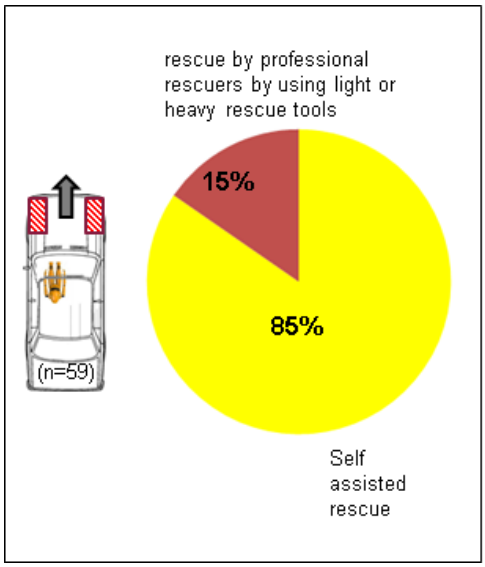

Figure 9. Technical rescue of the driver from the case car in car-to-car frontal collisions with a small overlap (n=59 case cars examined)

Severity of the injuries to protected drivers

Appendix 1 shows the maximum injury severity (MAIS code) and the individual injuries in accordance with the Abbreviated Injury Scale (AIS) [5] for the drivers of the case cars. Only those drivers who were wearing seat belts, whose airbag was deployed and whose car was impacted at the front on the left-hand side with a small overlap are included here. This information was available for exactly 24 drivers.

It is noteworthy that of 16 drivers who had minor injuries (MAIS 1), 11 had an AIS 1 injury of the neck (whiplash-type neck distortion), and only in five cases was the MAIS code obtained from a different injury. Two of these were elbow injuries, two were chest injuries, and one was a facial injury.
In the MAIS 2+ injury range, in addition to chest injuries and abdominal injuries, serious injuries to the upper extremities and, in particular, the lower extremities were relatively common. Only one driver suffered a serious head injury (AIS 3).
None of the drivers studied here suffered critical or fatal injuries (AIS 4+).

Analyses of the front-seat passengers

There were only relatively few front-seat passengers in this accident material, so detailed analyses were not carried out. However, the following statements

can be made as far as the front-seat passenger is concerned:

- In most cases, the front of the car was impacted on the left-hand side, most frequently at an angle.
- In cases where the front-passenger airbag was deployed and the impact was on the passenger's side, the front of the car sustained only slight to moderate damage, and there was therefore no serious deformation of the passenger compartment on the passenger's side.
- None of the front-seat passengers in a case car had to be freed by rescue services. In other words, they were not trapped.
- The injuries of the front-seat passengers protected by a seat belt and an airbag were almost exclusively AIS 1 injuries, most of which were whiplash-type neck distortions.

COMPARISON BETWEEN CAR-TO-CAR FRONTAL COLLISIONS WITH A SMALL OVERLAP AND THOSE WITH A LARGE OVERLAP

As indicated in the introductory section of this paper, small-overlap collisions are of not inconsiderable relevance in the car accident statistics, accounting for around 15% of all car accidents. In order to examine the importance of these accidents in detail, a number of comparative analyses were carried out. To this end, accidents that met all of the following criteria were taken from the group of n=1,930 car accidents involving a frontal collision (see figure 1):

- The cars had to be involved in a frontal collision with another car.
- The driver had to be wearing a seat belt.
- The extent of the overlap at the front of the car had to be known.

That left a pool of n=162 accidents involving a total of n=256 cars. In the first step, n=95 cars were identified in this pool that had sustained an impact with a small overlap (an overlap of up to 25% at the front of the car). The other n=161 cars in the pool were used as the comparison group. These were cars that were involved in a car-to-car frontal collision with a large overlap (an overlap of between 25% and 100% at the front of the car).
Figure 10 shows the distribution of the cars involved in car-to-car frontal collisions (n=256) in the two groups with a small overlap and a large overlap. Around a third of the cars involved in car-to-car frontal collisions sustained an impact with a small overlap at the front.

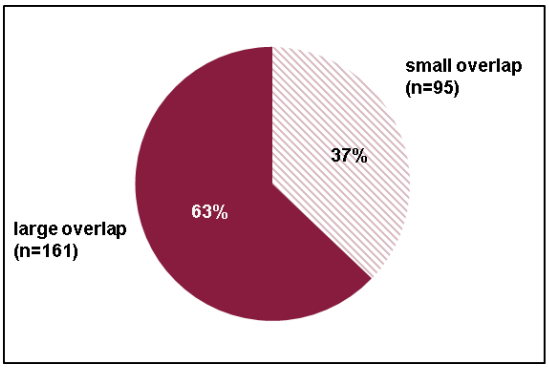

Figure 10. Percentages of cars with a small overlap and cars with a large overlap in car-to-car frontal collisions (n=256 cars)

When these two groups are compared in terms of the severity of the injuries of the drivers involved (drivers wearing seat belts only, with and without airbag), it becomes clear that small-overlap collisions have less serious consequences than large-overlap collisions (figure 11). The number of drivers killed in the latter group, for example, was many times higher.

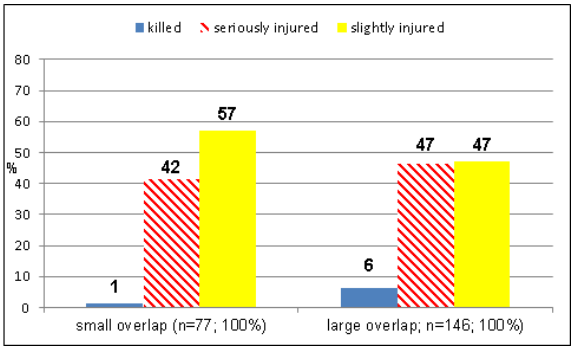

Figure 11. Injury severity of drivers wearing seat belts in small-overlap and large-overlap cars involved in car-to-car frontal collisions

Figure 12 shows a more in-depth analysis of injury severity. It is clear from this that around twice as many drivers wearing seat belts remain uninjured in cars with a small overlap compared to cars with a large overlap. In addition, AIS 2 injuries are more than twice as common in cars with a large overlap compared to cars with a small overlap. Only the injury severity MAIS 3 occurs with around the same frequency in both groups (11% and 12%). Injuries with a severity of MAIS 4+ only occurred in cars with a large overlap in this accident material.

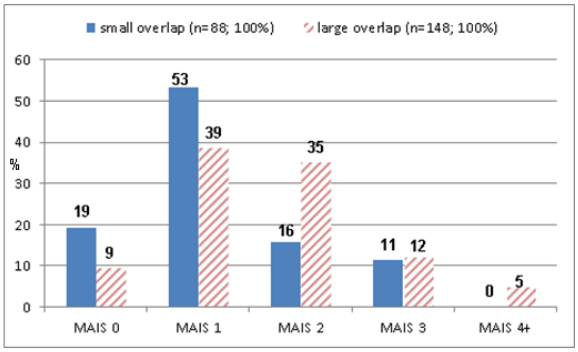

Figure 12. MAIS distribution for drivers wearing seat belts in small-overlap and large-overlap cars involved in car-to-car frontal collisions

Appendix 2 shows the individual AIS 3+ injuries of drivers wearing seat belts for the two groups. It indicates that around 40% of all AIS 3 injuries of drivers of cars with a small overlap were to their lower extremities (femur, lower leg, foot). In contrast, only 24% of drivers of cars with a large overlap had these injuries. The analyses of AIS 2 injuries revealed a similar picture.
Since experience shows that injuries to the lower extremities are associated with long healing processes and are thus cost intensive, the drivers involved were compared in terms of how long they were completely unable to work (figure 13). This revealed that drivers of cars with a small overlap are almost twice as likely to be completely unable to work for a lengthy period (three months or longer) than drivers of cars with a large overlap.

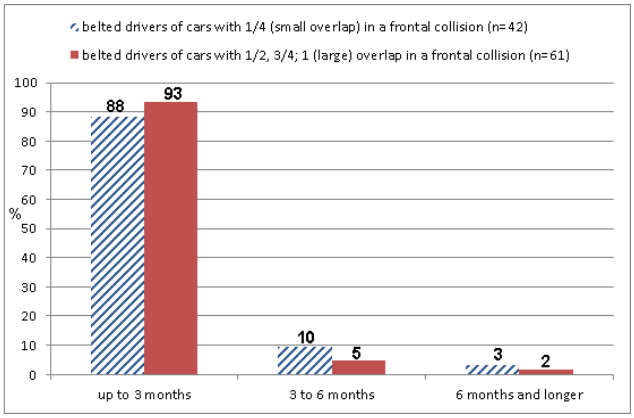

Figure 13. Duration of the period of being completely unable to work – comparison of drivers wearing seat belts in small-overlap and large-overlap cars involved in car-to-car frontal collisions

The longer period of being unable to work and the relatively cost-intensive injuries of the drivers of cars with a small overlap are also reflected in the documented claim costs of the insurers. The claim costs in cases involving a small overlap amounted to an average of around EUR 200,000 compared to EUR 80,000 for cases involving a large overlap. In the small-overlap cases, which were more costly, the high costs involved were demonstrably attributable to complex foot injuries of the drivers involved that take a long time to heal.

SUMMARY OF THE RESULTS

Frontal collisions with a small overlap account for around 15% of all car accidents and 25% of all car accidents involving a frontal collision. In accidents with a small overlap, the car collides with another car in 52% of the cases. Collisions with rigid obstacles (trees, posts) are very uncommon (1%).
The consequences of the accidents for the drivers involved tend to be less serious than for drivers involved in frontal collisions with a large overlap. Nevertheless, small-overlap collisions have specific patterns of injury for drivers protected by seat belts and airbags that differ from those of large-overlap collisions. In particular, cost-intensive injuries to the lower extremities, which entail a long period of treatment and frequently result in permanent damage, are considerably more common in cars with a small overlap than in cars with a large overlap.

It thus emerges that car accidents involving a small overlap are at least as relevant as accidents involving a large overlap in the damage claims of insurers following car accidents. This relevance increases or decreases depending on the reference level selected:

- In terms of fatalities, the relevance of small-overlap car accidents is low.
- In terms of serious injuries (AIS 2+) to the lower extremities, the relevance of small-overlap car accidents is high.
-

From the view of the UDV, following counter-measures can be derived from the analysis of car accidents involving a small overlap:

- Improved specific passive safety measures to the vehicle structure
- Active safety measures which are able to handle “turning off the road” accidents as well as “turning into or crossing a road” accidents.

REFERENCES

[1] Insurance Institute for Highway Safety. 2012. "Small overlap crashes." Status Report, Volume 47, Number 6. Arlington, VA

[2] Rudd, R., Scarboro, M. and Saunders, J. 2011. National Highway Traffic Safety Administration, USA. "Injury analysis of real-world small overlap and oblique frontal crashes." Paper number 11-0384, 22nd ESV Conference

[3] Stephan, W., Bernd, F., Wilhelm, B. and Hermann, S. 2001. "Sliding collisions in case of frontal crash with small lateral offset." Graz, Austria. Steyr-Daimler-Puch, Fahrzeug-technik. Available: http://www.tuev-sued.de/uploads/images/1134986822332304384899/Winkler.pdf

[4] Bostrom, O. and Kruse, D. Autoliv Research Sweden. 2011. "A sled test method for small overlap crashes and fatal head injuries." Paper number 11-0369, 22nd ESV Conference

[5] Association for the Advancement of Automotive Medicine. 1990. "Abbreviated Injury Scale – 1990 Revision." Des Plaines, IL

APPENDIX 1

Individual injuries by regions of the body for belted drivers of small overlap case cars in which the driver's airbag was deployed and the impact was sustained on the left-hand side of the front of the car

MAIS	Head	Face	Neck	Chest	Thorax	Arm	Forearm / Elbow	Hand	Abdomen	Lumbar Spine	Pelvis	Femur	Lower leg / Knee	Foot
1	0	0	1	0	0	0	0	1	0	1	0	0	0	0
	0	0	0	0	0	0	1	0	0	0	0	0	0	0
	0	0	1	0	0	0	0	0	0	0	0	0	0	0
	0	0	1	0	0	1	0	0	0	0	0	0	0	0
	0	0	1	0	0	0	0	1	0	0	0	0	0	0
	0	0	1	0	1	0	0	0	0	0	0	0	0	0
	0	0	0	1	0	0	0	0	0	0	0	0	0	0
	0	0	0	0	0	0	1	0	0	0	0	0	0	0
	0	0	1	0	0	0	0	0	0	0	0	0	0	0
	0	0	1	0	0	0	0	0	0	0	0	0	0	0
	0	0	1	0	0	0	0	0	0	0	0	0	0	0
	0	0	1	0	0	0	0	0	0	0	0	0	0	0
	0	0	1	0	0	0	0	0	0	0	1	0	0	0
	0	1	0	0	0	1	0	0	0	0	0	0	0	1
	0	0	1	0	0	0	0	0	0	0	1	0	0	0
	0	0	0	1	0	0	0	0	0	0	1	0	0	1
2	0	0	1	1	0	2	0	0	0	0	0	0	0	1
	0	0	0	1	0	1	0	2	0	0	0	0	1	2
	1	0	0	0	0	2	0	0	0	0	0	0	2	0
	0	0	0	2	0	0	0	0	0	0	0	0	0	0
3	0	0	0	3	0	2	3	0	3	2	2	3	3	2
	0	0	0	0	0	0	0	0	0	0	0	3	2	0
	3	0	0	3	0	0	0	0	3	0	0	0	0	0
	0	0	1	0	0	0	0	0	0	0	0	0	3	0

APPENDIX 2

Distribution of MAIS 3+ injuries by regions of the body for belted drivers of small-overlap and large-overlap cars involved in car-to-car frontal collisions

MAIS	Head	Face	Neck	Chest	Thorax	Arm	Forearm / Elbow	Hand	Abdomen	Lumbar Spine	Pelvis	Femur	Lower leg / Knee	Foot	Overlap
3	0	0	0	3	0	2	3	0	3	2	2	3	3	2	Small
	0	0	0	0	0	0	0	0	0	0	0	3	2	0	
	3	0	0	3	0	0	0	0	3	0	0	0	0	0	
	0	0	1	0	0	0	0	0	0	0	0	0	3	0	
3	0	0	0	2	0	0	3	0	0	0	0	0	1	2	Large
	0	0	0	3	0	0	1	0	0	0	0	0	0	0	
	2	0	0	0	0	3	2	0	0	0	0	0	0	0	
	0	0	0	3	0	0	2	0	0	0	0	0	0	0	
	0	0	0	3	0	0	0	0	0	0	0	0	0	0	
	0	1	0	1	0	0	0	1	0	0	1	0	3	0	
	0	0	0	0	0	0	2	0	0	0	0	3	0	2	
	0	0	1	3	0	0	0	0	0	0	0	0	1	2	
	0	0	1	2	0	0	0	0	3	1	0	0	0	0	
	3	0	0	0	0	0	0	0	0	0	0	0	3	0	
	0	0	0	0	0	2	0	0	0	0	0	3	1	1	
	0	0	0	3	0	0	0	2	2	0	0	0	0	2	
	0	1	0	3	0	3	1	0	3	0	0	0	0	0	
	0	0	0	3	0	2	0	0	0	0	0	0	0	0	
	0	0	0	3	0	0	0	0	0	0	2	0	0	0	
	0	0	0	3	0	0	0	0	0	0	0	0	0	2	
	0	0	0	3	0	2	0	2	0	0	0	0	3	1	
	0	1	0	0	0	0	2	0	0	2	0	3	2	0	
	1	0	1	0	0	0	0	0	0	3	1	0	1	0	
	0	0	0	0	0	0	0	0	0	0	0	0	3	0	
4	4	0	4	0	0	0	0	0	0	0	0	0	0	0	
	4	0	0	0	0	0	2	0	0	0	0	0	0	0	
	4	0	0	3	0	0	0	0	3	0	2	3	1	2	
5	0	0	5	0	0	0	0	0	0	0	0	0	0	0	
6	0	0	0	6	0	3	0	2	4	0	3	3	2	2	
	6														
	4	1	6	4	0	2	0	0	3	0	0	0	3	2	
	0	0	0	6	0	0	0	0	0	0	1	3	0	2	

Stamping effect application for crash CAE procedure with QUIKSTAMP

Hashik, Shin
Byoungjoo, Yoo
Renault Samsung Motors
Republic of Korea
Paper Number 13-0356

ABSTRACT

For having well-correlated crash CAE model, considering the thinning and the work hardening effect on CAE model is important to close to the physical BIW. QUIKSTAMP was used for considering the stamping effect in an early stage with short time instead of the conventional (incremental) approach. With considering the stamping effect, it is needed to predict the panel tearing behavior and the spot weld failure during impact.

INTRODUCTION

Many studies for considering the stamping effect like the work hardening and the thickness thinning behavior of BIW had been performed. Johnheon Yoon et al did the study regarding the stamping effect on the lateral crash model, they concluded that The result of the crash analysis demonstrates that the crash mode, the load- carrying capacity and energy absorption can be affected by the forming effect. It is noted that the design of an autobody should be carried out considering the forming effect for accurate assessment of crashworthiness. V. Grolleau et al did the study regarding the effect of thickness change and strian hardening of crash model; they stated that plastically at different thick strain levels ranging from −37% to −6% [2]. In this study, two different calculation approaches for the stamping operation were adopted as considering the work hardening and the thinning behavior: One is the incremental approach and the other is the inverse approach. Generally the incremental approach have been used for the stamping calculation , with this approach, many calculations are needed for each several stamping operation especially for intermediate shape operation and CAD data and tooling information are needed for this calculation. In inverse approach, just one-step calculation for the stamping operation is needed and CAE mesh model could be used for the calculation. Moreover, with the inverse approach, the calculation time could be reduced and the stamping calculation result could be applied on crash calculation from 1st CAE model build compared to the incremental approach.

STAMPING CALCULATION PROCEDURE

Stamping calculation method

The difference between the incremental and the inverse approach could be explained as below figure1 and figure2.
Figure1 shows the schematic drawing of the incremental approach. Several calculations are needed for each stamping operations and the stamping die design parameters and CAD data are necessary during calculation.

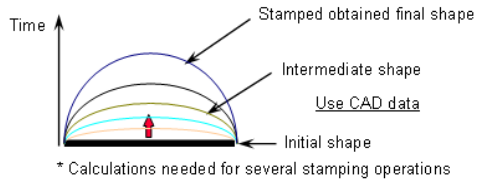

Figure1. Incremental approach

Figure2 shows the schematic drawing of the inverse approach. Different to the incremental approach, just one step calculation is needed for the stamping operation, and CAE mesh model is enough to make a calculation, this means that the stamping calculation results could be considered from 1st crash CAE model build without tooling information through the vehicle development process.

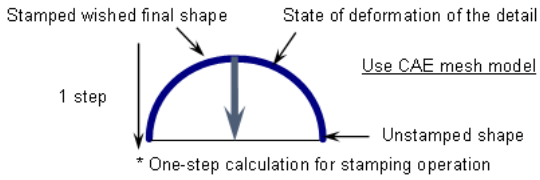

Figure2. Inverse approach

Figure3 shows the overall procedure considering the stamping calculation. The first step is to do the stamping calculation depended on the calculation types, and then the strain as a work hardening and the thickness profile as a thinning would be

exported and mapped to the crash CAE model as a M01 file format. After mapping the stamping calculation result, the crash calculation result could be obtained as considering the work hardening and thinning effect.

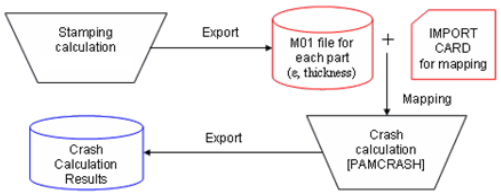

Figure3. Calculation procedure

Incremental vs. Inverse

Though the advantage of the inverse approach like the calculation time and the early application in the vehicle development process, the comparison study between the incremental and the inverse approach is necessary before adopting the inverse approach for the stamping effect.
For the comparison study, the study model is the mid-sized sedan vehicle with checking rear crash performance, Figure 4.

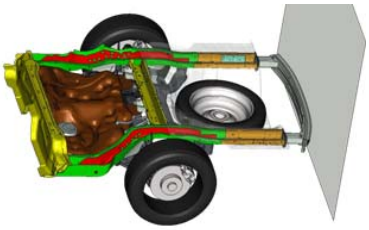

Figure4. Mid-sized sedan vehicle, rear crash performance

Rear side member of this vehicle was selected for the stamping calculation. AUTOFORM software was used for the incremental approach, and QUIKSTAMP software was used for the inverse approach.

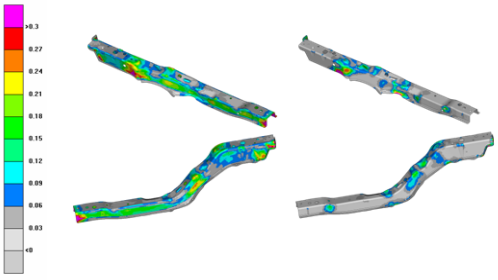

Figure5. Strain distribution

Figure5 shows the strain distribution on rear side member as a result of each stamping calculation approach: Left one for the incremental and right one for the inverse approach. The strain distribution on rear side member shows different between two approaches; however, the concentrated area followed well between two results. Figure6 shows the thickness profile, and the tendency was similar to the strain distribution.

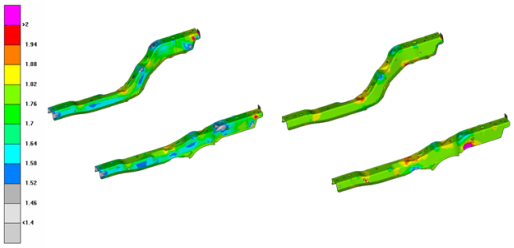

Figure6. Thickness profile

These strain distribution and thickness profile was mapped to the crash model, and the rear crash calculation performed. The section force of rear side member was compared to see the possibility for adopting the inverse approach instead of the incremental approach as considering the stamping effect on crash calculation.

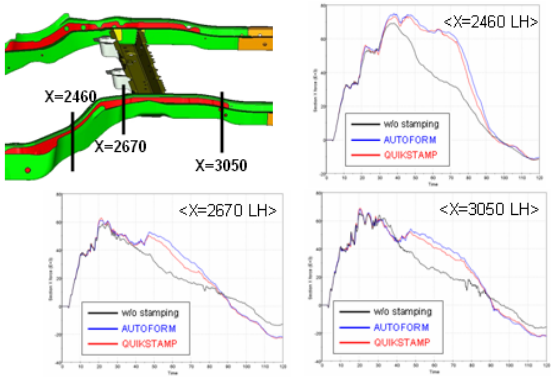

Figure7. Comparison of section forces on rear side member

Figure7 shows the section force results on rear side member in case of rear crash type, on each section definition, the stamping effect considered case was different to the others; however, the inverse case (red curve) followed well to the incremental case (blue curve), that means the inverse approach could be adopted for considering the stamping effect on crash calculation.

CRASH CALCULATION

Model definition

In this study, 65 KPH frontal crash calculation with 40% offset deformable barrier was performed for small family car, and 55KPH lateral crash calculation was performed for small MPV.

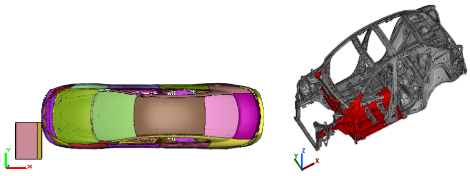

Figure8. 40% offset frontal crash model definition

Figure8 shows the model definition that was used for the frontal crash calculation, red colored parts located front left hand area of BIW was selected for the stamping calculation. These parts were selected in order of the part internal energy during crash calculation as below figure9.

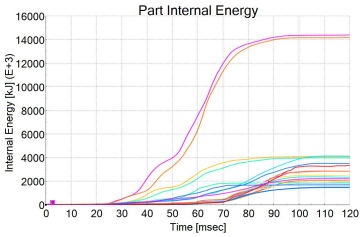

Figure9. Part internal energy of BIW during frontal crash calculation

Figure10 shows the model definition which was used for the lateral crash calculation. All BIW parts located in front left area were considered for the stamping calculation

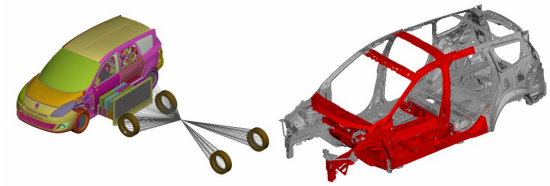

Figure10. Lateral crash model definition

Results: w/o stamping vs. w/ stamping

With 65 KPH frontal crash calculation, globally similar tendencies were found between two results, however, in some areas, the difference could be found. One of them is the A pillar area. In case of w/o stamping model, there's no bending behavior, but w/ stamping model, the bending behavior can be observed. This difference showed in Figure11. In the physical test, the bending behavior also could be found in Figure12.

Figure11. Global deformation on BIW

Figure12. Deformation view on BIW in the physical test

The level of section forces for stamping effect considered model was little higher than base.

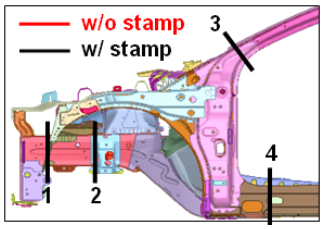

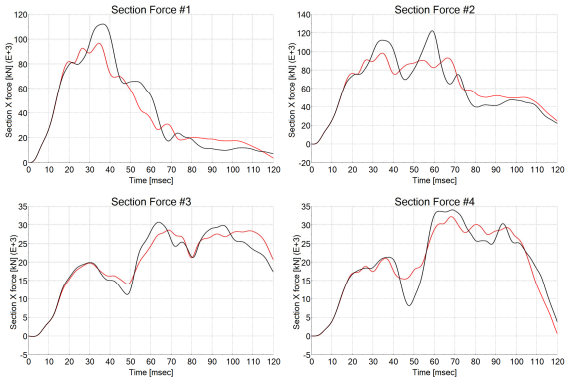

Figure13. Section forces on BIW in case of the frontal crash calculation

With 55 KPH lateral crash calculation, the front door velocity and B pillar intrusion was evaluated for checking the stamping effect. As showing in Figure14, the level of door velocity in the stamping effect considered model were lower than the model without the stamping effect.

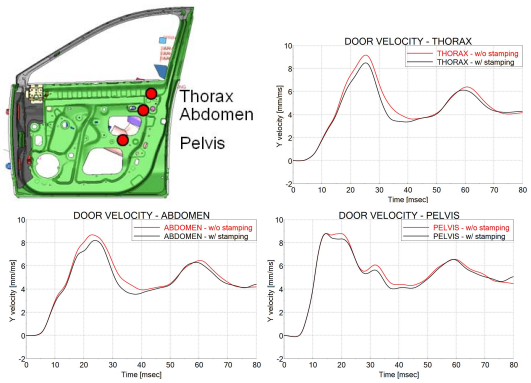

Figure14. Front door velocity

Compared to the model without the stamping effect, the pillar intrusion of the stamping model has been improved, it could be explained that the work hardening affected on BIW deformation. It would have a good effect on dummy injury criteria. See in Figure15.

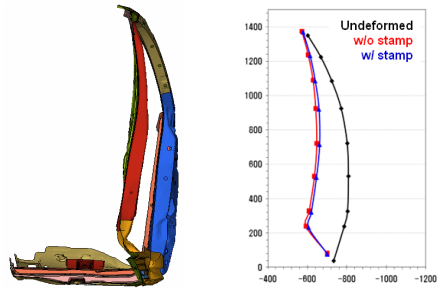

Figure15. B pillar intrusion

CONCLUSIONS

The stamping effect like the work hardening and the thinning effect are needed to be applied in crash calculation for building accurate crash CAE model in BIW point of view.
The crash calculation results with using inverse method was well matched to the results with using the incremental method even though the stamping results itself showed little difference of the initial strain distribution and thickness profile.
Work hardening effect on BIW affected on the crash results and showed stiffer behavior than the model that the stamping effect was not considered.
Comparing the physical test results, the deformation behavior on A pillar of the stamping effect considered model was well matched to the physical deformation.
The inverse method like QUIKSTAMP would be more efficient to build the crash CAE model considering the calculation time and the process focused on the project milestone than the incremental method.

REFERENCES

[1] Johnheon Yoon, Hoon Huh, Seho Kim, Hongkee Kim, Seungho Park 2006. “Side Impact Analysis of the ULSAB-AVC model with considering the forming effect.” Proc. KSTP, Fall Conference, No. 4, April: 37-40
[2] V. Grolleau, B. Galpin, A. Penin, G. Rio 2008 “Modelling the effect of forming history in impact simulations: evaluation of the effect of thickness change and strain hardening based on experiments.”, International Journal of Crashworthiness Vol. 13 No. 4 363p ~ 373p

STRUCTURAL PERFORMANCE: CHALLENGES WITHIN THE AREA OF TENSION BETWEEN SAFETY, LIGHTWEIGHT AND ECONOMICS

Thomas Unselt
Prof. Dr. Rodolfo Schöneburg
Dennis Waldherr
Daimler AG
Germany
Paper Number 13-0336

ABSTRACT

Structural safety still plays a significant role in the development and optimization of vehicle safety. This fact is reflected by the increase of rating and mandatory requirements like the revised FMVSS 208 and recently introduced small overlap test protocols. Related safety measures could lead to a major conflict when it comes to weight issues with impact on fuel efficiency and costs. To resolve this challenging conflict as far as possible, targeted measures such as innovative technical solutions and intelligent development methods are required. This paper will present an innovative vehicle safety and structure concept as well as balancing measures by the example of the new Mercedes-Benz SL roadster. The SL integrates an all-aluminum body and is the first mass-production Mercedes employing this type of design. Making the entire bodyshell from aluminum reduces the weight of the cell by 24 percent. Viewed across the entire life cycle (including the manufacturing phase), the new bodyshell concept of the SL reduces CO_2 emissions by 15 percent over the predecessor model. This innovative structure concept gives rise to a lightweight occupant cell with pronounced structural rigidity for high structural performance. It facilitates a light yet stable cell compound for a highly rigid occupant cell. This concept leads for example to good results in frontal small overlap tests without any additional measures**.** The crash test program for the development of the bodyshell was effectively supplemented with targeted simulations based on CAE methods. Therefore existing CAE methods had to be augmented to accommodate the lightweight construction of the new SL. Among the structural safety the SL has a wide portfolio of safety measures with respect to the Mercedes Benz integrated safety concept.

INTRODUCTION AND MOTIVATION

In the last few years, there has been a declining trend in the number of traffic accidents in the European Union. In 2011, for example, 4,009 people died in car accidents in Germany as opposed to the 7,503 traffic-related deaths recorded in the country in 2000. This 47 percent drop can be attributed to a number of traffic safety measures that have been implemented as well as ongoing advancements in vehicle safety. To propagate this trend, engineers will continue to place a great deal of emphasis on safety as they develop new passenger cars. Convertibles and roadsters pose a particular challenge in this regard. Whereas roadsters must offer a high level of agility and therefore integrate a lightweight design that has an effect on the vehicle's structure, convertibles by definition lack a permanent roof and therefore require more outlay than closed vehicles. Targeted compensation measures are needed to increase body rigidity and safety, especially when it comes to rollover accidents. Since these vehicles are usually not manufactured in high numbers, the fine line between safety, lightweight design, and cost effectiveness takes on new meaning. Development must therefore exploit technological possibilities and state-of-the-art methods to realize success in this segment.

METHODOLOGY

Four-Pillar Strategy for Integrated Safety

The development of the Mercedes-Benz SL shows how the safety equipment fitted to roadsters builds on the principle of integrated safety. This strategy takes into account the entire chain of events leading up to an accident and meets the legislative and rating requirements that provide a solid basis for safety as well as incorporates a "real-life safety concept" that is oriented toward actual traffic and accident scenarios and reflects the knowledge that has been gained from conducting accident research in

particular. The strategy of integrated safety from Mercedes-Benz comprises four pillars [1],[2]:

•Safe Driving

•Preventive Action

•Adaptive Protection

•Save and Rescue

Consistently applying this strategy translates into significant technical outlay in terms of development and manufacturing and can increase vehicle weight, thus going against the cost and weight objectives defined for the development program. To achieve as optimum a balance as possible, coordinated measures (*Figure 1*) must be implemented that require technical solutions and intelligent development methods and processes.

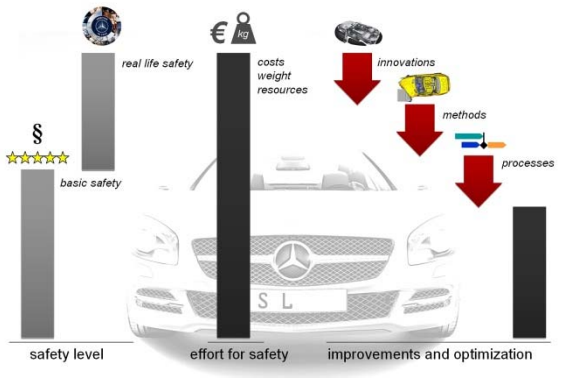

Figure1. Area of tension between safety, light-weight and economics

This paper discribes the safety concept as well as balancing measures as a result of the development process.

RESULTS

Safe Driving

The assistance systems in the new SL benefit safety and comfort. Speed Limit Assist detects posted speed limits via an on-board camera and displays them in the instrument cluster as well as on the head unit. Active Blind Spot Assist warns the driver of a potential collision when a lane is changed due to the presence of another vehicle occupying the neighboring lane in the driver's blind spot. If the driver ignores the warnings provided by the system and proceeds to change lanes, Active Blind Spot Assist engages by actively braking the vehicle to avoid an accident. Active Lane Keeping Assist engages if the roadster inadvertently crosses a solid or dotted line marking the left or right side of the lane. In this scenario, the driver is warned by a vibration of the steering wheel. Should the driver not respond to the warning indicating that a solid line is being crossed, Active Lane Keeping Assist can trigger targeted braking of the wheels on the opposite side of the car via the ESP system to guide the vehicle back into the lane.

Preventive Action

An advanced safety feature is the standard PRE-SAFE system, which is an anticipatory system designed to protect occupants. If it detects an acute risk of an accident, it reflexively activates precautionary protective measures for the vehicle occupants, also including the reversible belt tensioning function which ensures that the occupants are better secured so that the seat belts and airbags are able to perform their protective function to the full during an impact [3]. Passengers are also protected in the event of a rollover. During normal driving, two rollbars are fully retracted in two cartridges fixed to the bodyshell in the area behind the seat backrests. When the crash sensor detects a potential rollover, the airbag control unit sends a signal and the trigger mechanism is activated. Two pretensioned compression springs in each cassette then extend the rollbars to their support position in a fraction of a second. PRE-SAFE Brake is also available as an option and is ordered together with the DISTRONIC PLUS adaptive cruise control system. When PRE-SAFE Brake detects the acute risk of a rear-end collision, it is able to trigger autonomous emergency braking. This occurs in two stages. Approximately 1.6 seconds before the estimated time of the collision, the vehicle brakes autonomously using about 40 percent of maximum braking performance, at which time the driver is also haptically warned and the reversible PRE-SAFE occupant protection systems are activated as a preventive measure. If the driver does not respond, PRE-SAFE Brake autonomously activates the maximum braking power around 0.6 seconds before the collision to reduce the severity of the impact. The system acts as an "electronic crumple zone" that provides added protection for the vehicle occupants and the other parties involved in the accident.

Adaptive Protection

The restraint systems with two-stage driver and front passenger airbags have been enhanced. A headbag provides lateral protection for the head impact area. An additional thorax airbag in the seat backrest will protect the upper body in the event of a side impact.

The crash-responsive NECK-PRO head restraints now respond more quickly to support the driver and passenger in a rear-end collision, thus minimizing the risk of a whiplash injury [3]. Also fitted as standard is automatic child seat recognition. The ISOFIX child seat fastening system is available as an optional extra. During the development process for the new SL the requirements of Euro NCAP and other rating institutes as well as Mercedes-Benz internal requirements were taken into account. The basis for this is a new light-alloy bodyshell which is formed mainly by extruded sections and cast nodes made of aluminium. It facilitates a light yet stable cell compound for a highly rigid occupant cell. In conjunction with this the tail end and front are designed in such a way that in the event of an accident they can absorb high forces through deformation, thus considerably reducing the strain on the occupants in a crash in accordance with the principle of the crumple zone. The crash boxes behind the bumper trim and an exchangeable front module ensure that the damage sustained during a front impact at up to 15 km/h can be limited

Save and Rescue

The integrated safety concept from Mercedes-Benz also regards the phase after the accident has occurred. The new SL therefore integrates numerous post-crash measures. Depending on the type and severity of the accident, the doors can be automatically unlocked, the interior lights activated, and the side windows opened by 50 millimeters to provide better ventilation in the interior. In addition to this, the steering wheel can be slid upwards. The concept is completed by the Guidelines for Rescue Services and the rescue cards which can be downloaded from the internet free of charge and which can serve as a valuable support for fire brigades [3]. *Figure 2* shows the holistic “real-life safety concept” on the example of the new SL.

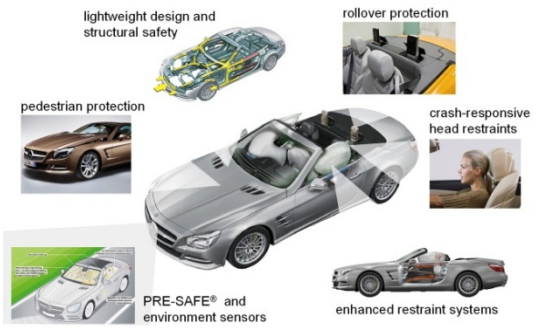

Figure2. Roadster specific “real life safety concept”

Simulations Reduce Numbers of Crash Tests

Crash testing plays a significant role in the development methods applied to optimize vehicle safety, whereby outlay to this end has increased considerably since the current SL was engineered for the global market with heightened rating and legislative requirements. In addition, Mercedes-Benz vehicles have to meet sophisticated internal safety standards. Had the development methods not been adapted accordingly, these requirements would have made it necessary to conduct three times the number of crash tests than were carried out for the predecessor model. By enhancing the crash test program with targeted CAE simulations, some 20 percent of the crash tests otherwise required did not have to be conducted. Before this "CAE offensive" could be leveraged, however, existing methods had to be augmented to accommodate the new lightweight construction of the SL. This investment already paid off in the optimized product quality that was achieved with the current SL, however .

Improved Safety with Lightweight Design

The SL is the first Mercedes-Benz model series after the SLS to integrate an all-aluminum body and is the first mass-production Mercedes employing this type of design (*Figure 3*). Making the entire bodyshell from aluminum reduces the weight of the cell by 24 percent as compared to the predecessor model, while CO_2 emissions are reduced by 15 percent when viewed across the entire life cycle (including the manufacturing phase) [4]. The design of the bodyshell takes into account all requirements pertaining to unit quantities, safety, noise, vibration, and harshness (NVH) characteristics, and cost effectiveness by employing an optimized mix of cast, extruded, and sheet metal parts made from aluminum. The aluminum bodyshell also offers improvements in safety. The underfloor, for example, comprises cast parts, hollow sections, and internal high-pressure forming parts [5]. This innovative, all-aluminum structure concept gives rise to a lightweight occupant cell with pronounced structural rigidity. Areas of the structure, which are exposed to specific strain, deviate from the all-aluminum construction**.** The A-pillars are one such area and combine steel with aluminum to provide the best protection possible in the event of an accident involving a rollover. Innovative safety systems also contribute to the lightweight design of the new SL. One example of this can be found in the pedestrian protection concept. In addition to passive measures such as the good deformation

characteristics of the engine hood and optimized foam material in the front bumper, an "active" engine hood is fitted that uses pyrotechnical actuators at the rear edge to raise the panel by 85 millimeters should a pedestrian impact occur [3]. This type of actuator benefits from its lower weight as compared to conventional mechanical actuators and shaves approximately 2 kilograms off of each vehicle – another example that lightweight design can go hand in hand with a high level of vehicle safety when an innovative strategy is employed.

Figure3. SL lightweight bodyshell

Modular Strategy

Mercedes-Benz Passenger Car Development pursues a single modular strategy via vehicle architectures that provide the basis for 90 standardized modules. This modular strategy was already applied to the new SL and its safety features in particular. The airbag and side protection components, for example, are shared with those of the SLK roadster. A key requirement in implementing this concept was to integrate standardized components in a manner that does not detract from any of the customer benefits the systems have to offer. The new SL not only features standardized components, but also standardized concepts. One of these concepts is the roll-over system, which uses protective cassettes that already have established a proven track record in other model series and reduce vehicle weight.

REFERENCES

[1] Fehring, M. 2012. “Integral Safety Concept on the example of the Mercedes-Benz SL-Class” In Proceedings of China Vehicle & Road Safety Summit 2012 (Beijing, August 16th-17th 2012)
[2] Schöneburg, R. and Breitling, T. 2012. „SL-Klasse Sicherheit - Integrale Sicherheit Unfallvermeidung und Insassenschutz” ATZextra, Der neue SL von Mercedes-Benz, April 2012
[3] Schöneburg, R.; Bachmann, R.;.Waldherr, D. and Hirschkorn, J. 2012. „SL-Klasse Sicherheit - Passive Sicherheit“ ATZextra, Der neue SL von Mercedes-Benz, April 2012
[4] Weissinger, J. and Scheihing, H. 2012.“SL-Klasse Leichtbau - Maßnahmen zur Gewichtsreduzierung” ATZextra, Der neue SL von Mercedes-Benz, April 2012
[5] Kelz, M.; Rudlaff, T.; Schretzlmeier, W.; Müller, M. and Bitzer, R. 2012. „SL-Klasse Karosserie - Leichtbaukarosserie” ATZextra, Der neue SL von Mercedes-Benz, April 2012

Development and validation of a reference vehicle for future research in passive safety

Thorsten, Adolph
Federal Highway Research Institute, BASt (1)
Germany
Richard, Damm
Ministry of Transport, Building and Urban Development (2)
Germany
Nimoy Kanjuparambil, Ulrich Langer
University of Applied Sciences Cologne (3)
Germany
Arno Meyna
University of Wuppertal (4)
Germany
Daniel Huster
University of Applied Sciences Dortmund (5)
Germany

Paper Number 13-0446

ABSTRACT

The objective was to develop and validate a crash trolley (reference vehicle) equipped with a compartment and a full restraint system for driver and front seat passenger which can be used in full scale crash testing. Furthermore, the crash trolley should have a suspension to show rotation and nick effects similar to real vehicles.
Within the development phase the reference vehicle was build based on a European family car. Special attention was needed to provide appropriate strength to the trolley and its suspension. The reference vehicle is equipped with a restraint system consisting of airbags, pedals, seats, dashboard, and windscreen. On the front of the vehicle different crash barriers can be installed to provide miscellaneous deceleration pulses.
For the validation phase a series of low and high speed crash tests with HIII dummies were conducted and compared with full scale tests. For the comparison deceleration pulse, dummy numbers and vehicle movement were analyzed.
Validation tests with velocities up to 60 km/h showed promising results. The compartment and the suspension systems stayed stable. Rotation effects were comparable with full scale car crash tests. The airbags and seat belt system worked reasonable. The acceleration pulse compared to an Euro NCAP test had a similar characteristic but was in general slightly lower.
After the successful validation the reference vehicle is already in use in different studies in the field of vehicle safety research at BASt.

INTRODUCTION

For crash tests usually two types of methods are used. The most realistic procedure is to use the whole vehicle, also called a full scale crash test. This kind of testing requires the full equipped vehicle including dummies. In contrast sled test are used for component development und dummy research. Sled tests are much cheaper and faster to perform, but have certain limitations in terms of rotational and pitching movement during the impact. In addition to this intrusions are difficult to apply.

For different research questions a test method would be useful which has the advantages of both methods, sled tests (cheap and repeatable usage) and reacting more like a real car including a chassis with suspension and a full restraint system. This was achieved by the modification of components of an existing real car which is durable enough for repeating crash tests. Therefore a crash trolley was developed which has a chassis with suspension and damper systems, in the following called reference vehicle. On the crash trolley a compartment of a European middle class vehicle is installed so a full restraint system can be integrated.

This reference vehicle could be for example applied in the field of dummy development, compatibility research and testing of road side barriers.

Accident analyses have identified improvements in regard to frontal impact and compatibility (1). However, it is difficult to describe the compatibility of a

car with a fixed barrier (2), (3) and (4). A mobile deformable barrier has different advantages particular with regard of the assessment of frontal stiffness to match deformation force levels between the colliding vehicles (5). The final test procedure for the MPDB (mobile progressive deformable barrier) is described in (6) and (7). The reference vehicle is in addition to this able to evaluate the frontend stiffness of the opponent car due to the assessment of the dummy loading.
Further research is planned for the testing and assessment of road side barriers. Often older cars will be used and no dummies are installed in the vehicle. The evaluation of the performance of the restraint system can be helpful to assess the acceleration level from the road side barrier in particular for small and stiff vehicles (8) und (9).

The objective of this paper was to describe the development and validation of a crash trolley (reference vehicle) equipped with a compartment and a full restraint system for driver and front seat passenger which can be used frequently for crash testing. Furthermore, the crash trolley should have a suspension to show rotation and pitch effects similar to real vehicles.
For the validation crash test data of the reference vehicle were compared to an Euro NCAP crash tested vehicle. Differences were analyzed to determine the advantages and disadvantages and to understand the boundary conditions of the reference vehicle for future investigations.

MATERIALS

Based on German registration statistics in 2006 the three most represented vehicles in road traffic with a test weight of about 1.500 kg were identified by their market share (10). The typical weight for a medium vehicle is about 1.500 kg (11) and also the test weight which was chosen for the MPDB crash test procedure within the FIMCAR project (3).
Three models were identified which had the largest market share: Volkswagen Golf/Jetta, Opel Astra and Audi A3. After comparing technical details and the effort to recreate them in a reference vehicle the Opel Astra was chosen. The Opel Astra had a relatively simple 3-point “Mc-Pherson” wheel suspension which makes it easier to recreate and stabilize.

To simulate the Astra the shortened passenger compartment was mounted and stiffened on a steel frame. The construction was designed to obtain the same mass distribution and inertia torque as the original Opel Astra. With the adjustable suspension the reference vehicle is able to simulate the rolling- and pitching motions as they were observed at the real vehicle. Furthermore the height adjustments allow the adaption of the ride heights of the reference vehicle to analyze the influence of different masses on the spring deflection.

The main framework is made of steel including the chassis. The compartment was integrated and reinforced. Special attention was needed to provide appropriate strength to the trolley and its suspension. The additionally reinforcement was chosen in such a way that the mass and the centre of gravity is still comparable to the original vehicle. Thus, a realistic behavior is given in car-to-car crash tests (10).

The chassis of the middle class vehicle was changed in a way that crash test pulses do not damage or bend the structure. Particular focus was laid on the suspension system, because the flexible parts need to be durable enough for repeating crash tests.

In order to provide miscellaneous deceleration pulses different types of crash test barriers can be attached to the front of the vehicle. The PDB (Progressive Deformable Barrier, (12)) was a good candidate because the stiffness is quite similar to a real front end of this type of car (13). The frontend of the vehicle needed strengthening and a flat stiff plate for the attachment of the barriers. The Figure 1 shows the reference vehicle positioned in front of the crash block with Hybrid III dummies installed.

Figure 1 Side view of the reference vehicle with a PDB attached and Hybrid III dummies

The reference vehicle is equipped with a restraint system consisting of airbags, pedals, seats, dashboard, and windscreen. The wind shield is made out of plastic which is durable enough for the crash tests. The front seat passenger airbag is supported by the wind shield as it does in a real vehicle.

In the back of the reference vehicle the installation of the trigger box for airbags and seatbelts, the emergency brake system, the data acquisition box and further systems can be installed for the tests.

METHODS

For the validation a series of low and high speed crash tests with HIII dummies was conducted and compared with full scale tests (14). For the comparison deceleration pulse, dummy numbers and vehicle movement were analyzed.

First a couple of low speed crash tests were performed at lower speeds to check the straight running, durability and the emergency brake systems. Inspections and static measurements were conducted before and afterwards to check the stability of the reference vehicle and to ensure the vehicle's crash resistance.

A high speed crash test was performed and compared with a Euro NCAP crash test using an equivalent Opel Astra. The full scale crash test with the Opel Astra was conducted according to the Euro NCAP frontal impact test protocol with 64 km/h, 40 % overlap against the ODB and with two Hybrid III Dummies. For the reference vehicle the test speed, overlap and barrier types were selected accordingly. The reference vehicle had a PDB barrier attached, version 8 XT (extended). On the crash test block an ODB (15) barrier was installed with a LCW behind. The following Figure 2 gives an overview of the final test procedure.

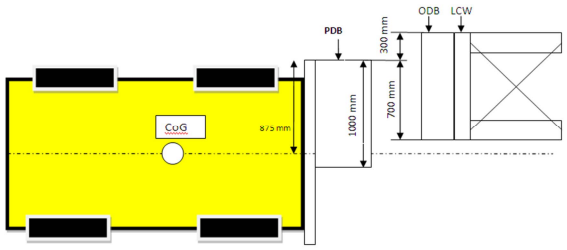

Figure 2 Overview of the test configuration reference vehicle against crash block

The test speed was calculated carefully with estimating the energy absorbed of the two barriers. The PDB barrier tends to be stiffer in particular the first parts so that a slightly lower test speed of 60 km/h was chosen for the reference vehicle.

Two Hybrid III 50% dummies were installed including the measurements according to the Euro NCAP frontal impact test protocol (16).

In the reference vehicle three axial acceleration sensors were placed at the centre of gravity and uniaxial acceleration sensors at the a- and b-pillar. The restraint system consisting of a dual stage driver airbag, one stage passenger airbag and seatbelt pretensions for driver and passenger side was manually triggered with a trigger box. The trigger times were chosen based on the Euro NCAP tests, see **Table** 1.

Table 1
Trigger Times for the Restraint System

	1st stage	2nd stage
Driver Airbag	20 ms	30 ms
Passenger Airbag	20 ms	-
Seatbelt pretensioner	20 ms	-

RESULTS

The measurements of the dummies and the vehicle of two similar crash tests were compared and the differences discussed. For the comparison deceleration pulse, dummy numbers and movements as well as the vehicle movement were analyzed.

Crash Data Reference Vehicle

Vehicle values

In Figure 3 the accelerations measured at the a-pillar for both sides are shown for the reference vehicle and the Opel Astra Euro NCAP test configuration. The maximum accelerations measured in the passenger compartment show a similar characteristic with slightly lower accelerations in the reference vehicle. In the beginning the acceleration of the reference vehicle is a little bit higher due to the stiffness of the

PDB element. The real Opel Astra is softer in the first part of the crash due to the bumper region.

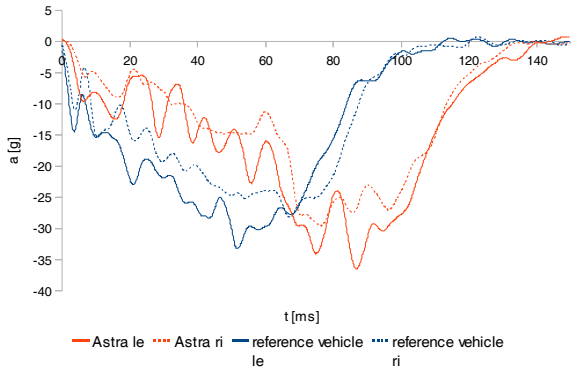

Figure 3 Comparison of the acceleration measured at the a-pillar

In the following Figure 4 the measured maximum accelerations in the vehicle are compared (tunnel, a-pillar and b-pillar). It turns out, that the measurements of the sensors placed in the vehicles are similar but in general slightly lower for the reference vehicle. Accelerations measured at the tunnel (Centre of Gravity) in z direction are lower for the reference vehicle which could indicate a lower pitch moment. This is comprehensible because the reference vehicle has less elastic parts compared to the Opel Astra.

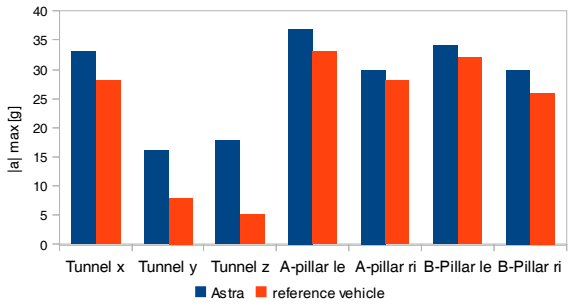

Figure 4 Comparison of maximum vehicle accelerations

Dummy values

Also the effects on the upper parts of the dummy bodies from head to pelvis can be simulated very well with the reference vehicle. Figure 5 shows the resulting chest-acceleration of all four involved dummies as an example. It is recognizable that the characteristic of the graphs is very similar. However there is a displacement of the points in time with the maximum accelerations. In the reference vehicle the dummy loadings occur earlier due to the used barrier which has a different structure compared with the front of the Astra.

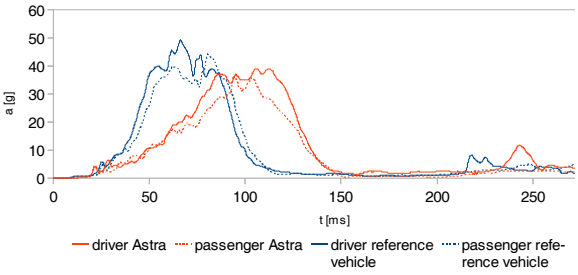

Figure 5 Comparison of the resulting chest acceleration

Figure 6 and Figure 7 show a comparison of the dummy values in relation to the ECE-R 94 limits (15). The limits for the different body regions as described in the regulatory frontal impact configuration are listed in Table 2.

Table 2 Biomechanical limits according to ECE-R94 (15)

Body region	Criterion	Limit
Head	HIC_{36}	1000
	a_{3ms}	80 g
Neck	My	57 Nm
Chest	ThCC	50 mm
	VC	1 m/s
Femur	Fz	7,58 kN (> 10 ms)
Knee	DS	15 mm
Tibia	Tibia-Index	1,3
	TCFC	8 kN

The dummy values for the driver side show similar numbers as for the dummy in the Opel Astra Euro NCAP test (see Figure 6). However, the head impact and the loading of the chest were in the reference vehicle higher. This can be explained by the higher pulse in the beginning of the crash due to the PDB element attached to the reference vehicle. In addition the dummy is loaded from the steering wheel airbag which should have been fired a few milliseconds earlier to substitute the increase of the deceleration pulse. The numbers for the lower extremities are in a comparable range. Due to the stiffened passenger compartment the footwell of the reference vehicle stays stable in a crash. For this reason the loadings on the lower extremities of the occupants differ from those recorded in the Opel Astra.

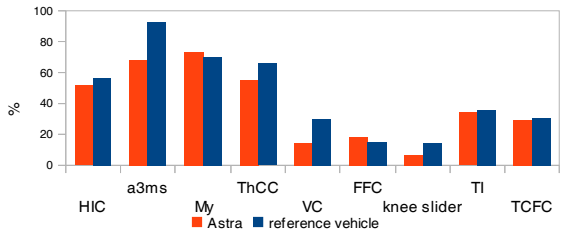

Figure 6 Comparison of the driver dummy values in percentage of ECE-R 94 limits

For the front seat passenger dummy the differences are in a similar range as for the driver dummy but are higher in absoluter numbers (Figure 7). Here, the chest deflection and head acceleration of the front seat passenger dummy is slightly higher, too.

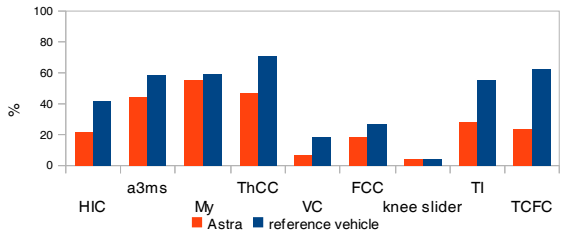

Figure 7 Comparison of the co-driver dummy values in percentage of ECE-R 94 limits

From the analyses of the high-speed movies it can be seen that the firing times for the airbag and the seatbelt of the reference vehicle were too late for the crash pulse. In contrast to this the forward movement of the dummies in the reference vehicle is earlier than in the Opel Astra. These differences explain the higher dummer loadings in the reference vehicle.
In Table 3 the timing of the dummy-vehicle interactions are summarized. The values were taken from the analyses of the high speed videos.

Table 3 Time of driver-dummy-interactions

	Driver		Co-Driver	
	Opel Astra	Ref-Vehicle	Opel Astra	Ref-Vehicle
Opening airbag lid	19 ms	22 ms	23 ms	24 ms
Seat belt motion	19 ms	22 ms	18 ms	22 ms
Airbag full opened	45 ms	50 ms	57 ms	59 ms
First dummy movement	40 ms	26 ms	43 ms	33 ms
Airbag-head-contact	64 ms	50 ms	66 ms	57 ms

DISCUSSIONS

The validation tests show that the reference vehicle is in principal suitable for crash testing. However, several limitations need to be considered.
The test was driven with a velocity of 60 km/h and therefore 4 km/h slower than the Opel Astra Euro NCAP test. Nevertheless the loadings on the Hybrid III Dummies were at a higher level in the reference vehicle. The higher loadings are caused due to the stiffness of the PDB element which is different compared to the frontend of the Opel Astra. Additionally in the Opel Astra has a certain amount of elasticity which is higher compared to the reference vehicle.
The barrier element is difficult to modify but the overlap and the test speed can be changed easily which has a direct influence on the deceleration gradient. It needs to be considered that the first part (e.g. bumper) of the Opel Astra is very soft while the PDB element is not.
The analyses of the dummy values indicated that the occupant loading of the upper body regions are realistic. The characteristics of the curve linearity are comparable to the Opel Astra. However, differences are present in the maximum values and can be explained with the higher pulse in the beginning of the crash. This should be considered for the selection of the fire times for the restraint systems in future investigations. The analyses of the firing times show that the trigger times should be reduced of approximately 5 ms for future tests with similar deceleration pulses.

Comparative analyses of the high-speed movies showed that the rotational effects due to the offset in the impact configuration are very similar to the real car. Pitch effects were present but less because elasticity of the suspension and the frame are different compared to the Opel Astra.

In general the results showed that the reference vehicle can be used for different kind of crash testing studies. However, there are some limitations due to the design which need to be considered for further investigations. The restraint system has to be triggered manually which has advantages in repeatability studies. The crash pulse is dependent of the barrier used and the overlap.

CONCLUSIONS

A reference vehicle equipped with a compartment and a restraint system for driver and front seat passenger dummies was developed and validated successfully. A variation of the deceleration pulses can be achieved due to the attachment of different deformable barriers. The reference vehicle was able to cope with accelerations up to 35 g.

The reference vehicle is a useful tool to answer further questions in different fields of passive automotive safety and road network. Compared to a traditional crash trolley dummies can be used as well as rotational and nick moments are present.
Future applications are planned in the field of dummy development, compatibility investigations and impacts with road side barriers.

ACKNOWLEDGEMENTS

The authors thank Kai Nebel for preliminary work conducted during his diploma theses.
In particular the authors thank the Opel AG for the support during this project with the allocation of parts and knowledge during the development.

REFERENCES

1. **Thomson A, Edwards M, Wisch M, Adolph Th, Krusper A, Thomson R,.** *Report detailing the analysis of national accident databases.* s.l. : European Commission, FP 7, FIMCAR frontal impact and compatibility assessment research, 2011. Deliverable 1.1.
2. **EEVC-WG15.** *Car Crash Compatibility and Frontal Impact, Final Report to Steering Committee.* www.eevc.org : European Enhanced Vehicle-safety Committee Working Group, 2008.
3. **Johannsen H, Edwards M, Lazaro I, Adolph Th, Thomson R, Versmissen T.** FIMCAR – Frontal Impact and Compatibility Assessment Research: How to test self and partner protection. *Transport Research Arena TRA.* 2012, Vol. Elsevier.
4. **Adolph T, Schwedhelm H, Lazaro I, Versmissen T, Edwards M, Thomson R, Johannsen H.** Development of Compatibility Assessments for Full Width and Offset Frontal Impact Test Procedures in FIMCAR. *ICRASH 2012 International Crashworthiness Conference.* Milano Italien, 2012.
5. **Schram, Richard and Versmissen, Ton.** *The Development of a mobile deformable barrier test procedure.* s.l. : ESV Conference, 2007. Paper Number 07-0327.
6. **Uittenbogaard, Jeroen and Versmissen, Ton.** *Test Protocol - Mobile Progressive Deformable Barrier.* s.l. : FIMCAR - FP7 Project of the European Commission, 2011.
7. **Versmissen T, Welten J, Rodarius C.** *MPDB test and simulation results.* s.l. : European Commission, FP 7, FIMCAR frontal impact and compatibility research, 2012.
8. **Gülich, H.-A.** Stahl oder Beton im Mittelstreifen? *Straße und Autobahn.* 12, 1996, Vol. 47, 12, S. 708-719.
9. **Ellmers, U.** *Eignung von Fahrzeug-Rückhaltesystemen gemäß den Anforderungen nach DIN EN 1317.* Bergisch Gladbach : Berichte der Bundesanstalt für Straßenwesen, August 2003. Verkehrstechnik Heft V 106.
10. **Nebel, K.** *Konzeption und Konstruktion eines Referenzfahrzeuges zur Untersuchung der Kompatibilität von Personenkraftwagen.* Wuppertal : Universität, 2006.
11. **Versmissen, Ton, Schram, Richard and McEvoy, Steve.** The development of a load sensing trolley for frontal offset testing. *International Journal of Crashworthiness.* 12, 2006, Vol. 01/2007, pp. 235-245.
12. **France.** *Regulation No. 94 (Frontal collision): Proposal for draft amendments PDB.* Geneva : Economic Commission for Europe – Inland Transport Committee – World Forum for Harmonization of Vehicle Regulations – Working Party on Passive Safety, 2007. http://www.unece.org/trans/doc/2007/wp29grsp/ECE-TRANS-WP29-GRSP-2007-17e.pdf.
13. **Edwards M, Coo P de, Zweep C van der , Thomson R, Damm R, Martin R, Delannoy P, Davies H, Wrige A, Malczyk A, Jongerius C, Stubenböck H, Knight I, Sjöberg M, Ait-Salem Duque O, Hashemi R.** *Improvement of Vehicle Crash Compatibility Through the Development of Crash Test Procedures (VC-Compat).* http://ec.europa.eu/transport/roadsafety_library/publications/vc-compat_final_report.pdf : Europen Commission 5th Framework Project GRD2/2001/50083, 2005.
14. **Kanjuparambil, N.** *Validierung der Kompatibilitätstauglichkeit eines Referenzfahrzeuges zur Analyse von Frontalkollisionen (diploma thesis).* s.l. : Fachhochschule Köln, 2012.
15. **UN/ECE.** *Regulation No. 94 (Frontal collision).* Genf : GRSP, 2010. http://www.unece.org/trans/main/wp29/wp29wgs/wp29gen/wp29fdocstts.html.
16. **Euro NCAP.** *Frontal Impact Testing Protocol v.5.2.* Brussels : Euro NCAP, 2011.

FIMCAR – INFLUENCE OF SEAS ON FRONTAL IMPACT COMPATIBILITY

Mathias Stein
Heiko Johannsen
Technische Universität Berlin
Germany
Robert Thomson
VTI
Sweden
Paper Number 13-0436

ABSTRACT

The aim of the FIMCAR project (Frontal Impact Compatibility and Assessment Research; co-funded by the European Commission within the 7th Framework Programme) was to develop and validate a frontal impact assessment approach that considers self and partner protection. Regarding the results of the FIMCAR accident analysis, one major issue of frontal impact compatibility is structural interaction. Not all car types have the potential to align their Primary Energy Absorbing Structures (PEAS) with the common interaction zone proposed by FIMCAR. Some cars use Secondary Energy Absorbing Structures (SEAS) to interact with external structures and thereby improve the structural interaction. There is a challenge to evaluate the different structural concepts, and in particular SEAS, in the possible variations of potential impact combinations.
The main objective of this study is the identification of characteristics of appropriate SEAS. Therefore this paper will give an overview about the investigations done within FICMAR to analyse parameters which improve the car-to-car crash performance. As part of the analysis physical test data as well as simulation results were used to study the interaction of the front end structures.
Within FIMCAR 10 car-to-car tests were conducted. The main outcome was that the alignment of the PEAS of both crash partners is crucial for the structural interaction. Furthermore the crash test showed that misaligned vehicles perform better if they are equipped with appropriate SEAS than vehicles without a lower load path. These investigations were supported by numerical simulations.
Within the FIMCAR project, amongst others, FEM vehicle models called Parametric Car Models (PCMs) were used for the assessment of car structures. For this study they were supplemented by the detailed FEM models provided by NCAC. For the SEAS analysis the PCMs were used to create several geometrical modifications. Due to the simplified design of the models the influence of the crash performance could be correlated well to the design of the SEAS.
The analysis of the simulations identified 3 geometrical parameters of the SEAS that had a positive influence in a car-to-car crash. The first parameter is the longitudinal position of the SEAS. A position of about 230mm behind the bumper beam (or further forward) improved the crash performance of both collision partners. The second parameter is the vertical connection between SEAS and PEAS. A robust connection located about 250mm behind the bumper beam was able to activate the penetrating structures of the striking vehicle and therefore to improve the structural interaction. The third geometrical parameter that was identified is the height of the cross section of the cross beam of the SEAS. An increase of the height by 50% to 60mm showed that the SEAS was able to support the penetrating structures better than the small SEAS.
According to the capabilities of assessment procedures to assess appropriate SEAS the OverRide Barrier (ORB), test configuration as well as the full width assessment metrics developed within FIMCAR were checked. The ORB test was not able to discriminate between appropriate and inappropriate SEAS. Regarding the full width test the Full Width Rigid Barrier (FWRB) configuration was not able to detect and assess the SEAS structures mainly due to the very short assessment interval, too. In contrast the Full Width Deformable Barrier (FWDB) was able to detect and correctly assess the SEAS that improved car-to-car crash performance due to their longer assessment period.

INTRODUCTION

Structural interaction was a high priority work item in the EC funded FIMCAR project (Frontal Impact Compatibility and Assessment Research). The project identified sub elements of structural interaction, i.e., structural alignment, horizontal load spreading and vertical load spreading. The latter is an issue that is in particular important to investigate the benefits of lower load paths. Secondary Energy Absorbing Structures (SEAS) have been identified in an earlier project [2], [7] relating to higher vehicles, like SUVs, to have a potential to address impact alignment in vehicles with a primary load path that is too high.

To further investigate vertical load spreading, three specific tasks were identified for this paper:

1) Report on recent international research related to evaluation and performance of lower load paths and SEAS
2) Identify the characteristics (geometrical parameters) of "appropriate" SEAS
3) Identify potential methods to assess or identify an appropriate SEAS

The benefits of vertical load spreading were identified in the VC-Compat project and confirmed in the FIMCAR car-to-car tests. Details of these tests will be presented in the following sections.

BACKGROUND

Within the last decade several relevant research activities were conducted to define requirements to address frontal impact compatibility requirements and to develop an assessment approach to address self and partner protection. Even though the vehicle fleets of different regions have specific compatibility requirements to fulfil, similar approaches to address compatibility issues like structural interaction can be found. A brief overview of the discussed test procedures is given in the following section.

Europe Amongst others, structural interaction has been detected as crucial to control the compatibility between passenger cars [1], [2], [7]]. To avoid car-to-car crash phenomena like over/underriding or fork effects, the focus was moved to the assessment of horizontal and vertical load spreading. Within VC-Compat different test procedures were evaluated regarding their potential to detect and correctly assess the height (and strength) of PEAS and SEAS [7]. Two test procedures were proposed to assess the structural interaction capabilities of a car: PDB and FWDB test [8]. However, no final metric for the PDB was evaluated and the proposed FWDB assessment still needed validation to show it could discriminate between good and poor performing cars.

USA A significant activity that was initiated by the automotive industry is the US voluntary commitment [6]. This was developed to ensure that Light Trucks and Vans (LTVs) have structures in alignment with a common interaction zone, also referred to as "Part 581 zone", measured vertically 16 to 20 inches (406mm – 508mm) from the ground to enable better interaction with cars. The US voluntary commitment states that all LTVs sold by participating manufacturers in the US must fulfil one of the two options below, see Figure 1:

OPTION 1

The light truck's PEAS shall overlap at least 50 percent of the Part 581 zone (Option 1a)

AND at least 50 percent of the light truck's PEAS shall overlap the Part 581 zone (Option 1b)

OPTION 2

If a light truck does not meet the criteria of Option 1, there must be a SEAS, connected to the primary structure, whose lower edge shall be not higher than the bottom of the Part 581 bumper zone.

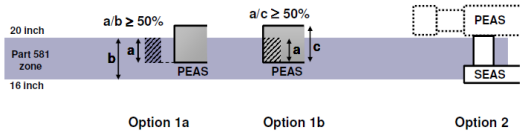

Figure 1. US voluntary commitment for improved compatibility of LTVs [18]

The assessment of the SEAS capabilities was evaluated with an additional test configuration, the OverRide Barrier (ORB) [12]. Thereby a rigid barrier equipped with Load Cells (LC) and positioned below the PEAS measures the forces applied by the SEAS during the test. The forces must reach 100kN within 400mm displacement measured from the most forward point of the vehicle structure, see Figure 2.

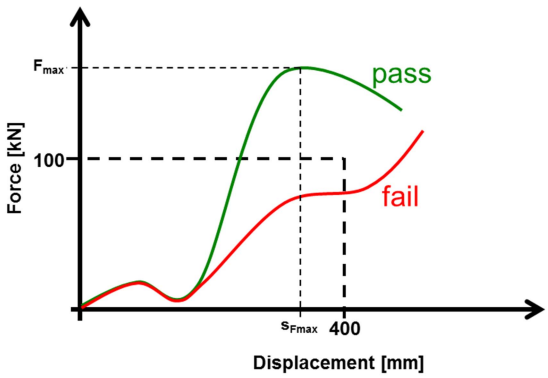

Figure 2. ORB test criterion

Japan The Japanese proposal to evaluate structural interaction consists of a combination of FWRB and ORB test [16]. The ORB test is used as a 2nd stage criterion, if the vehicle fails the proposed FWRB metric, see Figure 3. In contrast to the dynamic test configuration preferred by NHTSA the Japanese describe a static test, where an impactor loads the SEAS which has to withstand 100kN within 400mm displacement, too.

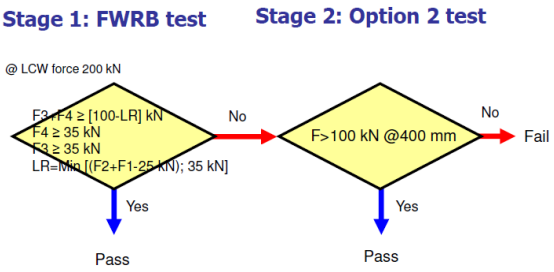

Figure 3. Japanese recommendation for full frontal test procedure [16]

FULL WIDTH ASSESSMENT PROCEDURES

Within FIMCAR two full width test procedures (FWRB and FWDB) were evaluated regarding their potential to address the defined priority items and are described in detail in [10]. Compatibility metrics were developed which should allow an assessment of the structural interaction capabilities of passenger cars. The final proposal for a frontal impact and compatibility assessment approach is to use the FWDB and its corresponding assessment metric in combination with the ODB (ECE R 94).

Structural alignment metric [10]:

- Up to time of 40ms:
  - F4 + F3 ≥ [MIN(200, 0.4FT40) kN
  - F4 ≥ [MIN(100, 0.2FT40) kN
  - F3 ≥ [MIN((100-LR), (0.2FT40-LR))]
  - where:
    - FT40 = Maximum of total LCW force up to time of 40ms
    - Limit Reduction (LR) = [F2-70] kN and 0kN ≤ LR ≤ 50kN*
    - *Note values to be confirmed taking into account the new test velocity

Even though both full width test procedures have a lot of similarities there are also some important differences which mainly have an influence on the assessment metrics. The most important influence is the engine dump effect which makes the evaluation of forces contributed by Energy Absorbing Structures (EAS; PEAS & SEAS) in the LCW measurements impossible. Yonezawa et al. [18] showed that the engine typically starts to decelerate after 200mm displacement (depending on the vehicle - 10ms to 15ms) in the FWRB test. The disadvantage of a relatively short assessment period is overcome in the FWDB test configuration, due to the two honeycomb layers in front of the wall [2]. The crushable element ensures a longer assessment period because the honeycombs prevent the engine to directly impact the wall. Thus an assessment period of 40ms is possible, which offers the potential to assess the EAS of about 50% of the crash period. One further advantage is that a far rearward located SEAS which does not penetrate the second stiffer layer, does not apply relevant forces to the LCW. This was identified as a positive characteristic, because a far rearward placed SEAS will not contribute in car-to-car crashes and therefore will not be assessed as an appropriate SEAS.

CAR-TO-CAR TESTING

Within FIMCAR a large vehicle crash test program was envisaged. Car-to-barrier crashes were planned for the evaluation of the proposed test procedures and assessment approaches while car-to-car crashes were conducted to investigate the influence of structural misalignment.
The car-to-car crashes were classified into three test series. The main objective of all three test series was the evaluation of the SEAS in frontal and side impacts.

Table 1.
FIMCAR car-to-car test program [13]

Test series	Vehicle	Aim of the test	Test setup
1	Supermini 1 (PEAS) Supermini 2 (PEAS & SEAS)	The effect of structural alignment in vehicle equipped with lower load path compared to a case without a lower load path	Frontal car-car 56km/h 50% offset
2	Small family car 1 (PEAS & SEAS) SUV 1 (PEAS & SEAS)	The effect of structural alignment and lower load path in SUV type vehicles crashing against a small family car	Frontal car-car 56km/h 50% offset
3	Large family car 1 SUV 2 (PEAS & SEAS)	Investigate the importance of lower load paths for SUV type vehicles in side impact crash	Side impact car-car 50km/h

Table 1 gives an overview about the car-to-car crashes conducted within FIMCAR. A detailed summary about the results can be found in [13]. However the main findings will be described shortly in the following section.

Test series 1 – Super Mini vs. Super Mini

Regarding the decelerations, higher mean values for the first 300mm displacement and higher maximum values for Super Mini 2 (SM 2) could be observed for the aligned tests. Both misaligned configurations showed a delayed increase of the decelerations at the beginning of the crash compared to the aligned configurations, but the delay is longer for Super Mini 1 (SM 1; without SEAS).
The intrusions of the SM 2 were generally lower than for SM 1 in both configurations. Both configurations showed the same trend in the case of the misaligned structures in that the differences of intrusions for the two crash partners increased.
The dummy values showed no obvious trends. However some injury criteria were higher than the corresponding Euro NCAP criteria (a_{3ms} and HIC36 for SM 2 aligned).

Test series 2 – SUV vs. Small Family Car

The mean decelerations within the first 300mm displacement are again lower for the misaligned Small Family Car (SFC) compared to the aligned one. The maximum decelerations show hardly any differences. The deceleration measurement for the misaligned SUV failed, thus no comparison to the aligned configuration was possible.
Regarding the intrusions, the SFC had higher values in both configurations than the SUV. However, only the dashboard intrusions were lower in the aligned configuration. The aligned configuration led to less override of the SFC, but the structures were overloaded by the heavier SUV which resulted in higher intrusions in areas directly affected by the main load path.
No clear trends could be observed regarding the dummy measurements. With respect to the ECE R94 limits all measurements showed lower values.

Test series 3 – LFC vs. SUV

Comparing the deformation patterns of both crash configurations, the following observations could be made. The B-pillar intrusions of the LFC in the reference configurations were higher than those in the other configuration. Due to the loading of bumper beam and cross beam of the SEAS above the sill, the B-pillar displacement was higher. In the second configuration the bumper beam was the only structure that loads the B-pillar and the door intrusions increased due to the penetrating longitudinals of the SUV. Even though the door intrusions were higher in the modified configuration, the dummy measurements were lower because the longitudinals of the SUV penetrated the doors outside the contact area of dummy and inner door. It was expected that the dummy would be loaded more if the impact location moved rearwards. However the loads in the reference test were spread more homogenously than in the second configuration and demonstrate the importance of vertical load spreading.

Summary of car-to-car testing

Summarising the results of the car-to-car testing conducted within VC-Compat [7] and FIMCAR [13] the following observations were made:

- Cars with aligned PEAS show better results than misaligned.
- Vehicles with PEAS aligned in row 3 and row 4 were more stable when equipped with a lower path.
- Vehicles with PEAS in row 4 performed well if a SEAS was identified in FWDB metric in row 3 and/or row 2.

In addition to the car-to-car crashes, the test objects were also crashed against the FWDB. The FWDB metric assessment of well performing SEAS readings regarding car-to-car crash results was always positive.

FE MODEL APPROACHES

To support the development of frontal impact compatibility assessment metrics, an extensive virtual testing program was established within the FIMCAR project. For this purpose two different FE model approaches were used to create FE vehicle models. The first approach was based on the Generic Car Models (GCMs) already used within the APROSYS project [3]. The second modelling approach is the Parametric Car Models (PCMs). Supplementing the FIMCAR activities, a third FEM model type was used. The NCAC provides detailed FEM models of specific cars of different vehicle classes (e.g. Ford Taurus and Ford F250) [4]. The NCAC models used for the following investigations are comparable to the GCMs, except they represent a real vehicle and its corresponding crash performance. Table 2 summarises the main characteristics of the two modelling approaches. A more detailed description is given in [14].

Table 2.
Comparison of FE model approaches (information in brackets according to NCAC models)

	GCM (NCAC)	PCM
Number of elements	600,000 (750,000-1,000,000)	200,000
Level of detail	high	low
Computational effort	high	low
Number of models - modifications	5 – no modification (only minor modifications possible)	3 – theoretically unlimited number of modifications possible
Intended field of application	detailed analysis of structural interaction, representative crash behaviour	identification of influence of crash relevant parameters

Due to the high level of detail the GCMs/NCAC models offer the possibility for in-depth analysis of the crash performance of the corresponding structural concepts (SEAS designs) as well as a quantitative estimation of injury severity level controlling parameters like accelerations and intrusions. However, the detailed models did not allow structural modifications with acceptable efforts in the scope of this investigation. To overcome limitations w.r.t. modifications of detailed FE car models, PCMs were used for the investigation of different structural concepts and their influence in frontal impacts. An implicit parametric CAD model allowed fast modifications

of the main crash relevant structures and a specific pre-defined simulation environment ensures that the simplified FE models could be computed directly without further pre-processing [15].

SEAS ANALYSIS

The study is subdivided into three parts. The first part is based on an NHTSA study analysing the capabilities of the ORB and their potential to assess SEAS properly. In part two and three, characteristics of SEAS are identified which bring benefits in car-to-car crashes. Furthermore the potential of the full width assessment candidates proposed by FIMCAR to detect SEAS is analysed.

Capability of ORB

The capability of the ORB was already investigated by Patel et al. [12]. As part of this study the influence of SEAS of Option 2 vehicles was investigated using car-to-car crashes as well as numerical simulations. The main conclusion was that the ORB test did not lead to a significant assessment of the SEAS with respect to the analysed SEAS designs. Even though the two investigated LTVs (Ford F250 and Chevrolet Silverado [4]) pass the ORB test, only the F250 showed an improved crash performance in car-to-car crashes compared to a modified F250 with removed SEAS.
Because the passenger car (1996 Dodge Neon) used for the study of Patel et al. [12] did not represent a modern car, the presented methodology was adopted and the passenger car was replaced by one of the PCMs developed within FIMCAR. Additionally both LTVs were crashed against the FWDB at 50km/h to analyse the Load Cell Wall (LCW) force distributions.

ORB simulations with and without SEAS Because the two LTV FEM models were not validated for the ORB, the performance of both vehicles was checked in ORB simulations. The SEAS of the F250 consists of a blocker beam which is attached about 250mm below and 55mm behind the PEAS. For the configuration without SEAS only this blocker beam was removed, while the attachment was kept. The SEAS of the Silverado consists of two separate brackets that are attached directly to the PEAS and are located about 280mm behind the bumper beam. For the Silverado without SEAS, these brackets were removed. Table 3 summarises the simulation results (s_{Fmax} and F_{max} are explained in Figure 2).

Table 3.
ORB results for LTV modifications

	Modification	s_{Fmax} [mm]	F_{max} [kN]
Ford F250	with SEAS	300	360
	without SEAS	330	340
Chevrolet Silverado	with SEAS	240	420
	without SEAS	400	0

The LTVs equipped with SEAS pass the test. Compared to the crash test data, the forces applied by the numerical models are much higher. This mainly depends on the ORB barrier type used for the F250 crash test where only the blocker beam impacted the ORB (3 LCs 250x250mm were used). The vertical connections between blocker beam and SEAS were not activated. In contrast to this, the ORB barrier used for the simulations overlapped the front of the trucks completely. Due to this the F250 with removed blocker beam was also able to pass the test. The higher loads computed for the Silverado resulted due to the fact, that no failure was defined in the FEM model. The SEAS remain connected for the whole impact and could apply much higher forces compared to the original SEAS which broke off. Due to numerical problems during the computation, the Silverado bumper had to be removed whereby no forces could be applied to the ORB in the configuration without SEAS.

Car-to-car simulations with and without SEAS A crash configuration for the car-to-car simulations similar to Patel et al. [12] was used but a PCM model replaced the Dodge Neon as the target vehicle. Both vehicles were crashed against each other with 100% horizontal overlap and a 100km/h closing speed for this study. An overview about of the structural alignment is given in Figure 4 and Figure 5.

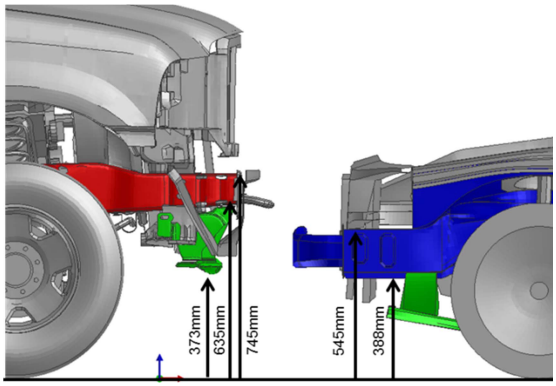

Figure 4. Vertical alignment of Ford F250 (left) and PCM LFC (right)

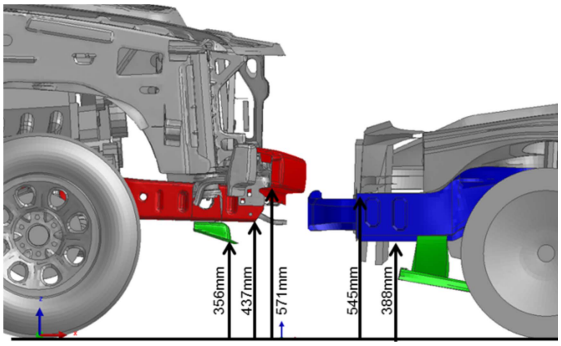

Figure 5. Vertical alignment of Chevrolet Silverado (left) and PCM LFC (right)

The PCMs were designed to meet the proposed assessment criteria within FIMCAR. Based on this the PEAS of the LFC are in alignment with row 4 and row 3 of the full width Load Cell Wall (LCW) and therefore within the Part 581 zone. The alignments of the Energy Absorbing Structures (EAS) of F250 and Silverado with the PEAS of the LFC are comparable to the original alignment used with the Dodge Neon. The PEAS of the LFC are aligned with the SEAS of the F250 only. However, the distance between the longitudinals of the F250 (980mm) is higher compared to the Silverado (800mm). Thus there is a vertical alignment of the PEAS of Silverado and LFC but there is a horizontal geometrical mismatch, see Figure 6.

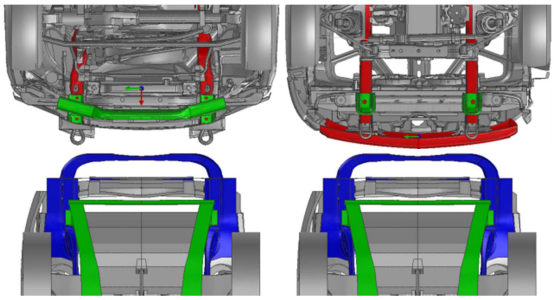

Figure 6. Horizontal alignment (top: left – Ford F250, right – Chevrolet Silverado; bottom: PCM LFC)

Figure 7 shows exemplarily the deceleration-displacement curves of the F250-to-PCM simulations. The solid graphs show the configuration where the LTV (red curves) was equipped with SEAS, the dotted graph without SEAS.

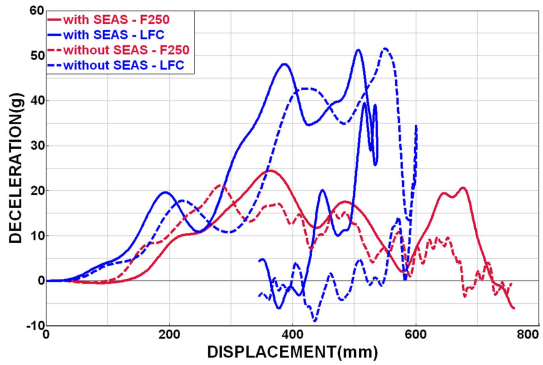

Figure 7. Deceleration-displacement curves F250 vs. LFC (solid lines – with SEAS, dotted lines – without SEAS)

The simulations show a reduction in the stopping distance by 50mm of the PCM (blue curves) and a slight increase of the deceleration of the F250, which can be related to improved structural interaction. Thus the trend to override the PCM was also reduced in the configuration with SEAS.
Regarding the results of the Silverado simulations no significant influence of the presence of the SEAS could be observed on the collision partner. The Silverado overrides the LFC in both configurations and no interaction of the brackets with the PEAS of the LFC was detected. The analysis of the intrusions showed also no differences.

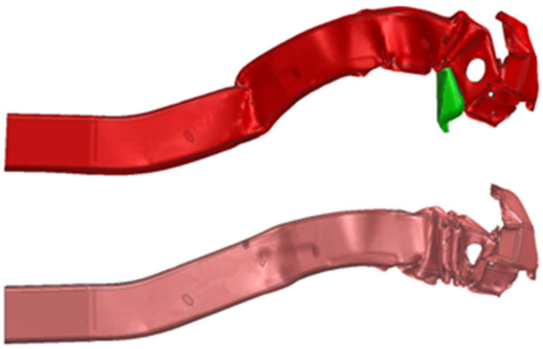

Figure 8. Change in deformation mode due to absence of SEAS (longitudinal of Silverado; top with SEAS, bottom without SEAS)

As Patel et al. [12] already mentioned, the deformation behaviour of the PEAS changed due to the removal of the SEAS. Without the SEAS, the PEAS have a better buckling behaviour which resulted in slightly higher decelerations and in a more efficient energy absorption mechanism, see Figure 8. Comparable observations were made in frame of another study conducted within FIMCAR, where the influence of the towing eye on the full width assessment metrics was analysed [5].

FWDB simulations with and without SEAS In the last step the LTVs were crashed against the FWDB at 50km/h. The main objective was to check if this assessment procedure is able to detect the SEAS and if these specific types of SEAS are able to load the barrier enough to pass the test. Especially for the F250, there was the question if the attachment and the blocker beam is stiff enough to load the barrier significantly, because the PEAS does not overlap row 4 (distance of lower edge of PEAS to the ground 635mm) and therefore does not contribute to the loads that have to be applied into the common interaction zone.

Table 4.
LCW forces (up to 40ms) of FWDB simulations with modified LTVs

	Ford F250		Chevrolet Silverado	
	w SEAS	w/o SEAS	w SEAS	w/o SEAS
F_{tot} [kN]	849	825	753	724
F4 [kN]	142	137	266	266
F3 [kN]	25	10	308	258
F2 [kN]	4	4	23	9
	fail	fail	pass	pass

Table 4 summarises the computed results of the FWDB simulations. Regarding the F250 the SEAS could not apply enough loads to row 3 to pass the test. Compared with the configuration without the blocker beam, the results show that the attachment is the only structures which applied loads to row 4 and row 3. The blocker beam itself had just a minor influence, even though it had a positive influence in the car-to-car crashes. Basically the same observations were made regarding the Silverado. However, due to the removed brackets the deformation behaviour of the PEAS changed and the forces decreased.

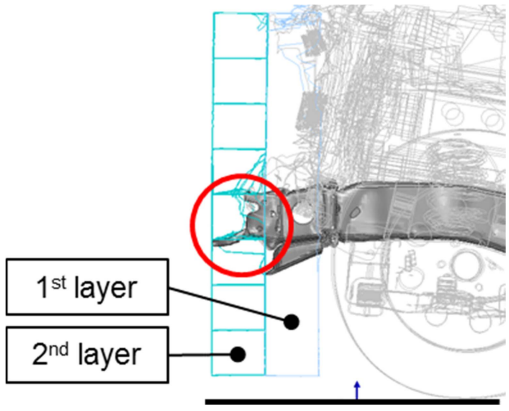

Figure 9. Towing eye contact in FWDB test (Chevrolet Silverado)

Even though the PEAS of the Silverado overlaps row 3 only with 14% the sum forces of row 3 are relative high. The reason for that is the towing eye in front of the PEAS, see Figure 9. Due to this very stiff part effects of the PEAS were covered and an assessment of crash relevant structures was not possible. Therefore the towing eye was removed and the simulations were repeated. Even with the overlap of the longitudinal with row 3 enough forces were applied and the vehicle passed the FWDB test again.

Summary of LTV simulations The conducted simulations confirm the results of Patel et al. [12] and also show that they can be transferred to modern cars.
The assessment of the SEAS with the ORB did not necessarily provide benefits in a car-to-car crash. The following main reasons could be identified:

1. The acceptance criteria are too generous. The requirement to meet a force threshold in the first 400mm of travel can result in significant interaction of a stiff PEAS before any contribution of a SEAS with the collision partner in car-to-car accidents.
2. The force measurement in a rigid load measurement system can overestimate the contribution of structures when a displacement based procedure is used to evaluate stiff structures like steel components.
3. The test method has no requirement for energy absorption of the structures and thus no demands are placed on the SEAS to maintain the threshold force.

Regarding the results of the Silverado simulations the assessment of the FWDB metric gives contradictory information (pass FWDB test but overrides PCM). The main reason for that is the design of the PEAS of the Silverado which has the bumper beam above its PEAS (typically in front of the PEAS). The bumper beam position resulted in a poor horizontal load spreading between the longitudinals which is not being assessed by the FWDB metric. Furthermore, heavy vehicles have less problems to apply 100kN in row 3 and row 4 due to their mass. Thus a relative small overlap of PEAS and row 3 is sufficient for the Silverado to pass the FWDB metric. Assessment metric improvements like a load distribution criterion (see proposed FWRB metrics in [9]) or an increased LCW resolution could lead to a more sensitive assessment.

Analysis of SEAS characteristics with PCMs

The goal of this study was to investigate the influence of the SEAS in car-to-car crashes and to identify characteristics of appropriate SEAS that are able to improve structural interaction. Therefore geometrical modifications in terms of varied stiffness and SEAS positions were simulated. In a first step the modified PCM models were crashed in an adapted ORB test to identify the force level of the SEAS. Furthermore it should be checked, if this test configuration is able to assess a SEAS in a correct manner (distinguish between SEAS that provide benefits in car-to car crashes and others). After that the PCMs were run against the FWRB and FWDB with 50km/h. The main objective was to check if the SEAS could be detected on the LCW.

First modifications Figure 10 shows the baseline configuration of the used PCM (Large Family Car – LFC). The PEAS are in alignment with row 3 and 4 and the SEAS are in alignment with row 2.

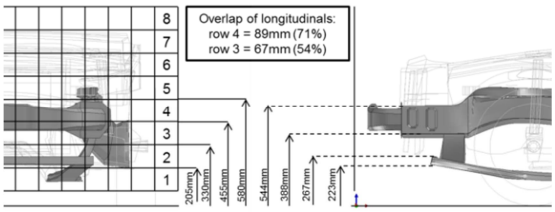

Figure 10. Baseline configuration of the PCM (LFC)

In a first step the position of the SEAS in longitudinal direction was modified, see Figure 11. These modifications only affected the longitudinals and the cross beam of the SEAS. The position of the vertical connection was not changed in this first step. Earlier simulations with a modified Ford Taurus model indicated that an appropriate SEAS will bring benefits if it is located between 180mm and 400mm behind the bumper beam [11].

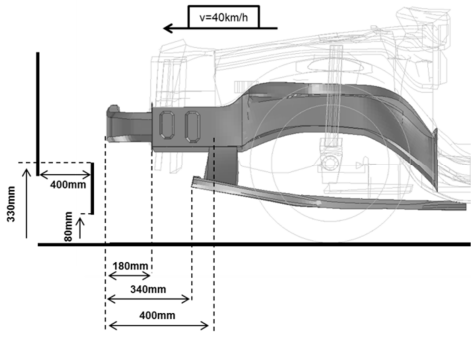

Figure 11. Adapted ORB crash configuration and geometry of PEAS and SEAS and lower boundary (400mm) for SEAS modification

In addition to the baseline configuration five modifications were created, see Table 5.

Table 5.
First modifications of SEAS

Modification	Distance between bumper beam and SEAS [mm]
D200	**200**
D250	**250**
D300	**300**
D350	**350**
D400	**400**

ORB simulations Regarding the stiffness level of the SEAS, other simulations within FIMCAR indicated that the sub frame of the baseline LFC was relative weak. For this purpose the stiffness of the sub frame was increased by factor 2. The results of the ORB simulations are summarised in Table 6 and Table 7.

Table 6.
ORB results for LFC SEAS modifications

Modification	s_{Fmax} [mm]	F_{max} [kN]
D200	288	203
D250	337	198
D300	387	186
Baseline	400	73
D350	400	68
D400	400	26

Table 7.
ORB results for LFC with reinforced SEAS (stiffness increased by factor 2) modifications

Modification	s_{Fmax} [mm]	F_{max} [kN]
D200	288	457
D250	338	468
D300	388	446
Baseline	400	257
D350	400	183
D400	331	25

The configurations with the standard SEAS pass the ORB test if the SEAS was located 200mm to 300mm behind the bumper beam. After the reinforcement of the SEAS the baseline LFC and the D350 modification pass the ORB test too.
Following the intention of the ORB test to assess SEAS on vehicles that do not meet the US volunteer commitment, it should be expected that all configuration that pass the metric (configurations that are highlighted in Table 6 and Table 7) should bring benefits in car-to-car crashes.

FWRB and FWDB simulations To address the vertical load spreading initially the PDB was the most promising crash configuration to detect and assess the capabilities of lower load paths [9]. However, the FW test procedures also offer the possibility to detect those structures. To define suitable thresholds for the assessment metrics force levels had to be specified which could be related to corresponding SEAS and their capability to improve car-to-car crashes. Furthermore both full width test candidates had to be evaluated regarding their potential to identify appropriate SEAS.

To compare the results of the ORB tests the six LFC configurations were crashed against the FWRB and FWDB with and impact velocity of 50km/h.

The row sum forces of the FWRB and FWDB crash simulations are shown in Figure 20 and Figure 21 in the appendix. Compared to the FWDB, the FWRB clearly detects the sub frame of all configurations except modification D400. For the three configurations with the far forward located sub frame (D200, D250 and D300) the maximum forces are higher than 100kN and were applied to the wall within 20ms to 40ms of the crash (red circles). The baseline model and the modification D350 apply also forces in row 2 to the LCW but after 40ms which is relative late in the crash (red dotted circles). The FWDB detects also loads in row 2 but below 100kN and the maximum was not reached within the first 40ms of the impact (blue cirlces). However, the forces start to increase after 20ms.

The results of the simulations with the reinforced sub frame showed for the FWRB configuration unrealistic high peak forces when the sub frame contacted the wall but at the same point in time compared to the simulations with the baseline sub frame. In the FWDB configuration the reinforced sub frame was able to apply significant loads to the wall. The forces were up to 150kN for the D200 configuration but the maximum was reached not until after 50ms. The further back the sub frame was located, the lower the load applied in row 2. Due to the load spreading of the deformable element a small proportion of the forces was also applied to row 1.

Table 8.
Differences in SEAS detection between FWRB and FWDB

	FWRB	FWDB
Detection of SEAS	yes	yes
Detected SEAS configurations	D200 to D350	D200 to D350
Clearly detected SEAS configurations	D200 to D350	D200 to D300
Force level of sum force in row 2 of clearly detected SEAS	>100kN	50kN <F2 <100kN
t_{maxF2} for configuration D200	23ms	45ms
Force progression in row 2	Relatively short peak (Δt = 10ms)	Continuously loading (Δt = 40ms)

Table 8 summarizes the results of the car-to-FWB simulations of the first SEAS modifications. Both FW tests were able to clearly detect the baseline sub frame located between 200mm and 300mm (350mm for FWRB) behind the bumper beam. Furthermore, both test procedures were able to detect the reinforced SEAS except the sub frame was located 400mm behind the bumper beam (D400). The forces in row 2 did not reach their maximum within the assessment periods of the corresponding test procedure. The main differences between FWRB and FWDB were, that the forces measured in row 2 were higher in the FWRB (>100kN) test than in the FWDB (50kN <F2 <100kN) test and the characteristic of the force progression in both configurations. The forces applied to the LCW in the FWRB test occurred only a relative short moment ($\Delta t \approx 10$ms) compared to the longer duration ($\Delta t \approx 40$ms) in the FWDB test. In comparison to the FWRB, the forces applied in row 2 started to increase within the first 40ms in the FWDB and reached about 75% of the maximum sum forces of row 2 within this period (modification D200). These results were not influenced due to engine dump because the simplified engine is located about 610mm behind the bumper and does not contribute to the load distribution in the FWB tests.

Car-to-car simulations For the identification of the benefit of a far forward located sub frame, the LFC configurations were crashed against the three available reference PCMs (Super Mini – SM, Large Family Car – LFC and Executive – Exe), henceforth referred to as bullet vehicles. The vehicles were crashed against each other with a horizontal overlap of 50%, with respect to the modified LFC, and a closing speed of 112km/h. The modified LFCs were raised by 70mm to simulate a vertical mismatch between the PEAS and to estimate the influence of the SEAS, see

Figure 12. This offset was identified in another study within FIMCAR as a configuration where the LFC failed the FWRB and FWDB criteria, because the forces applied to row 3 were too low. Baseline runs were simulated to compare the geometrical misalignment with a perfect match of the PEAS.
The most important differences between SM, LFC and Exe (beside dimension and mass) are the position of the sub frame (LFC and Executive are equipped with an SEAS which is located about 350mm behind the bumper beam) and the cross section of the SEAS (SM has the smallest cross sections compared to LFC and Exe).

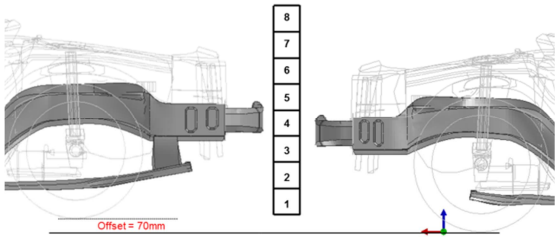

Figure 12. Car-to-car crash configuration (LFC (left) vs. SM (right))

In general the assessment of the occupant loading was done by calculation of simplified occupant load criteria (e.g. OLC) and comparison of the intrusions on the firewall. For the car-to-car simulations the assessment was done by analysing the deceleration-displacement curves and the intrusions of the colliding vehicles.
The analysis of the deceleration-displacement curves showed a reduction of the maximum decelerations for all cars in the misaligned configuration compared to the corresponding aligned configuration. The structural mismatch resulted in an under/overriding and the total displacement of the crash partners increased. For that reason the intrusions increased in both crash partners. However, no trend could be observed regarding the position of the sub frame and an improved car-to-car crash performance, neither in the baseline nor in the reinforced configuration.
The analysis of the structural interaction of the PEAS/SEAS during the crash showed that the SEAS had a too small cross section to support penetrating structures properly. Thus the PEAS of the bullet vehicles slid between PEAS and SEAS of the modified and raised LFCs. But the vertical connection between PEAS and SEAS offered support, although the contact occurred relatively late in the impact due the large distance of this vertical link to the bumper beam (about 420mm, see Figure 11).

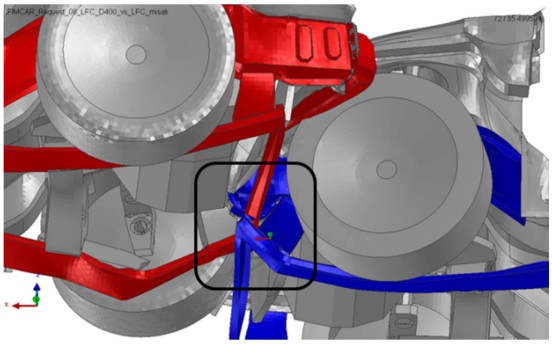

Figure 13. Contact between vertical connection and sub frame (D400 (red) vs. bullet vehicle (blue))

As highlighted in Figure 13 the results indicated that the vertical connection between the SEAS and the PEAS offered a good support to the penetrating structures. In almost every case the SEAS were not activated before they meet this part of the sub frame.

Summary of results of first modifications The simulations showed that the ORB test does not discriminated between appropriate (provides benefits in car-to-car crashes) and inappropriate SEAS. Thus the ORB test produces "false positives" which means that the test assesses a car structure as good while the car-to-car test showed no improvements in the structural interaction. Both full width tests showed their potential to detect a sub frame, especially SEAS which are located between 200mm and 300mm behind the bumper beam. However the FWRB clearly detected the SEAS although the forces were not measured within the first 15ms (before engine dump occurs) and although the SEAS modifications showed no benefit in car-to-car crashes. Thus the FWRB also produces false positives in terms of SEAS detection.
Because the main loads contributed by the SEAS in the FWRB tests occurred only in a relative short time ($\Delta t \approx 10ms$) an assessment of the SEAS performance is not possible compared to the FWDB tests ($\Delta t \approx 40ms$). In addition to an assessment of the forces within the first 40ms of the crash the FWDB also offers the potential to assess the energy absorbing capabilities of the SEAS over a significant period of the crash.
Because the results of the car-to-car simulations indicated that the vertical connection between PEAS and SEAS can bring benefits in car-to-car crashes additional modifications were done.

Second modifications In a second step the sub frame was modified as illustrated in Figure 14.

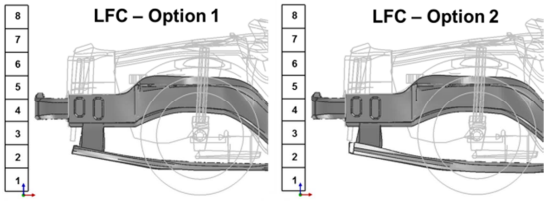

Figure 14. Second modifications of LFC SEAS

The second modifications were added to the D200 version (cross beam of the sub frame 200mm behind the bumper beam). The vertical connection was positioned 250mm behind the bumper beam (distance in the baseline configuration was about 420mm). Additionally the cross section of the cross beam was increased from 40mm to 60mm in vertical direction (LFC-Option 2). Both modification were also raised to align the PEAS with row 4.
Taking the results of the first modifications into account it was expected that the far forward located vertical conneting is able to catch the penetrating structures and that the increased cross section of the cross beam offers additional support to activate the EAS of the collision partner.
The LFC-Option 1 and Option 2 were based on the D200 modification so the ORB simulation was needless, because the D200 modification already passed the test.

FWDB simulations The FWRB simulation was not conducted, due to the relatively short assessment period. The LFCs were crashed against the FWDB with 50km/h.

Table 9.
LCW forces (up to 40ms) of FWDB simulations with raised LFC

	Baseline	Option 1	Option 2
F_{tot} [kN]	458	427	457
F4 [kN]	190	146	155
F3 [kN]	61	66	81
F2 [kN]	32	46	63
	fail	fail	fail

The results of the LCW forces of the FWDB simulations are summarized in Table 9, an overview about the force progression is given in the appendix. Compared to the baseline LFC the LFC-Option 2 was able to apply almost twice of the forces in row 2 within the first 40ms. The forces applied to row 3 also increased by 33% which could be related to the strong assembly of the far forward located vertical connection between PEAS and SEAS and the increased cross section of the cross beam of the sub frame.

Car-to-car simulations In the last step of this analysis the performance of the second modifications should be checked in car-to-car crash simulations. For this purpose the modified LFCs were raised by 70mm and crashed against the baseline LFC with 56km/h and a horizontal overlap of 50%, see Figure 15.

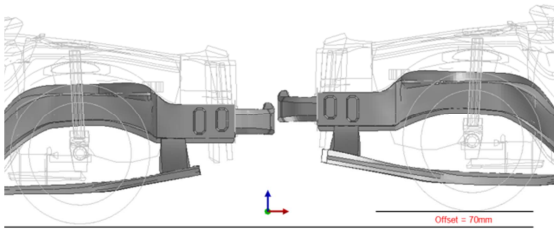

Figure 15. Car-to-car crash configuration with second modifications (baseline LFC - left and LFC-Option 2 - right)

As already described the analysis was performed regarding the deceleration-displacement curves and the intrusions. The results were compared to the car-to-car crash configuration LFC baseline vs. raised LFC baseline (misaligned).

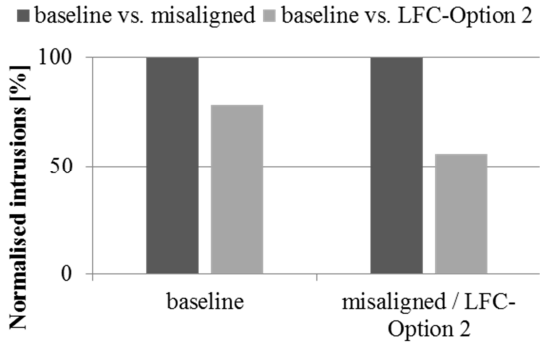

Figure 16. Normalised intrusions of car-to-car crash simulations (second modifications)

Figure 16 shows the improvement in the intrusion behavior. With respect to the baseline crash configuration the intrusions were reduced by almost 25% for the baseline LFC and by almost 50% for the LFC-Option 2. The reason for that is the improved structural interaction, see Figure 17, due to the activation of the sub frame.

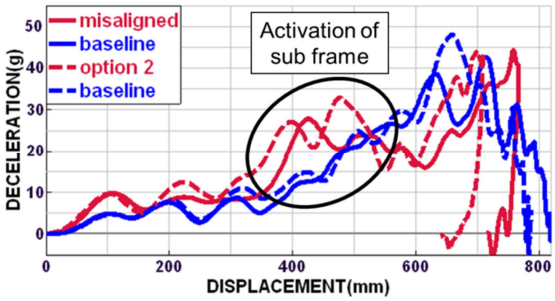

Figure 17. Deceleration-displacement curves (solid lines – baseline vs. misaligned, dotted lines baseline vs. LFC-Option 2)

A comparison of the red (modified) to blue (baseline) lines show that the decelerations increase earlier and reach a higher level (red dotted line) than in the misaligned configuration with the baseline SEAS (red solid line). The analyses of the crash performance of the LFC-Option 2 showed, that the SEAS modifications fulfilled their tasks to support the penetrating structures, which resulted in higher deceleration for the bullet vehicle too (blue dotted line at 650mm). Comparable trends could be observed for LFC-Option 1, however the benefit in the car-to-car crashes was higher due the increased cross section in option 2, which could be related to the increased stiffness of the sub frame.

Summary of results of second modifications
The second modifications of the SEAS were able to improve the car-to-car crash performance. The further forward vertical connection was able to catch the penetrating structures of the collision partner. In combination with an increased cross section of the SEAS cross beam, a relative large surface and high stiffness of the sub frame could be modelled which could partially compensate for the vertical misalignment between the PEAS. In addition the FWDB showed the potential to detect this type of SEAS. A clear trend could be observed showing the higher forces applied to the LCW due to the modified sub frame.
To promote SEAS structures and multiple load path designs, respectively, an assessment metric for the FWDB was developed within FIMCAR that should take into account forces applied in row 2. This should help cars to pass the test which were not able to bring down their PEAS into row 3 (e.g. SUVs). A limit reduction was introduced to reduce the minimum forces need to be applied to row 3 depending on the forces applied in row 2. But to reduce the limit at least 70kN needed to be applied in row 2 which was not the case for the simulations. The main reason for that was that the threshold of 70kN was identified in FW tests conducted with 56km/h. The finally proposed collision velocity was 50km/h which should lead to a lower criterion for the limit reduction. Therefore the forces applied by LFC-Option 2 could be enough to satisfy new minimum force requirements for row 3 and the vehicle may pass the test.

Crash simulations with other vehicle models

Chalmers and VTI had conducted an earlier study on the effect of sub frame on car-to-car impacts [11], [17]. These simulations indicated how modifications of the public available and detailed FE model of a Ford Taurus [4] affected the crash response.
In addition to the studies the modified Ford Taurus models were crashed against the FWDB. The objective was to check the correlation of the FWDB metrics to the car-to-car crash performance.

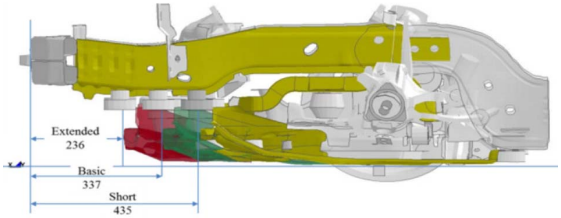

Figure 18. Sub frame modifications of Ford Taurus (based on [11])

The sub frame configurations investigated are shown in Figure 18. The basic sub frame is more than 300mm and the shortened sub frame is more than 400mm behind the bumper beam. The results of the car-to-car simulations were presented in [17]. What is significant to note is that the extended sub frame (Figure 18, red) tended to improve the vehicle performance while the shortened sub frame (Figure 18, yellow) tended to decrease the performance compared to the baseline vehicle.

FWDB simulations The FWDB tests were simulated with the Taurus in its raised conditions. (Based on the car-to-car simulations where the Taurus had a vertical offset of 25% - 25% of the vertical section height of the longitudinals were in contact.) The row loads calculated for the cases are shown in Figure 23 in the appendix. All three cases meet the FWDB metric. It can be seen that the shortened sub frame configuration case just meets the 100kN in row 3. The raised Taurus still has parts of its PEAS overlapping row 3 and this is enough to load this area of the barrier sufficiently for a positive evaluation. In contrast the row 2 loads show significant differences for the three Taurus configurations. Figure 19 shows a section cut of the three modifications at 40ms of the crash. Because the sub frame of the shortened sub frame (orange) did not contact the first layer of the crush element no significant forces were applied to the wall below row 3.

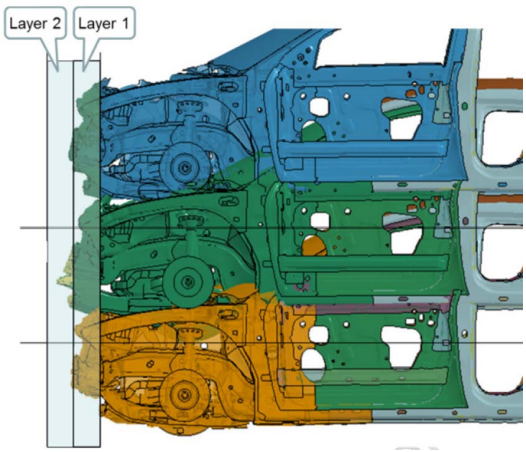

Figure 19. FWDB simulations with Ford Taurus modifications at 40ms (short sub frame – orange, baseline sub frame – green, extended sub frame - blue)

…..**Summary of results of Taurus modifications**
The results of the Taurus simulations showed that vehicles barely meeting the FWDB metric had poorer performance than those with higher loads in row 3 and 4. The results also showed that vehicles producing row 2 loads over 80kN were better than those with only 40kN in car-to-car crashes. The barrier was starting to detect sub frames 337mm behind the bumper beam and it was this region 300mm to 400mm that sub frames could be seen to introduce differences in car-to-car crash performance.

DISCUSSION

A general point that needs to be discussed is the limitation of the validity of the FEM models used for this study as well as the number and the type of the vehicles used for testing. However, in combination with test results of former research projects principle conclusions are possible.
Regarding the used FEM models two different types of model approaches can be distinguished with respect to the level of detail. On the one hand very detailed car models provided by NCAC were used to assess the specific design of crash structures and the corresponding crash performance in car-to-barrier and car-to-car crashes. Some simulations showed relevant differences between the original car and the corresponding model (e.g. brackets of Silverado) performance due to the fact that these models were not validated for these crash configurations. On the other hand there are the simplified PCMs which were used to investigate different structural concepts. The addition of a lower load path into an existing vehicle architecture will affect the stiffness level and therefore the force level of PEAS and SEAS should be adjusted. The modifications investigated in these studies did not take into account those effects. Another relevant issue is the simplified front end design of the PCMs. Regarding the FWB simulations, real cars often apply relevant loads into lower rows of the LCW even though they are not equipped with a SEAS. The PCMs only have energy absorbing structures (PEAS and SEAS) respectively load path creating structures (e.g. wheel-sill, engine-firewall). No other mechanisms that can create significant forces (such as radiator and battery support structures) loading the barrier or collision partner were included in detail. However, the conducted investigations show the influence and the potential of different SEAS designs as well as the presence of a lower load path.

CONCLUSIONS

The main objectives of this study were to analyse the influence of SEAS in car-to-car crashes and to identify characteristics of a SEAS that contribute positively in a car-to-car crash. Furthermore the capability of different test procedures was investigated regarding their potential to assess appropriate SEAS correctly.
Based on the test series conducted within VC Compat and FIMCAR the improvement of structural interaction due to the presence of SEAS in case of vertical misaligned PEAS was verified. In almost every case an improved interaction of the EAS resulted in an increase of the compartment decelerations and in a reduction of the intrusions (in particular for the overriden car), except the case if the compartment was overloaded due to a disadvantageous mass ratio of the crash partners. Simultaneously improved structural interaction also means that a transfer of injury causalities from “contact by intrusions” to occupant protection systems or “contact without intrusions” may occur. Furthermore in car-to-car crashes with different mass ratios the stiffness level of the front end structures become more relevant if the EAS are in alignment and will be activated in the crash. Finally the following priorities for structural interaction were made:

1) Cars with aligned PEAS show better results than misaligned.
2) Vehicles with PEAS aligned in row 3 and row 4 were more stable when equipped with a lower path.
3) Vehicles with PEAS in row 4 performed well if a SEAS was identified in FWDB metric in row 3 and/or row 2.
4) FWDB metric assessment of well performing SEAS readings regarding car-to-car crash results was always positive.

The simulations identified some geometrical characteristics of SEAS that help to improve the car-to-car crash performance. The main factor that

had a positive influence was the distance between SEAS and bumper beam. The simulations with the modified Ford Taurus showed that the contribution of the SEAS in car-to-car crashes is positive if it is located no more than 230mm behind the bumper beam. A distance of about 400mm resulted in negative effects. However, the PCM simulations showed that not only the position in longitudinal direction was crucial for a good crash performance. Other important factors were the height of the cross section of the SEAS cross beam and the position of the vertical connection to the PEAS. A connection positioned about 250mm behind the bumper beam was able to activate penetrating structures which resulted in an improved car-to-car crash performance.
To assess appropriate SEAS three different test procedures were evaluated. The ORB test proposed by NHTSA to evaluate the performance of Option 2 vehicles seems not to be suitable to discriminate between appropriate and inappropriate SEAS. Previous studies and the conducted simulations showed that the assessment of the ORB does not correlate with a good car-to-car crash performance. Within FIMCAR two full width tests were proposed to assess structural alignment. Both candidates were also evaluated regarding their potential to assess SEAS that bring benefits in car-to-car crashes. Due to the very short time window for the assessment of EAS (FWRB: 10ms to 15ms; FWDB: 40ms) the FWRB is not suitable for the assessment of SEAS, because the simulations showed that the SEAS starts to load the barrier after 20ms even in the case where the SEAS was in the most forward position. Furthermore the progression of the loads applied by the SEAS is a relative short peak, which makes the assessment of the performance difficult. In contrast the FWDB was able to detect and correctly assess the SEAS that improved car-to-car crash performance due to their longer assessment period. In addition the SEAS loaded the barrier for a longer period and maintained a relative high level.

ACKNOWLEDGEMENT

The paper is based on research results of the FIMCAR project. The FIMCAR project is co-funded by the European Commission under the 7th Framework Programme (Grant Agreement no. 234216). The members of the FIMCAR consortium were: Technische Universität Berlin, Bundesanstalt für Straßenwesen. Chalmers tekniska hoegskola AB, Centro Ricerche Fiat S.C.p.A., Daimler AG, FIAT Group Automobiles Spa, Humanetics GmbH, IAT Ingenieurgesellschaft für Automobiltechnik mbH, IDIADA Automotive Technology SA, Adam Opel AG, Peugeot Citroën Automobiles SA, Renault s.a.s, TNO, TRL Limited, UTAC, Volvo Car Corporation, Volkswagen AG, TÜV Rheinland TNO Automotive International BV.
Further information is available at the FIMCAR web site www.fimcar.eu.

REFERENCES

[1] "*Developments of Criteria and Standards for Vehilce Compatibility (EUCAR - Final Technical Report)*". 2000.

[2] "*EEVC WG 15 Final Report to EEVC Steering Committee*". www.eevc.org.

[3] "*Generic car (FE) models for categories super minis, small family cars, large family / executive cars, MPV, heavy vehicle (APROSYS Deliverable D7.1.4 A)*".

[4] "*NCAC - Finite Element Model Archive*". http://www.ncac.gwu.edu/vml/models.html.

[5] Adolph, T. Wisch, M.; Edwards, M.; Thomson, R.; Stein, M.; Puppini, R.:"*D3.1 - Report analysis performed to develop assessment criteria and associated performance limits for full width test*".

[6] Barbat, S.: "*Status of Enhanced Front-to-Front Vehicle Compatibility Technical Working Group Research and Commitments*". 19th Enhanced Safety Vehicle Conference 2005. Paper Number: 05-463. Washington D.C. 2005.

[7] Edwards, M. Coo, P. de; van der Zweep, C.; Thomson, R.; Damm, R. M. T.; Delannoy, P.; Davis, H.; Wrige, A.; Malczyk, A.; Jongerius, C.; Stubenböck, H.; Knight, I.; Sjoberg, M.; Ait-Salem Duque, O.; Hashemi, R.:"*Improvement of Vehicle Crash Compatibility through the Development of Crash Test Procedures (VC-Compat - Final Technical Report)*". 2007.

[8] Faerber, E.: "*EEVC Approach to Develop Test Procedures for the Improvement of Crash Compatibility between Passenger Cars*". 20th Enhanced Safety Vehicle Conference 2007. Paper Number: 07-0331. Lyon. 2007.

[9] Johannsen, H. Adolph, T.; Thomson, R.; Edwards, M.; Lazaro, I.; Versmissen, T.: "*FIMCAR - Frontal Impact and Compatibility Assessment Research - Strategy and first results for future frontal impact assessment*". 22nd Enhanced Safety Vehicle Conference 2011. Paper Number: 11-0286. Washington D.C. 2011.

[10] Johannsen, H. Adolph, T.; Edwards, M.; Lazaro, I.; Versmissen, T.; Thomson, R.:

"*Proposal for a Frontal Impact and Compatibility Assessment Approach based on the European FIMCAR Project*". 23rd Enhanced Safety Vehicle Conference. Paper Number: 13-0104. Seoul. 2013.

[11] Park, C.-K. Thomson, R.; Krusper, A.; Kan, C.-D.: "*The Influence of Sub-Frame Geometry on a Vehicle's Frontal Crash Response*". 21st Enhanced Safety Vehicle Conference 2009. Paper Number: 09-0403. Stuttgart. 2009.

[12] Patel, S. Prasad, A.; Mohan, P.: "*NHTSA's Recent Test Program on Vehicle Compatibility*". 21st Enhanced Safety Vehicle Conference 2009. Paper Number: 09-0416. Stuttgart. 2009.

[13] Sandqvist, P. Thomson, R.; Kling, A.; Wågtröm, L.; Delannoy, P.; Vie, N.; Lazaro, I.; Candellero, S.; Nicaise, J.-L.; Duboc, F.:"*D6.1 - Report on car2car test results*".

[14] Stein, M. Johannsen, H.; Puppini, R.: "*FIMCAR Models for the Assessment of Frontal Impact Compatibility*". ICrash Conference 2012. Mailand. 2012.

[15] Stein, M. Friedemann, D.; Eisenach, A.; Zimmer, H.; Johannsen, H.: "*Parametric Modelling of Simplified Car Models for Assessment of Frontal Impact Compatibility*". 8th LS Dyna User Conference. Strasbourg. 2011.

[16] Tanaka, Y.:"*Japanese Test Plan for Full Frontal Impact*". 16th meeting of the GRSP Informal Group on Frontal Impact. Paris. 10.11.2012. https://www2.unece.org/wiki/download/attachments/4064596/FI-16-04e.pdf.

[17] Thomson, R. Krusper, A.; Avramov, N.; Rachid, K.: "*The Role of Vehicle Design on Structural Interaction*". ICrash Conference 2008. Kyoto. 2008.

[18] Yonezawa, H. Mizuno, K.; Hirasawa, T.; Kanoshima, H.; Ichikawa, H.; Yamada, S.; Koga, H.; Yamaguchi, A.; Arai, Y.; Kikuchi, A.: "*Summary Activities Compatibility Group Japan*". 21st Enhanced Safety Vehicle Conference 2009. Paper Number: 09-0203. Stuttgart. 2009. http://www-nrd.nhtsa.dot.gov/departments/esv/21st/.

APPENDICES

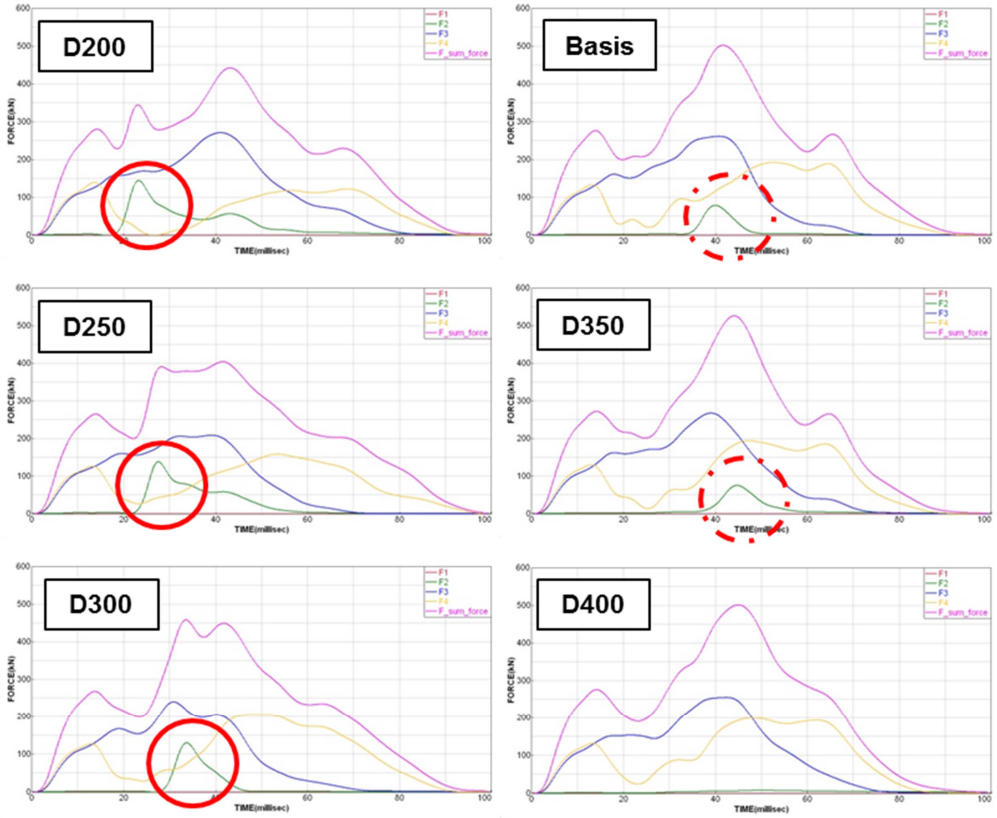

Figure 20. LCW sum forces of FWRB simulations (first modifications)

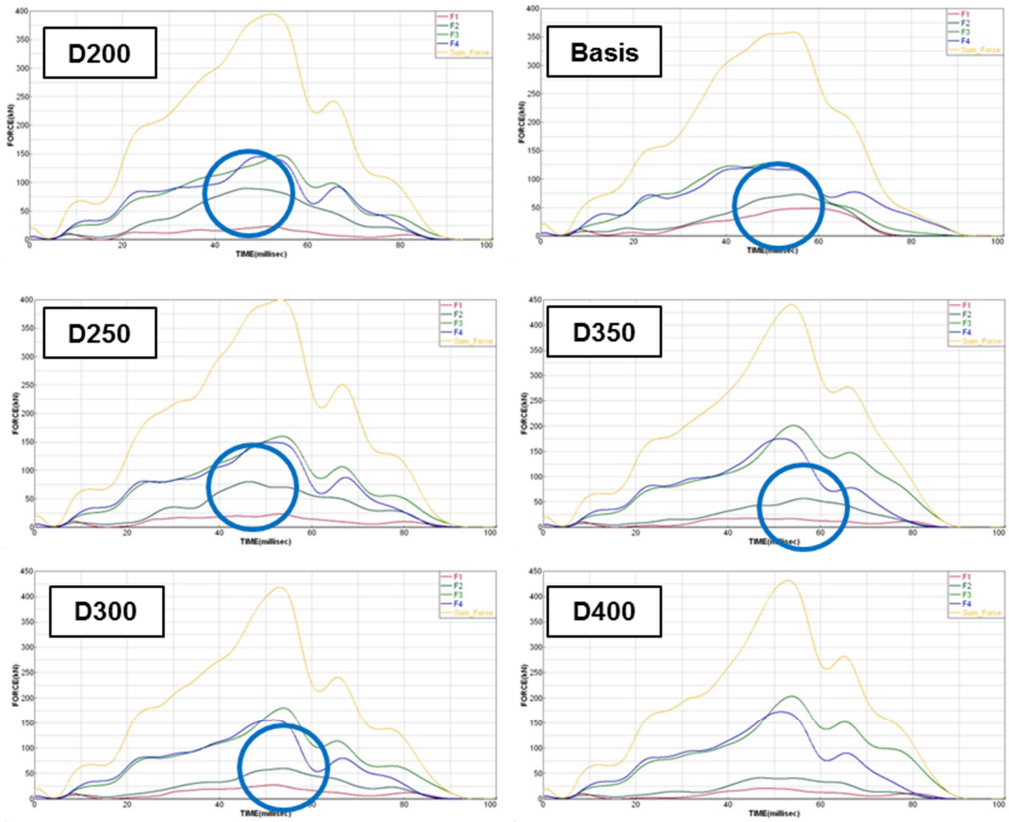

Figure 21. LCW sum forces of FWDB simulations (first modifications)

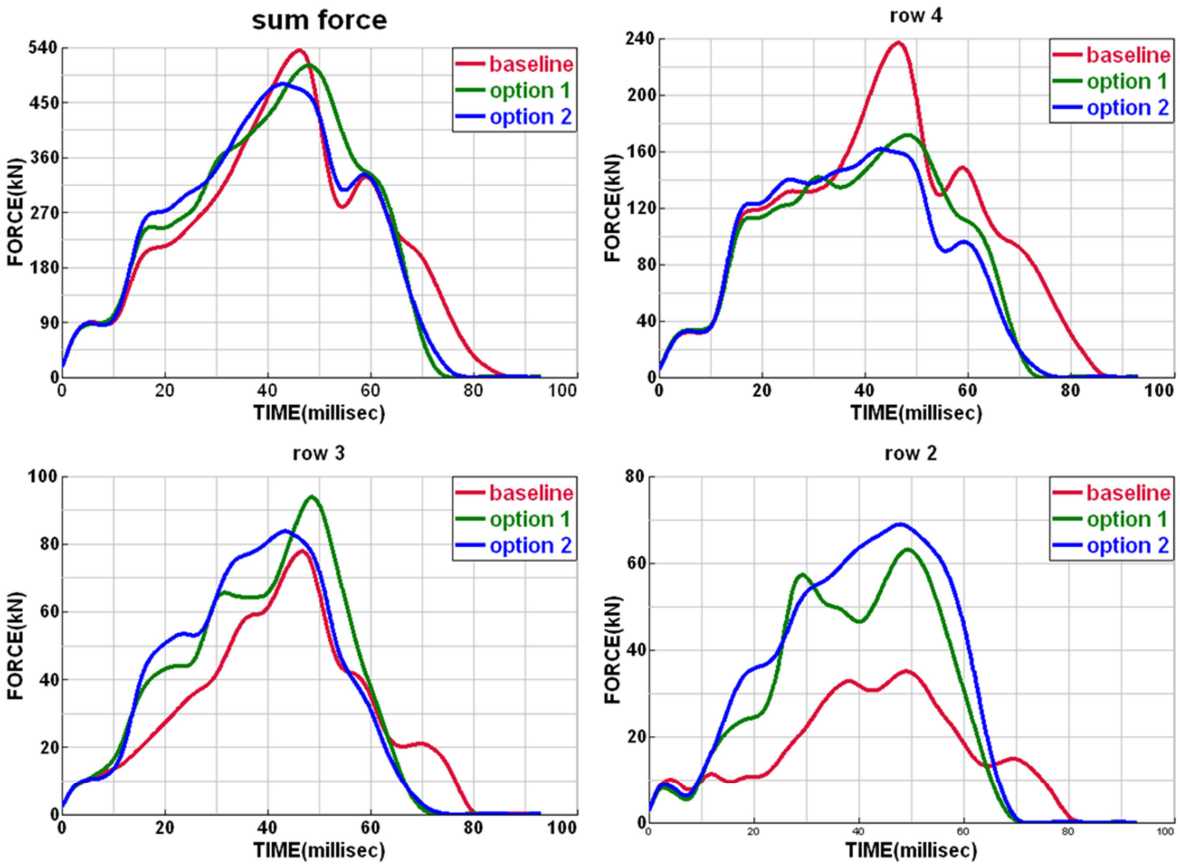

Figure 22. LCW sum forces of FWDB simulations with raised LFCs (second modifications)

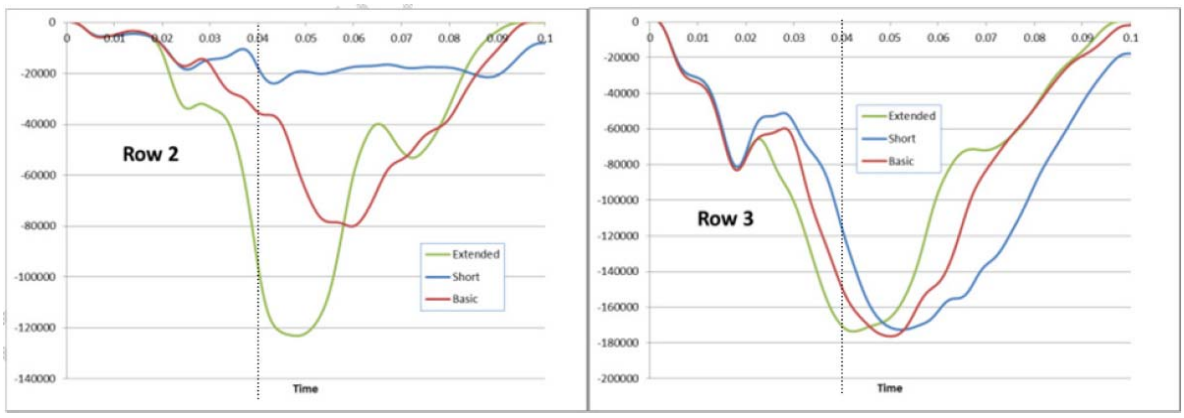

Figure 23. LCW row forces in FWDB Ford Taurus simulations

OCCUPANT AND VEHICLE RESPONSE FOR OFFSET POLE CRASH SCENARIOS

Donata Gierczycka-Zbrozek
Visiting Scholar at University of Waterloo, from Warsaw University of Technology
Poland
Duane Cronin
Phil Lockhart
Brock Watson
University of Waterloo
Canada
Paper Number 13-0435

ABSTRACT

Vehicle impacts with fixed roadside structures, such as poles, constitute a significant portion of road fatalities in North America. The purpose of this study was to evaluate occupant response in pole crash scenarios for varying offsets, and to compare the current occupant-based metrics with vehicle-based. A Hybrid III ATD was integrated with a mid-size sedan equipped with seatbelts and airbag. Impacts with deformable and rigid poles were investigated. The predicted response was higher for the rigid pole, and varied significantly with offset from the vehicle centreline.

INTRODUCTION

Vehicle impact with fixed roadside structures can result in significant occupant injury. In 2009, the Fatality Analysis Reporting System (FARS, NHTSA) reported 1759 fatalities resulting from crashes involving poles (National Highway Traffic Safety Administration FARS, 2011). Recent work has demonstrated that offset impacts (offset from the vehicle centreline) may result in different vehicle and occupant kinematics compared to central impacts (Lockhart et al., 2012). The goal of this study was to apply previously developed coupled vehicle, occupant, restraint and pole structure models to investigate occupant kinematics and the potential for head and chest injury in offset crash scenarios. This study is an extension of research performed by Lockhart et al. (2012).

METHODS

A detailed human surrogate model (Hybrid III v7.1.6 50th percentile male, Humanetics Innovative Solutions Inc.) was integrated with a seat model and restraint system into a mid-sized sedan (2001 Ford Taurus, NCAC) and validated using NHTSA frontal crash tests. The energy absorbing pole and rigid pole models were developed, validated against a physical pendulum test, and coupled with the vehicle-occupant model (Lockhart et al., 2012). The impact location was varied left (driver side) and right (passenger side) from the vehicle centreline at impact velocities of 50 and 70 kph. The current North American Test standard (Ross et al., 2007) uses different test levels (weight and initial velocity of the vehicle) depending on the application of the roadside structure. The range of test vehicle weights is 700, 820 or 2000 kg with an initial velocity of 30, 50, 70 or 100 kph. Occupant response was investigated by calculating the potential for head injury (HIC_{15}) and thorax injury (chest compression).

Rigid pole model

The rigid pole (Figure 1) was modeled as a column of hexagonal cross-section with a major diameter of 330mm (Ontario Provincial Standard Specification, 2010), attached rigidly to the ground. Steel material properties were used for contact purposes only and the pole did not deform during the impact. The model consisted of 25,200 shell elements.

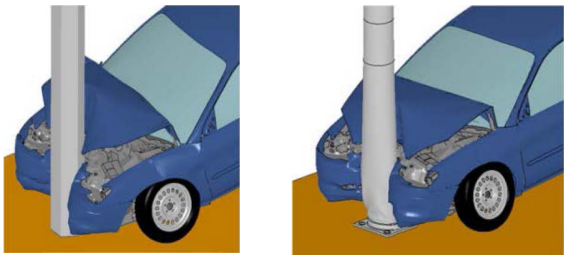

Figure 1. Rigid [Left] and deformable [Right] pole impact**.**

Energy absorbing pole model

The energy absorbing pole was modeled as a 12.34m high tapered column with 7 sections, and fixed to the ground (rigid) with a 12.7mm thick base plate and four deformable bolts (Figure 1). The nominal diameter was 329mm in the impact zone and the mesh comprised 215,344 solid elements and 33,280

shell elements, 10x10mm in size in the impacted area. An incremental plasticity material model with isotropic hardening was used. The material model was rate independent following the model validation given by Lockhart et al. (2012).

Vehicle, restraint system and occupant models

The vehicle model used for this study was a 2001 Ford Taurus mid-sized sedan (1,057,113 elements), developed by NCAC (Opiela, 2008) and validated under frontal impact conditions. The model was enhanced to include a seat and restraint system and was validated using available NHTSA frontal impact crash data (Lockhart et al., 2012).

The 50th percentile Hybrid III ATD was positioned in the seat during a separate simulation, prior to the crash simulation, to achieve an equilibrium position with the ATD. The seat foam was pre-compressed and integrated with the standard seat frame. The ATD was then coupled with a restraint system including a single stage airbag, seatbelt with a pre-tensioner (60mm in 7.5 ms) and a 6 kN force limiter. Two-dimensional shell elements were used for the seatbelt sections in contact with the ATD and 1-D elements were used for the parts of the belt that were outside the contact zone. The belt was fit to the occupant using a pre-processor fitting option (LS-PrePost, LSTC, Livermore, CA).

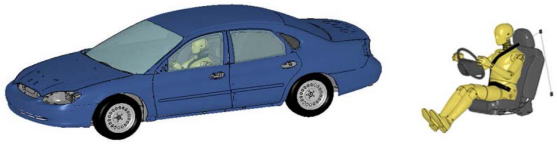

Figure 2. ATD seated in the car and coupled with the restraints.

Impact at the vehicle centreline (0mm offset, Figure 3) was the reference case, and the pole location was varied symmetrically on both sides of the centerline. The 570mm offset case was aligned with the vehicle axial crush structures.

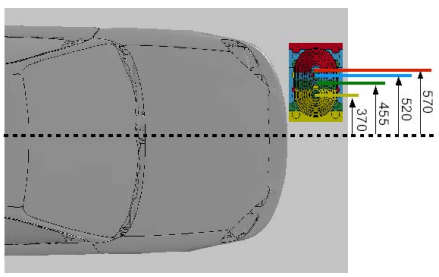

Figure 3. Offset locations from the vehicle centreline (top view, driver side shown for clarity).

Offsets outboard of the crush structure were also considered; however, this scenario requires further investigation and model development to verify the interaction with the vehicle tire, wheel and suspension during the impact. Therefore, the injury assessment for these offsets is not included in this paper. All the offset simulations were performed for both deformable and rigid pole and relevant results are presented.

Injury criteria

The injury criteria considered were HIC_{15} and chest compression. HIC_{15} and chest compression were used according to the Canadian Motor Vehicle Safety Standard (CMVSS) 208 Protection Criteria for Frontal Impact Tests. Future studies will consider the knee-thigh-hip (KTH) injury criteria to assess lower extremity response.

Head injury risk was evaluated using the HIC_{15} criterion calculated based on the resultant head CG acceleration over a 15ms duration. The threshold values determined by US and Canadian federal regulations are given in Table 1. The threshold value of 700 corresponds to 31% probability of a skull fracture for a 50th percentile male (Schmitt, 2010).

Chest injury risk was evaluated based on chest compression measured as the maximum deflection between the spine and the sternum of the ATD. A CC value equal to 50mm (Transport Canada threshold) corresponds to a 50% probability of the serious (AIS 3+) chest injury.

Table 1.
Occupant-based criteria for the 50th percentile male

Federal code	Head injury criterion	Chest injury criterion
FMVSS 208	HIC_{15}<700	CC<63mm
CMVSS 208	HIC_{15}<700	CC<50mm

Vehicle based metrics

A vehicle-based metric, recommended by the National Cooperative Highway Research Program (NCHRP) 350 report, was used in this study. The Occupant Ride Down Acceleration (RA) has a maximum value of 20.49 G and preferred limit

of 15 G. This value is determined from the centre of gravity of the vehicle, where acceleration data was filtered with a 10ms moving average in accordance with the NCHRP 350 report. Another vehicle-based metric, Occupant Impact Velocity or OIV, was not investigated in this study since previous work has shown that this value produces very different results and trends compared to the occupant-based metrics.

RESULTS

The occupant injury metrics are presented for both rigid and deformable poles at different offsets for the 50 kph impact speed (Figures 4 and 5). The negative offset values correspond to the passenger side, and positive offset values correspond to the driver side.

HIC_{15} values did not exceed the threshold of 700 for the 50 kph impacts. For the deformable pole, the highest HIC value was predicted for a 370 mm offset from the vehicle centreline on the driver side. The rigid pole impacts result in higher values of HIC and the peak was shifted to the passenger side, at 370mm offset. The difference in HIC_{15} value for the centerline impact was significant between the rigid and deformable poles (373 versus 78).

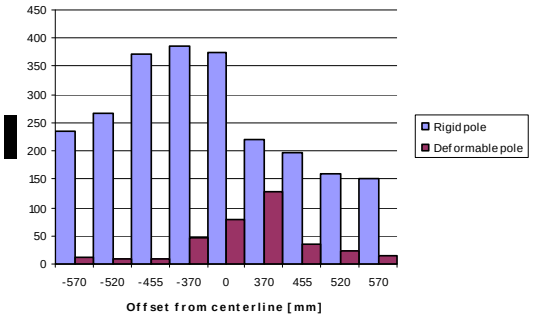

Figure 4. Head Injury Criterion values at different offsets for both pole types at 50kph impacts.

The chest compression values for the deformable pole were symmetric about the vehicle centreline, while the values were higher for the passenger side offsets in the rigid pole impacts (Figure 5).

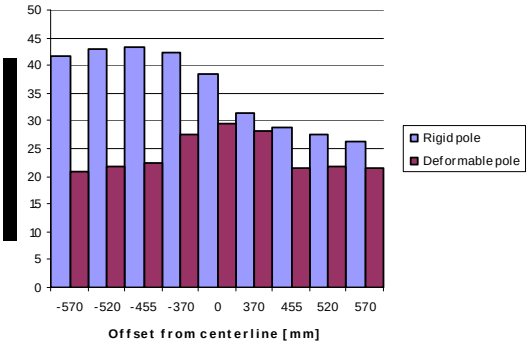

Figure 5. Chest compression values at different offsets for both pole types at 50kph impacts.

DISCUSSION

The occupant and vehicle injury metrics were normalized using the threshold values (Table 1) for comparison.

For the deformable pole, the predicted occupant response depended on the offset location. The maximum HIC_{15} value was predicted for the 370mm driver side offset while the chest compression values were highest for the vehicle centreline, from 370mm passenger to the 370mm driver offset (Figure 6). In all cases, the injury criteria values decreased when the pole was aligned with the vehicle crush structure. For 70 kph impacts (Figure 7), similar trends were noted; however both HIC_{15} and chest compression values were lower since the pole sheared off at the base with a reduced effect on the vehicle kinematics.

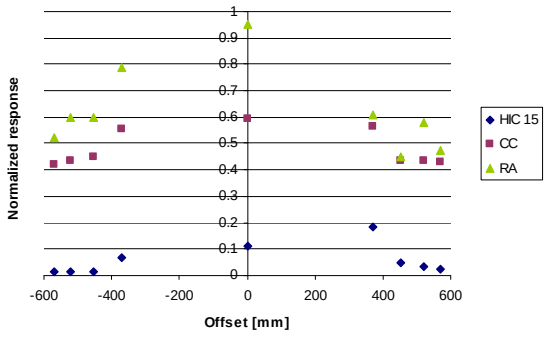

Figure 6. Normalized occupant and vehicle metrics – deformable pole at 50kph.

The vehicle based injury metric (Ride Down Acceleration or RA, Figure 6) was normalized using the threshold value of 20.49 G and compared to the occupant based metrics trends (Figure 6). The RA values over-predicted injury, compared to the occupant based metrics. The highest RA values were

measured for the vehicle centreline and decreased when the offset moved towards the crush structures on either side.

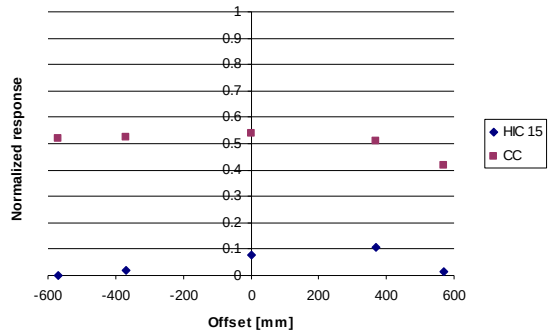

Figure 7. Normalized occupant metrics – deformable pole at 70kph.

For the rigid pole impacts at 50 kph, the passenger side offsets resulted in higher predicted injury risk (Figure 9) compared to the deformable pole. The maximum value of chest compression was predicted when the impact location was aligned with the vehicle crush structure on the passenger side and the maximum value for the HIC_{15} was predicted for the 370mm offset on the passenger side. Both criteria predicted decreased injury risk when the impact moved towards the vehicle crush structure on the driver side where the responses were a minimum. The increase in response for passenger-side impacts was related to the occupant kinematics and interaction with the seatbelt (Figure 8).

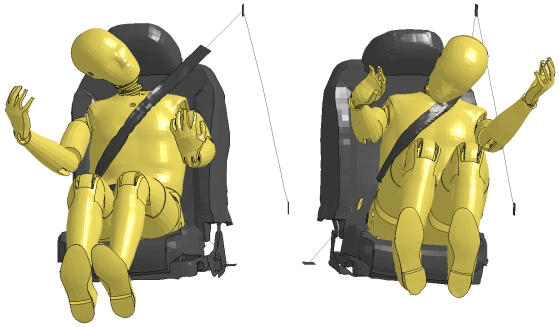

Figure 8: Comparison of the occupant kinematics for the 520mm passenger [Left] and 520mm driver side [Right] rigid pole offset impact at the final stage of the simulation (160ms). Front view.

For driver side offsets, the shoulder belt slid upwards towards the neck and led to a decrease in the chest compression value. For passenger side offsets, rotation of the vehicle caused higher belt loads on the occupant leading to higher chest compression and increased head acceleration values, particularly in the lateral direction, leading to higher predicted HIC_{15} values. The 70 kph rigid pole simulations terminated early due to the aggressive nature of the impact; however, the data available for the limited simulation time suggests that the occupant and vehicle-based injury metrics would be exceeded in all cases.

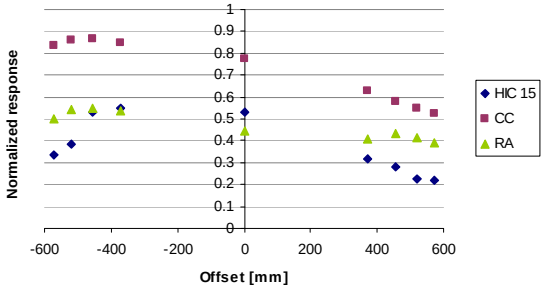

Figure 9. Normalized occupant and vehicle metrics – rigid pole at 50kph.

The RA trend (Figure 9) was in reasonable agreement with the trends for HIC_{15} and CC. The highest values were measured for the passenger side offsets and decreased when the impact moved towards the crush structure on the driver side.

CONCLUSIONS

The predicted response and injury risk for frontal pole impacts was found to depend on the impact location relative to the vehicle centreline. In general, impacts that were directly aligned with a vehicle crush structure resulted in the lowest predicted response for HIC_{15} and chest compression. Trends with offset distance were consistent between 50 and 70 kph impacts with the deformable pole, with the maximum response occurring for impacts located between the vehicle crush structures. The maximum response for the rigid pole impacts was predicted for offsets on the passenger side of the vehicle, attributed to vehicle rotation and occupant interaction with the shoulder belt. The vehicle-based metric, Ride Down Acceleration, was comparable to the occupant metrics for the rigid pole, but over-predicted injury for the deformable pole. The deformable pole resulted in lower levels of predicted injury compared to the rigid pole for the impact scenarios investigated in this study.

LIMITATIONS OF THE STUDY

A standard seating position was considered in this study. Future studies should also consider the effect of occupant position on predicted response. The simulations were run for 200ms, which covers initial contact between the pole and the vehicle as well as between the ATD and vehicle interior; however, secondary impacts between the ATD and vehicle interior or between the vehicle and surrounding structures were not considered. A standard mid-sized sedan was used for this study which represents only part of the car fleet in terms of the mass and geometry. The maximum impact speed was limited by the available validation data for the numerical models.

ACKNOWLEDGMENTS

The authors would like to acknowledge Polefab Inc., Humanetics Innovative Solutions and the National Crash Analysis Center for the use of their numerical models in this work and NHTSA for providing the validation data.

REFERENCES

Humanetics Innovative Solutions, Inc. 2010. H350 Adult Dummy Model LS-Dyna. Release Version 7.1.6.

Lockhart, PA, Cronin, DS, Watson, B. 2012. "Frontal Impact Response for Pole Crash Scenarios." Traffic Injury Prevention, 2012.
DOI 10.1080/15389588.2012.732718

National Crash Analysis Center. Finite Element Model Archive. Available at:
http://www.ncac.gwu.edu/vml/models.html.
Accessed June 3, 2011.

National Highway Traffic Safety Administration FARS. Fatality Analysis Reporting Reporting System Encyclopedia. Available at
http://wwwfars.nhtsa.dot.gov/QueryTool/QuerySection/CaseListingReport.aspx. Accessed November 20, 2011.

Ontario Provincial Standard Specification. 2010. "Material Specification for Steel Poles, Base Mounted." OPSS 2423.

Opiela KS. 2008. Finite element model of Ford Taurus. NHTSA Finite Element Model Archive. Available at:
http://www.ncac.gwu.edu/vml/archive/ncac/vehicle/taurus-v3.pdf. Accessed June 3, 2011.

Ross HE Jr, Sicking DL, Zimmer RA, Michie JD. 2007. "Recommended Procedures for the Safety Performance Evaluation of Highway Features." Washington, D.C. National Cooperative Highway Research Program.

Schmitt K, Walz F. 2010. "Trauma Biomechanics Accidental Injury in Traffic and Sports." 3rd ed. Heidelberg: Springer.

Transport Canada. "Occupant Restraint Systems in Frontal Impact (Standard 208)." Available at: http://www.tc.gc.ca/eng/acts-regulations/regulations-crc-c1038-sch-iv-208.htm. Accessed December 10, 2011.

US Dept. Of Transportation. 2012. "Standard No. 208; Occupant crash protection." Federal Motor Carrier Safety Administration,. Available at:
http://www.fmcsa.dot.gov/rules-regulations/administration/fmcsr/fmcsrruletext.aspx?reg=571.208. Accessed June 15, 2012

IMPACT OF DRIVER ASSISTANCE SYSTEMS ON SAFETY AND REPAIR

Helge Kiebach
KTI GmbH & Co. KG
Germany
Paper Number 13-0418

ABSTRACT

Driver assistance systems, such as autonomous pre-crash braking systems can reduce the impact velocity (particularly the impact energy) or can even avoid the crash completely. Thus, by reducing the impact speed in order to decrease the number of serious accidents, the subsequent repair costs of the crashed vehicle can also be lowered. However, the testing and assessment of new cars still involves using tests which do not take into account the significant additional potential of integrated safety measures.

In order to investigate the differences during crashes as a consequence of altered kinetic energy at the vehicle front, KTI teamed up with DEKRA and BMW to carry out joint crash tests with the latest BMW 5 series vehicles. The vehicles involved braked automatically from 64 km/h initial test velocity down to different impact speeds.

The paper will describe and discuss some relevant details and results of the crash tests regarding passenger safety and repair costs.

INTRODUCTION

In the last decade, automatic braking and pre-crash occupant positioning systems are offered by an increasing number of automobile manufacturers firstly in their high class vehicles. And now the new systems find their way into all vehicle classes.

The main effects of pre-crash braking are the reduction of velocity and kinetic energy before the car hits the impact barrier. This reduces the biomechanical occupant load and the extent of damage on the car. In addition, the pre-crash-system activated reversible belt pretensioner limits the forward displacement of the driver and passenger dummy during the pre-crash-braking phase to a small extent until the impact starts. Thereby, the occupant safety can additionally be improved.

First results of a test using a pre-crash braked BMW 5 are given in [1]. This paper includes results of two additional tests using the same car model.

TEST VEHICLES

In all tests conducted the vehicle used was a BMW 5 series (type F10/F11) with inline six-cylinder diesel engine and rear wheel drive. The non-braked car for the typical Euro NCAP frontal impact was equipped with standard features.

The autonomous braked cars was, in addition to other serial and prototype safety systems, fitted with the currently available active speed control system including Stop&Go function and an additional head-on collision warning with braking function. It is a radar-based speed and distance regulation system. The system can also monitor the traffic environment in front of the vehicle if the conventional speed control system is not activated. When a critical head-on situation is detected, the driver is warned in two stages. If the risk of a head-on collision situation is very high, an intense visual-acoustic warning is additionally activated that initiates an automatic partial braking with a deceleration of 3 m/s². This means the speed is already being reduced during the driver's reaction time. If the driver reacts, he already encounters a pre-filled brake and swiftly reaches full deceleration – with the aid of the brake assistant – when depressing the brake pedal. This equipment, which is currently found on production models, was taken as a basis for the development of a prototype front safety system, which finally fulfils the requirements for tests in the laboratory crash-test hall. This means that it was first assured that the radar sensor can also reliably detect the target object (in this case the barrier). It is essential that this detection is assured despite the difficult conditions prevailing in the test hall. The vehicle was still equipped with electromotive reversible belt retractors for both driver and front passenger. A pre-crash deactivation of the fuel pump was envisioned as well.

CRASH TESTS

The tests were run by the new intelligent drive system at the DEKRA crash test facility. This required several modifications to be made to the test facility as well as to the vehicle.

The test set up followed the Euro NCAP frontal impact configuration. This is an offset crash test with 40% overlap against a deformable barrier and Hybrid III 50th percentile male dummies on the driver's and passenger's seats. The collision speed is given at 64 km/h. This speed was chosen as the initial speed for the autonomous braking. The cars brake then with different braking scenarios. As consequence of this, the impact speeds was reduced to 51 and 38 km/h.

For comparison, a similar car was crashed without the activation of an active safety system (impact speed 64 km/h). The test set-up is shown in Figure 1.

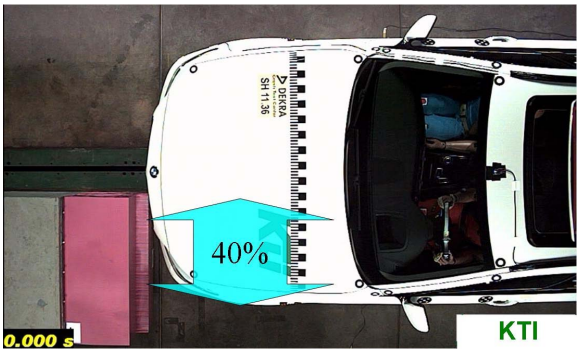

Figure 1. Impact position with 40% overlap.

Approaching the barrier the sensor detected the obstacle and the full braking power was automatically triggered 0.9 seconds before the impact. The collision speed was reduced to 51 and 38 km/h. The collision energy was, thus, reduced from 343kJ to 215kJ respectively 112kJ. The reductions of kinetic energy in the pre-crash phase for each test vehicle are shown in Table 1.

Table1.
Mass, impact velocity and kinetic energy of the test vehicles at start and end of the pre-crash phase

Test	Mass of vehicle	Impact velocity	Kinetic energy
1	2,164 kg	64 km/h	343 kJ
2	2,164 kg	51 km/h	215 kJ
3	2,072 kg	38 km/h	112 kJ

OCCUPANT SAFETY

Basically, reductions in speed and the kinetic energy of the vehicle during the impact with the block must also be reflected in correspondingly reduced load values on the dummy occupants. The tested vehicle (BMW 5 series) has already demonstrated very good results, achieving a top score (5 stars) in a conventional EuroNCAP crash test at 64km/h impact speed [2].

Figure 2 illustrates the results for the head injury criterion (HIC36) for the driver and front passenger dummies in the tests. These injury numbers are greatly reduced when compared to the EuroNCAP test at 64 km/h impact velocity. The reduction in the case of impact at 51 km/h for the driver dummy and the front passenger dummy is 42% and 36%, respectively. For the impact velocity of 38 km/h, there was a reduction of the HIC36 numbers of 76% and 78% for the driver and passenger, respectively.

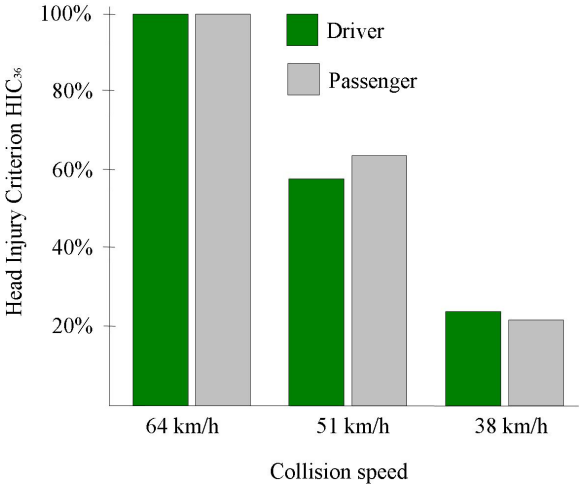

Figure 2. Relative values of the HIC.

It is worthy of note that the reduction of the maximum resultant head deceleration is less significant over a duration of 3 ms (a3ms) as shown in Figure 3. Apparently, at the low load value given here, which is well below the associated biomechanical maximums, the HIC36 values better reflect the reduced load of the head than the a3ms values.

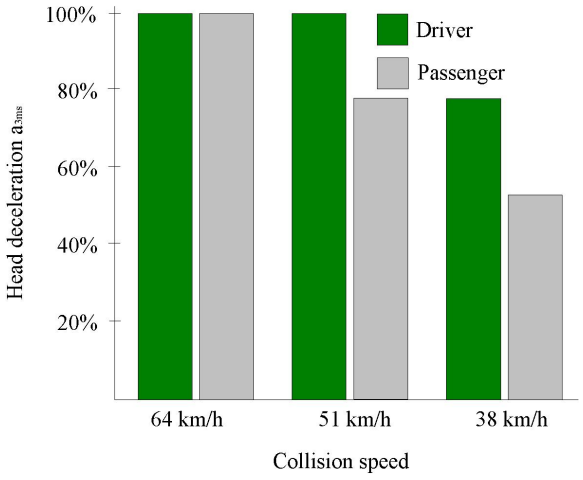

Figure 3. Relative values of the resultant head deceleration.

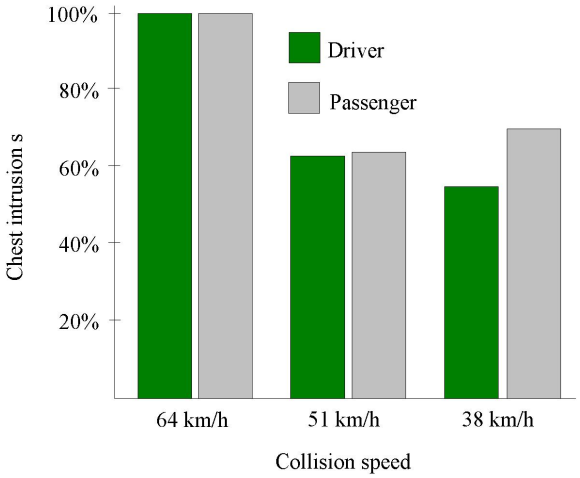

Figure 4. Relative values of the chest intrusion.

A considerable reduction of the dummy chest load in the tests involving pre-crash braking very clearly show the data recorded for chest intrusion (see Figure 4). The values of the resultant chest deceleration a3ms also fail to adequately reflect the reduction of this low load level (see Figure 5).

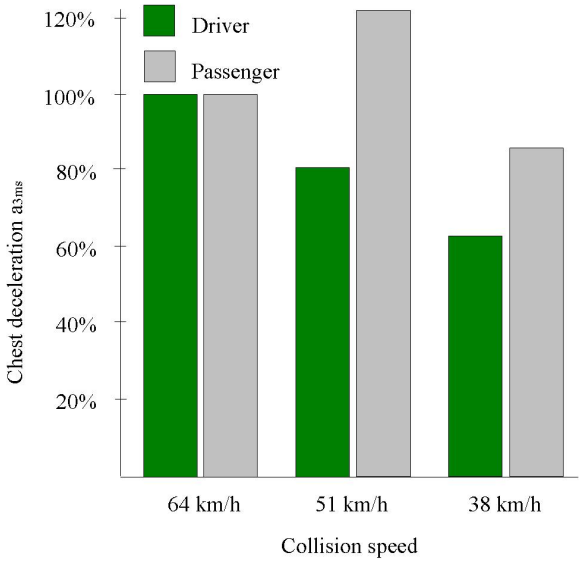

Figure 5. Relative values of the chest deceleration.

VEHICLE DEFORMATIONS

Figure 6 shows a comparison of the front deformation of three test vehicles. In particular, the area around the left front wheel shows a significantly lower deformation of the vehicle, which was involved in a crash test with pre-crash braking at a resulting impact speed of 38 km/h.

Figure 6. Comparison of the deformation of the front of the test vehicles (top down: 64, 51 and 38 km/h impact speed).

The results showed the effectiveness of a pre-crash braking system. The vehicle damage could clearly be reduced due to the reduction of impact speed. The damages on all cars were analyzed. It turned out that the car at 64 km/h impact suffered damage, among other things, on the front bulkhead, A-pillar, windscreen, right side member and left front door.

At 50 km/h impact speed, there are less significant intrusion. The frontleg is deformed and it's necessary to be replace completely this part (up to the passenger compartment). The drive shaft channel damaged but the engine block and gearbox not damaged.

At an impact velocity of 38 km/h, the car has less significant intrusion. The frontleg is damaged and in addition to the deformation of the wheel arches and other load-bearing part in the front structure. No deformation have been detected of the passenger compartment nor the drive shaft channel. A repair of the front light (right side) and the ACC radar sensor (without damage) can carried out.

REPAIR COSTS

The software "Audatex AudaPad" was used to calculate the damages on all three crashed vehicles. AudaPad is a special software used for calculating repair costs on vehicles. The comparison of these results with the ones of a similar crash test with deactivated systems and a collision speed of 64 km/h showed significant differences. The repair costs were reduced by more than 29% respectively 37% in the 38 km/h test depending on the configuration (Figure 7).

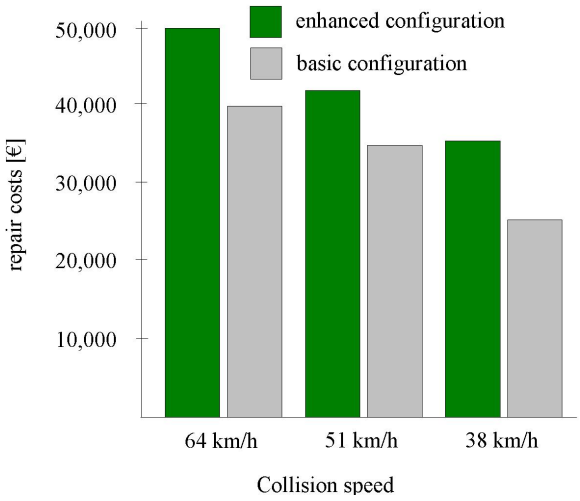

Figure 7. Repair savements depend on vehicle configuration and impact speed.

At all tested cars, the airbag and belt tensioner is triggered. This needs a replacement of the dashboard (passenger air bag deployment) and other expensive parts. Therefore at all crashed cars the repair costs are relatively high. Significantly lower repair costs can be expected when the collision speed is below the threshold triggering the restraint systems.

Bottom line is reflected a serious influence of the configuration. Depend on the vehicle configuration, the additional repair costs in consequence of optional equipment can reach almost one third of the total repair cost. In the crash test with 38 km/h for example, the repair costs at the car with enhanced configuration is circa 10,000 € higher compared to the vehicle in basis configuration. The analysis of calculated repair costs show furthermore the influence of the vehicle electronics of modern cars: electronic systems increases spare part costs up to Euro 8000.

MASTER PROCESS

In the KTI's body shop, a master process and documentation was carried out on the car at 38 km/h impact (Figure 8).

Figure 8. Deformations resulting from the 38 km/h impact.

The OEM’s introduction of new materials and production techniques in cars makes it increasingly important that the repair of such vehicles is carried out with the appropriate techniques and quality. Studies conducted at the KTI have shown that the professional repaired vehicles perform in a similar way to that of an original undamaged vehicle [3]. Non-professional repairs in contrast can have a negative influence on the deformation behaviour of a vehicle involved in a crash [4]. Therefore, OEM information was used during the repair.

Because of aluminium`s electrical flow characteristics, welding is not permitted anywhere on the front structure of the BMW F10; front end components are partially attached with rivets and a high-strength glue. Therefore, it is a requirement that

appropriate technical equipment and parts are used, such as rivet insertion and extraction tool, factory-specified structural adhesive and siliconcoated rivets.

Initially, for proper diagnosis an electronic measurement of the car body was carried out. After additional check with a tear test-spray-set, we found that the right aluminium front shock tower section was not damaged. After removal of exterior attachment parts (such as bumper, headlights, fender, bonnet), the car was fixed on a bench. The repair started with a raw reshaping of the car chassis on a universal straightening bench. During straightening, we measured the dimensions at reference points. The vehicle was then raised on a lift. Windscreen and dashboard were removed (access and front-seat passenger airbag had been deployed). The engine and front suspension were also removed in order to properly access the damaged components. The front end of the car was fully disassembled while mounted on the repair bench to ensure manufacturer`s tolerance would be met (Figure 9).

Figure 9. Car on the repair bench with disassembled front.

To prepare the new parts, were marked the cutting lines and then cut them at those points. We then made a rough cut of the brace (between firewall and strut tower), side member and inner fender apron near the installation area. Welded connections were opened and wheel arch with engine support was removed. In order to replace the parts correctly, we used alignment brackets to mount to the firewall. To preparation of new parts, were severance cut marked and cut. By repairing this vehicle on a bench, we were able to restore it to factory specifications. New components were attached with welding, adhesive and rivets. Thereby, to avoid contact corrosion, we grinded the new wheel arch part in the area of the bonding surfaces. The vehicle had to remain on the bench for 12 hours (at a temperature of 20°) after the structural adhesive was applied to allow it to set properly. The car was then taped and protected so that it could be primed. A factory-recommended seam sealer was then applied to all new joined seams and painted, see Figure 10. Then, the engine and front suspension were installed as a single unit; all systems were installed and checked prior to painting. Finally the errors were deleted in the error memory.

Figure 10. New components were attached with welding and adhesive.

It was clear that electronic components require a extensive diagnostic and system calibration. However that's absolutely essential because the quality of calibration affects the system functionality. The outcome of this are high investments for equipment and training for body shops.

In this context, for accident research arises the question how far the benefit of driver assistance systems in the real world accident occurrence could be reduced as a consequence of non-professional repairs.

CONCLUSIONS

Results of the crash tests described above show that pre-crash braking makes it possible to substantially reduce the severity of a crash in terms of impact velocity, impact energy, and the resulting occupant injuries plus repair costs.

In the crash test with braked cars, the injury numbers are greatly reduced when compared to the EuroNCAP test at 64 km/h impact velocity. The reduction in the case of impact at 51 km/h for the dummies is up to 42%. For the impact velocity of 38 km/h, there was a reduction of the HIC36 numbers up to 78%.

The comparison of the results regarding repair costs also showed significant differences. Compared to the car with deactivated systems and a collision speed of 64 km/h, the repair costs were reduced by more than 29% respectively 37% in the 38 km/h test depending on the configuration. Regarding repair costs, it turned out that airbag firing and vehicle configuration are key factors.

A extensive diagnostic and system calibration is a precondition for the correct functionality of driver assistance systems.

Further tests regarding repair costs at low speed impacts, will be conducted at the KTI in the future.

REFERENCES

[1] Kiebach H. Influence of driver assistance systems on repair costs. ESV paper no 11-0350. Washington 2011.

[2] http://www.euroncap.com/results/bmw/5_series/2010/401.aspx

[3] Kiebach H., Heidrich S., Schmortte U. Passive Sicherheit fachgerecht instand gesetzter Pkw. VKU - Verkehrsunfall und Fahrzeugtechnik, no. 10/2012

[4] Kiebach H., Heidrich S. Passive Sicherheit nicht fachgerecht instand gesetzter Pkw. VKU - Verkehrsunfall und Fahrzeugtechnik, no. 9/2010

Experimental Study of the Possibility of Using of External Inversion Crash Box on Sloped Crash Barrier

Joon Geun, Cha
Chul Hong, Bae
Hyundai Motor Company
Republic of Korea
Byoung Kee, Han
Hongik University
Republic of Korea
Paper Number 13-0119

ABSTRACT

A new crash box system in the vehicle frontal crash is considering by energy absorbing of the pre-inverted pipe, which is a useful compression force based on the external inversion phenomenon. As a result of the application of the pre-inverted pipe, this paper describes the benefits of the uniform energy absorbing and the space utilization of the crash box systems with 3 thicknesses of pipes during the frontal collision.

INTRODUCTION

The most of the physical phenomena to absorb crash energy were the local buckling and overall buckling of the crash boxes, frontal side members and other structural parts on the vehicle during a frontal collision. The phenomenon on the crash box and side member during a frontal collision is primarily accordion-like deformation. It is regarded as the ideal design. And it has a deformed region about 70% of the total length of the crash boxes.
The previous researches of the external inversion of pipe were conducted by Guist et al in 1966 [1], Al-Hassani et al in 1972 [2], and Rosa in 2003 [3]. The external pipe research conducted by Guist1) was to invent the test machine to develop the landing system of the space ship for NASA. Al-Hanssani2) used the various dies to invert the pipe for the internal and external inversion. And the validation research of external inversion of thin-walled tubes using the inversion die between the physical tests and theoretical investigation was conducted by Rosa et al [3].

In this study this paper reports the results of the compression tests of the pipes which is 80 mm in outer diameter and the thicknesses are 1, 1.6 and 2 mm with external inversion. And it is compared to the results of the simple compression tests of the pipe which is same size with the accordion-like deformation. The external inversion phenomenon on pipe type crash box allows for uniform energy absorption and gives us the advantage of space utilization during the frontal collisions.

Static and Dynamic Compression Tests

Crash Box with Pre-Inverted Pipe

The longitudinal compression of pipe on the die which is useful to external inversion or internal inversion are necessary a certain level of force to change the shape of thin-walled tube. Figure 1 shows the sectional shape of the pipe during the static compression tests of external inversion and internal inversion. Figure 1-(a) represents the phenomenon of external inversion which the inner surface of pipe is inverted into outer surface along the expanded slope of die. Figure 1-(b) also represents the phenomenon of internal inversion. The outer surface of pipe is inverted into inner surface along the reduced slope of die.

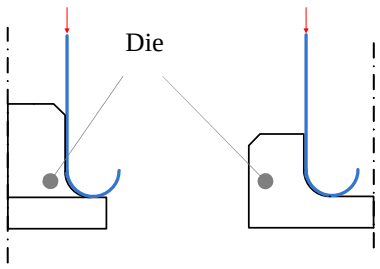

a) External Inversion (b) Internal Inversion
Figure 1. Inversion of pipe

Fabrication of Pre-Inverted of Pipe The test specimen of crash box was consist of pipe pre-inverted. Figure 2 represents the fabrication process of the external inversion of pipe and the installation of pipe into the side member. The space between the outer surface of die and the inner surface of pipe is 0.125 mm used in the research conducted by Al-Hassani et al [1]. And the pre-inverted pipe was installed into the side member with TIG welding.

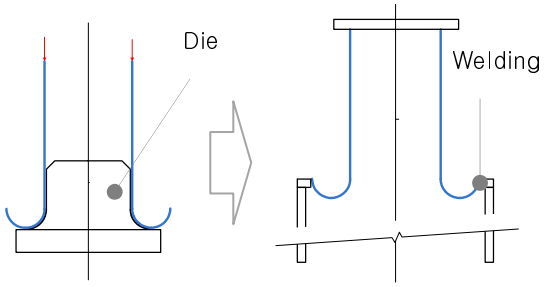

(a) Pre Inversion (b) Installation
Figure 2. Installation of pre inverted pipe

Test Specimen of Crash Box
Figure 3 represents the configuration of the crash box as test specimen. The pre inverted crash box is installed on side member with TIG welding. A thin plate is welded on the crash box. In the B-B section of figure 3 one side of the side member is opened to take the pictures during tests.

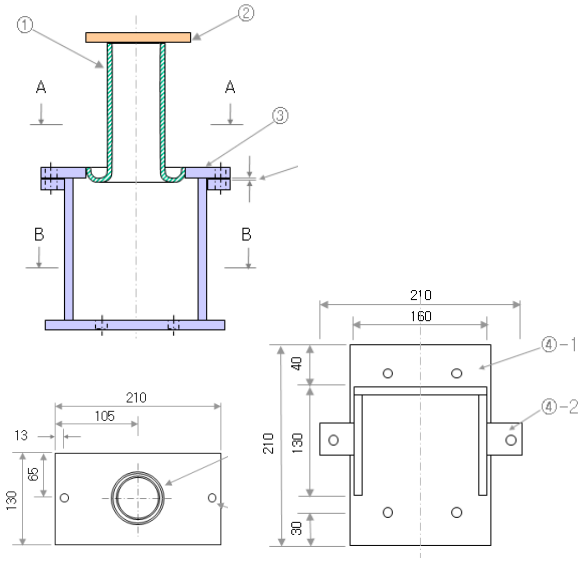

(a) Section A-A (b) Section B-B
Figure 3. Assembling of the crash box

Tensile Test of the Material The pipe for this research was tested to get the material characteristics using the universal test machine. Figure 4 shows the setup of the tensile test according to the KS B 0801 standard. The thickness of specimen was 1 mm. The dimension of it was 12.5 mm of width, 50 mm of reference distance, and 75 mm of parallel section. Figure 5 shows the characteristics of test specimen in the tensile condition. The yield stress, σ_y, was calculated according to the offset standard of metallic material tensile test method of KS B 0802. The calculated yield stress was 546 MPa and the maximum tensile stress, σ_b, was 570 MPa. In this research the calculated flow stress, σ_p, is 558 MPa of the average between 546 to 570 MPa.

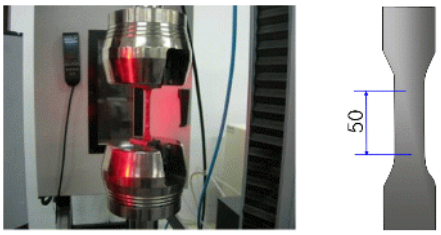

Figure 4. Tensile Test of test specimen

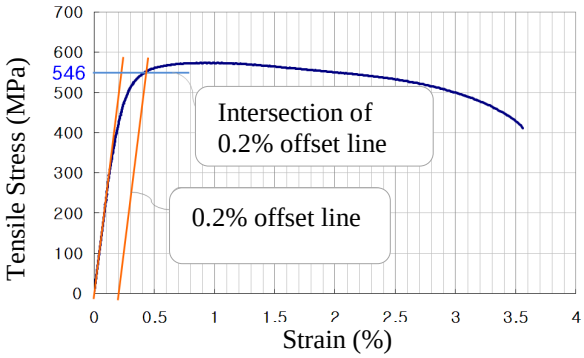

Figure 5. Characteristics of test specimen

Table 1.
Tensile test result of specimen

Thickness	Young's Modulus	Yield Stress(σ_y)	Tensile(σ_B)
1.0t	234.8 GPa	546 MPa	570 MPa

Static Compression Test of Pre External Inversion Crash Box

The static compression tests using the universal test machine were conducted to compare the energy absorption performance of crash box with same material under the different test conditions. Three pipes are compressed in different test conditions of simple compression, simple compression on 10-degree slope, and pre-external inversion respectively. The compression rate of the static compression tests were 10 mm a minute.

Comparison between simple compression and pre external inversion of pipe

Figure 6 shows the deformed pipes during the test. The pipes of the simple compression and the pre-external inversion were symmetric and the pipe of the simple compression on 10-degree slope was asymmetric during the static test.

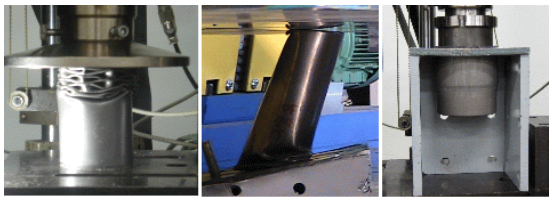

Figure 6. Static compression test of simple pipes and pre external inverted pipe

Figure 7 shows the compression force compared to the displacement of pipes in the different compression conditions. The compression force level of the simple compression of pipe was fluctuated the range between 60 kN and 20 kN. The simple pipe on 10 degree of slope surface was slipped and not compressed properly. The pre-external inverted pipe was compressed with flat shape of the compression force during the plastic deformation.

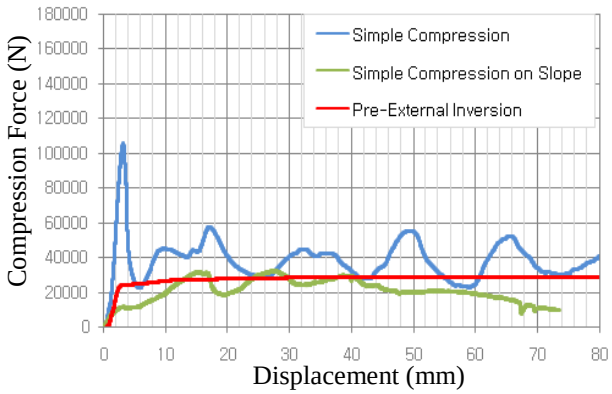

Figure 7. Test graph of static compression test of simple and pre external inversion pipes

Table 2 describes the results of the energy absorption of the pipes under the three different test conditions. The absorption energy of pipes pre-inverted was 61.3% when that of simple compression is based. The pipe on the slope condition was slipped and not reached to the compression force of simple compression.

Table 2.
Test result of static compression test of simple and pre external inversion pipes (1t, 50 mm deformation and based on simple compression)

Test Conditions	Section Area(mm^2)	Average Force(N)	Energy(J)	%
Simple Compression	248.2	41,382.7	2,069.1	100.0%
Slope	248.2	23,084.2	1,154.2	55.8%
Pre Inverted	248.2	25,377.2	1,268.9	61.3%

Comparison between rectangular section crash box and pre external inversion of pipe

The static compression tests were also conducted to compare the energy absorption performance of crash boxes between pre-external inversion of pipe and conventional rectangular. Figure 8 shows the test setup of these tests. The rectangular crash box was mounted and compressed on universal test machine guiding vertically.

Figure 8. Static compression test of pre external inversion pipes and rectangular section crash box

Figure 9 shows the compression force on time history of the crash boxes of pre-external inverted pipe type and rectangular type. The compression force level of the crash boxes of the pre-external inverted pipe type were flat shape within the certain levels during the static test. But the compression force of the rectangular crash box was fluctuated the range between 30 kN and 100 kN.

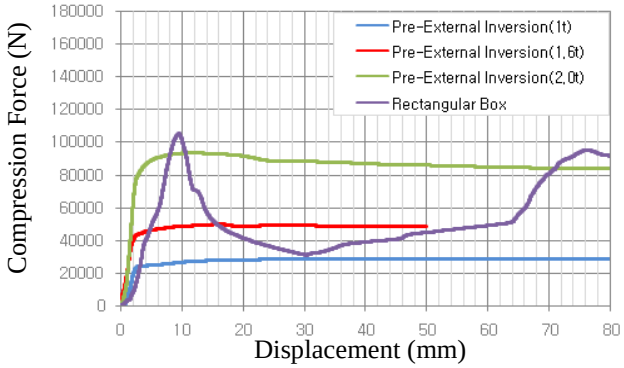

Figure 9. Test graph of Static compression test of rectangular section crash box and pre external inversion pipes

Table 3.
Test result of Static compression test of rectangular section crash box and pre external inversion pipes (50 mm deformation and based on simple compression)

Test Specimen	Section Area(mm^2)	Average Force(N)	Energy(J)	%
Pipe 1.0t	248.2	25,377.2	1,268.9	60.2%
Pipe 1.6t	394.1	46,254.1	2,312.7	109.8%
Pipe 2.0t	490.1	84,074.7	4,203.7	199.5%
Rectangular 1.6/2.0t	629.6	42,136.2	2,106.8	100.0%

Dynamic Comparison Tests with Moving Crash Barrier

The crash tests using the moving barrier were conducted to verify the energy absorption performance of crash box with pre inverted pipe material in the dynamic condition.
The weight of the moving barrier was set to 1400 kg before the test. One of the crash box was installed on the mid of the front surface of the moving barrier firmly. The load cell was installed between the crash box and the moving barrier to measure the compression force. Three axis accelerometers are also installed on C.G. of the moving barrier to measure the deceleration during the crash test. And these accelerations were used to calculating the displacement of the moving barrier. The moving barrier was guided in rails and travelled into the concrete crash barrier with a speed of 16 kilometers an hour.

Comparison the pipes of 1t, 1.6t and 2t

Figure 10 shows the test setup and the crash box of the pre and post-test. The crash boxes with thickness of 1 mm, 1.6 mm and 2 mm respectively were fully deformed into the inside of the side member during the tests.

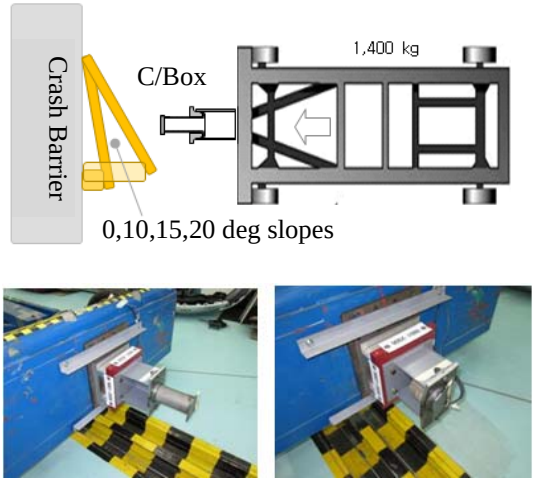

Figure 10. Dynamic test using the moving crash barrier

Figure 11 shows the compression force compared to the displacement of the crash boxes with the thickness of 1 mm, 1.6 mm, and 2 mm respectively in the 0-degree crash barrier conditions. The levels of compression force for the crash boxes with different thickness are flat within the certain levels during the moving barrier crash test.

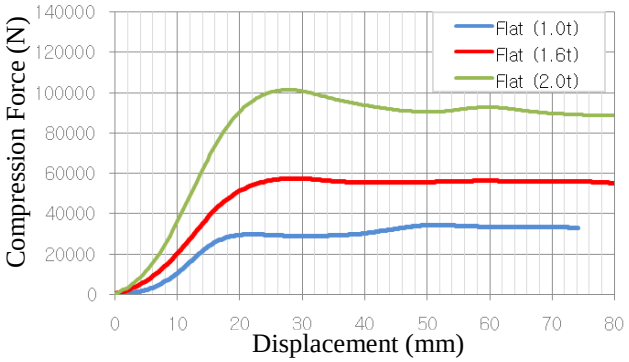

Figure 11. Graph of dynamic test using the moving crash barrier

Table 4 describes the results of the energy absorption of the crash box with the different thicknesses of pipe material. The absorption energy of crash box with the thickness of 1 mm, 1.6 mm, and 2 mm respectively were increased 100%, 174.6%, and 301.2% gradually when that of 1.0t is based.

Table 4.
Test result of dynamic test with pre-inverted crash box using the moving crash barrier (70 mm deformation and based on 0 degree)

Test Conditions	Section Area(mm^2)	Average Force(N)	Energy(J)	%
1.0t	248.2	26,795.9	1,875.7	100.0%
1.6t	394.1	46,777.3	3,274.4	174.6%
2.0t	490.1	80,716.5	5,650.2	301.2%

Comparison the oblique conditions, 0, 10, 15, and 20 degrees

The dynamic moving barrier tests were conducted on the 0, 10, 15, and 20 degree of rigid slope surfaces using the crash boxes with 1.6 mm thickness of pipe material. Figure 12 shows the slope surface of the moving barrier test.

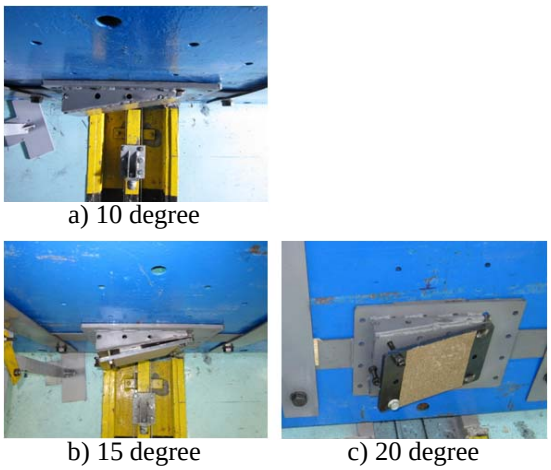

Figure 12. Dynamic test for oblique conditions

Figure 13 shows the compression force compared to the displacement of the moving barrier tests in the slope surface conditions. The compression forces among the 0, 10, and 15 degree of slope surfaces are similar each other and reduced in 20 degree of the slope surface.

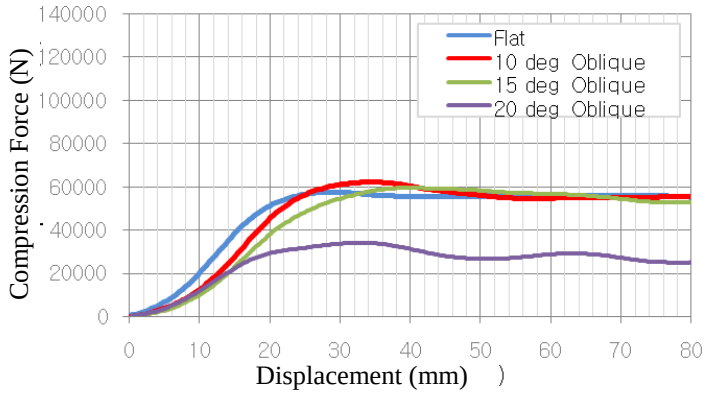

Figure 13. Graph of dynamic test for oblique conditions

Table 5 describes the results of the energy absorption of the crash boxes with pipe material of 1.6 mm thickness in the slope conditions. The absorption energy values of crash box in 0, 10, 15, and 20 degree slope surfaces were reduced 100%, 99.4%, 95.3% and 54.0% gradually when that of 0 degree is based.

Table 5.
Test results of dynamic test for oblique conditions (70 mm deformation and based on 0 degree)

Test Conditions	Section Area(mm^2)	Average Force(N)	Energy(J)	%
Flat	394.1	46,777.3	3,274.4	100.0%
10 deg	394.1	46,518.1	3,256.3	99.4%
15 deg	394.1	44,587.4	3,121.1	95.3%
20 deg	394.1	25,240.6	1,766.8	54.0%

Calculation of Compression Force

The required force for the compression of the pre inverted pipe material was calculated. The average diameter and the thickness of pipe is 79 mm and 1 mm each. The flow stress (σ_p) of the pre inverted pipe through tensile test is 558 MPa.
To calculate the compression force(P) it was used the equation suggested by Guist et al [1] in 1966.

$$P\,(N) = \pi\ D\ t\ \sigma_p\ \sqrt{(2\ t / D)} = 4.44\ \sigma_p\ t^{3/2}\ D^{1/2}$$

where D is diameter and t is thickness of pipe material.
The calculated compression force was compared to that of the test on the Table 6.

Table 6.
Comparison of compression force between calculation and test

Diameter of Pipe	Force of Compression (N)			Remark
	Test	Calculation	%	
79 mm	24,694	22,035	10.8	

The calculated compression force is 10.8% lower than that of the test. The cause of this difference is assumed to only using of the plastic deformation energy in the equation of Guist et al [1]. It is possible to use in early stage of the vehicle engineering design to predict the crash performance.

CONCLUSIONS

The following conclusions were obtained from the static compression tests and the dynamic moving barrier tests with the crash box using the pre inverted pipe material.

With the application of the pre inverted crash box, it was possible to improve the space utilization efficiency of the crumble zone in the frontal collision.
As results of pre inverted pipe application with various thicknesses, it was also possible to control the level of the crash energy for the different size of the vehicles.
With the benefit of the external inversion of pipe material, it was also possible to have the consistent compression force of crash box in the 15-degree slope conditions.

REFERENCES

[1] L.R. Guist, D.P. Marble “Prediction of the inversion load of a circular tube”, NASA TND, p. 3622, 1966
[2] S. Al-Hassani, W. Johnson, W.T. Lowe “Characterization of inversion tubes under axial loading” J. Mech. Eng. Sci. 14 370, 1972
[3] P.A.R. Rosa, J.M.C. Rodrigues, P.A.F. Martins “External inversion of thin-walled tubes using a die: experimental and theoretical investigation” McGraw-Hill, New York, 2003
[4] T. Wierzbicki, S.U. Bhat ″A moving hinge solution for axisymmetric crushing of tubes″ Int. J. Mech. Sci Vol. 28, No. 3, pp. 135~151, 1986
[5] Byoung Kee Han, ″Research for the local buckling and global bending of the rectangular section tube (1), (2)″ KSAE A-22 vol 4 pp. 887 ~894, 1998

INVESTIGATION OF OPPORTUNITIES FOR LIGHT-WEIGHTING A BODY-ON-FRAME VEHICLE USING ADVANCED PLASTICS AND COMPOSITES

Chung-Kyu Park
Cing-Dao (Steve) Kan
National Crash Analysis Center, The George Washington University
USA
William Thomas Hollowell
WTH Consulting LLC
USA
Paper Number 13-0023

ABSTRACT

This paper investigates the opportunities for light-weighting a current body-on-frame type vehicle using advanced plastics and composites. In addition, the safety benefits of structural plastics and composites applications in future lighter vehicles are identified and evaluated by frontal impact simulations as part of implementing the plastics and composites intensive vehicle (PCIV) safety roadmap of the National Highway Traffic Safety Administration (NHTSA). The methodology of the study includes two steps: (1) developing a light-weight vehicle based on a current finite element (FE) vehicle using advanced plastics and composites, and (2) evaluating the crashworthiness of the light-weighted vehicle by frontal New Car Assessment Program (NCAP) test simulations. An FE model of a 2007 Chevrolet Silverado, which is a body-on-frame pickup truck, was selected as the baseline vehicle for light-weighting.

By light-weighting components in the Silverado, the vehicle weight was reduced 19%. As a result, the content of plastics and composite in the light-weight vehicle becomes about 23.6% of the total weight of the light-weight vehicle. Frontal NCAP simulations of the light-weighted vehicle show that the light-weighted vehicles using advanced plastics and composites provide equivalent structural performance (intrusion and crash pulse) to the baseline vehicle in the full frontal impact condition. This study demonstrates that (1) using plastics and composites can reduce the vehicle weight efficiently; and (2) the Silverado, light-weighted using advanced plastics and composites, provides equivalent structural performance in the frontal impact condition as the baseline vehicle.

INTRODUCTION

According to the U.S. Department of Energy (DOE), the United States consumed nearly 20 million barrels per day in 2010 [1,2]. The transportation sector accounted for 28% of total U.S. energy use, two-thirds of the nation's petroleum consumption, and a third of the nation's carbon emissions. Nearly, 32% of U.S. greenhouse gas (GHG) emissions are generated from transportation, the second-largest source after electricity generation. It was estimated that 75% of fuel consumption directly relates to vehicle weight [3]. With everything else remaining the same and considering mass compounding, a 6 to 8 percent increase in fuel economy can be realized for every 10 percent reduction in vehicle weight [4,5]. However, there are several barriers to weight reduction in automobiles: (1) historically low prices of fuel in the United States, (2) higher costs of advanced light-weight materials, (3) lack of familiarity with light-weight materials, (4) extensive capital investment in metal-forming technologies, (5) lack of large automotive composites and magnesium industries, (6) preferences for large vehicles, (7) perceptions of safety, (8) recycling issues of plastics and composites, (9) increased emphasis on alternative fuels such as non-conventional petroleum, biofuels and electricity, (10) alternative propulsion systems such as hybrids and fuel cells, and (11) the automotive industry's lack of long-term pricing strategies and stable long-term partners [4,6].

The Corporate Average Fuel Economy (CAFE) standards in the United State had remained mostly unchanged for past three decades since 1975. The new CAFE standards issued in 2010 proposed that new passenger cars and light trucks, including minivans, sport utility vehicles (SUVs), and pickups, are now required to achieve at least 14.5 kilometers per liter (34.1 miles per gallon) automaker fleet wide average by model year (MY) 2016 [7]. Recent changes to the CAFE standards were driving automakers to seek more aggressive methods for fuel consumption deductions. Light-weighting of vehicles will be an important factor to meet these requirements due to the inherent relationship between vehicle mass and fuel consumption.

Vehicle weight reduction is a known method to improve fuel economy in vehicles. However, Cheah addressed that the opportunity to reduce vehicle weight is not simple on three different aspects [5]; (1) the average new U.S. vehicle weight has increased steadily over the past two decades [8]; (2) the topic of vehicle weight reduction should be studied with a life-cycle perspective, considering energy-intensive production and recycling of light-weight materials [9,10]; and (3) while the effectiveness of weight reduction at a vehicle-level is reasonably well understood, the effectiveness at a vehicle fleet-level is less so [11]. Reductions in vehicle weight can be achieved by a combination of (1) vehicle downsizing, (2) vehicle redesign and contents reduction, and (3) material substitution [5,11,12]. Actually, there are a number of major research projects that have sought to determine the mass-reduction technology and materials potential for future vehicles. Lutsey reviewed seventeen vehicle mass-reduction studies and summarized achieved mass-reductions and cost impacting findings [13]. In those studies, the new manufacturing technologies and the light-weight materials, such as high strength steel (HSS), aluminum, magnesium, plastics, and composites, are utilized to reduce the vehicle weight; and a range of mass reduction is 16 to 57% in body and 19 to 52% in vehicle with the average of these vehicle designs achieving about 30% mass reduction. More recently, a study by EDAG showed that mass reduction of up to 23% is likely feasible by MY 2020 while maintaining vehicle performance and safety functionality and staying within a10% increase of the original baseline midsize sedan's MSRP (manufacturer's suggested retail price) [14].

Schewel identified that light-weight vehicle could be a potent solution to triple safety (safety of climate, drivers and other road users) simultaneously, without compromise [15]. Clearly, light-weight automobiles enhance the global environment (climate) safety through their higher fuel efficiency. However, the safety (self- and partner-protections) of light-weight vehicles is not clearly evaluated yet. There have been many debates about the relationship about between safety and vehicle weight and size. The Rocky Mountain Institute (RMI) reviewed the light-weight automotive safety studies and summarized conclusions of these studies [16]. The conclusions of light-weight safety studies have not provided clearly the safety implications of light-weight vehicles to vehicle weight and size. These light-weight safety concerns are still actively studied by many researchers [17,18].

In 2006, the U. S. Congress directed the National Highway Traffic Safety Administration (NHTSA) of the U.S. Department of Transportation (DOT) to begin development of a program to examine the possible safety benefits of light-weight Plastics and Composite Intensive Vehicles (PCIVs) and to develop a foundation for cooperation with the DOE, industry and other automotive safety stakeholders [19]. In the 2008 PCIV safety workshop sponsored by NHTSA in supporting of implementing this mandate, attendees indicated that a minimum of 30% to 40% (by weight) plastics and composite content in one or more subsystems beyond interior trim could qualify a vehicle as a PCIV [20]. There are two roadmaps for PCIVs [21]; (1) a government-led roadmap under the direction of the NHTSA focuses on a holistic safety-centered approach to PCIV innovation [17,20,22-24], and (2) an industry-led roadmap developed by the American Chemistry Council - Plastics Division (ACC-PD) outlines the industry's action priorities for achieving the technology and manufacturing innovations required to realize PCIVs [21,25-27].

NHTSA concentrated on the safety-related research issues affecting the deployment of PCIVs in 2020. In 2007, the Volpe Center developed a safety roadmap for future PCIVs and described the approach, activities, and results of an evaluation of potential safety benefits of PCIVs [22,23]. Barnes *et al*. identified outstanding safety issues and research needs for PCIVs to facilitate their safety deployment by 2020, and recommended three topics pertinent to crashworthiness of PCIVs: (1) material database, (2) crashworthiness test method development, and (3) crash modelling [24]. In the vehicle mass-size-safety workshop in 2011, NHTSA brought together experts to discuss about the effect of vehicle mass and size on safety, vehicle structural crashworthiness, occupant safety, and advanced vehicle design; and to understand what might be appropriate level of mass reduction for future CAFE rulemaking [17].

In 2001, the American Plastics Council (APC), now the ACC-PD, outlined a vision and technology roadmap for the automotive and plastics industries [25]. In the technology integration workshop in 2005, the ACC-PD provided an expansive safety road mapping effort examining PCIVs [26]. In 2009, the ACC-PD updated the vision and technology roadmap to outline the industry's action priorities for achieving the technology and manufacturing innovations required to realize PCIVs [27]. Also, the ACC-PD recommended three research activities: (1) improve the understanding of composite component response in vehicle crashes,

(2) development a database of relevant parameters for composite materials, and (3) enhance predictive models to avoid costly overdesign [21].

Since composites were introduced firstly to automotive industry in 1950's [28,29], the use of composites in vehicles has increased steadily. Today's average U.S. light vehicle contains about 174 kg (384 pounds) of plastics and composites in 2009 – about 10% of total vehicle weight but more than 50% of vehicle volume [1,21]. Advantages of composites compared to steels for automotive and transportation are: (1) weight reduction of 20-40%, (2) styling flexibility in terms of deep drawn panels, which is limited in metal stampings, (3) 40-60% savings in tooling cost, (4) reduced assembly costs and time in part consolidation, (5) resistance to corrosion, scratches and dents, and improvement in damping and NVH (noise, vibration and harshness), (6) materials and process innovations capable of adding value while providing cost saving, and (7) safer structure due to the composite material's higher specific energy absorption (SEA) [4,6]. Sehanobish reported that the use of 45.4 kg (100 pounds) of plastics could replace approximately 90.7 kg (200 pounds) to 136.0 kg (300 pounds) of mass from the use of traditional materials [30].

Although the benefit of composites are well recognized by the industry, composite use has been dampened by (1) high material costs [31,32], (2) slow production rates [31], and (3) the lack of design experience and knowledge caused by different material characteristics from conventional metal [6,33]. Thus, the application of plastics and composites is still limited mostly to non- or semi-structural components of vehicles [6,30,33]. However, many studies have shown the potential and future use of composites for light-weighting vehicle structural components [34-38]. Actually, numerous investigations of composite intensive automotive body have taken place over 30 years [28,39-43]. Bonnet [39] and Beardmore [40] designed the body-in-white (BIW) and front-end module of a passenger car using carbon fiber reinforced plastic (CFRP) composites and achieved about 65% reduction in weight. Boeman and Johnson [41] developed the composite intensive BIW of a passenger car with CFRP composites and achieved 60% mass reduction. Fuchs [42] studied about designing the composite intensive passenger vehicle while satisfying all safety requirements. Deb *et al*. [43] compared the frontal impact performances of the glass-FRP (GFRP) composite and steel rails of a passenger car. Those studies were dealing with unibody structures. There was a study to develop a light-weight optimized frame in a body-on-frame type SUV by using high-strength steel, not composites [44].

In this paper, the opportunities for light-weighting a current body-on-frame type vehicle using advanced plastics and composites are investigated as part of implementing the PCIV safety roadmap of the NHTSA. In addition, the safety benefits of structural plastics and composites applications in future lighter vehicles are identified and evaluated by frontal impact simulations.

METHODS

The methodology of the research includes two steps: (1) developing a light-weight vehicle based on a current finite element (FE) vehicle model using advanced plastics and composites, and (2) evaluating the crashworthiness of the light-weighted vehicle by frontal impact simulations. At first, a light-weight vehicle is developed to investigate the light-weighting opportunities in a current vehicle. An FE model of a 2007 Chevrolet Silverado, which is a body-on-frame pickup truck, was selected as the baseline vehicle for light-weighting. Plastics and composites were considered as the primary substitute materials in this study. Based on the literature review and with help from the ACC-PD's member companies, candidate steel vehicle components in the Silverado were identified and light-weighted by substituting advanced plastics and composites for the heavier steel components. After that, the frontal New Car Assessment Program (NCAP) tests of the light-weighted vehicle were simulated to investigate the weight reduction effect on vehicle crashworthiness, to evaluate the crash performance of the composite structural component, and to look into the opportunities of using plastics and composites for weight reduction in a current vehicle. In this study, only the frontal impact configuration is considered.

In addition, costs were not considered in this study. In particular, a cost increase as compared to the used of other advanced materials (e.g., ultra high strength steel) is one of the critical barriers to using plastics and composites in automobiles. However, in order to investigate opportunities for light-weighting vehicles using plastics and composites and indentifying the potential safety benefits of plastics and composites applications in future lighter, this study mainly focused on identifying currently available plastics and composite materials and their applicability to current vehicle components, and did not consider cost variations. Also, the manufacturability for vehicle components using plastics and composites is another critical issue. Instead, the existing vehicle design,

which has optimal structures for steel material and steel manufacturing technologies, was utilized to develop the light-weight vehicle using plastics and composite as material substitutes in this study. So, the design changes of original vehicle structures and components were limited to replacing components, and therefore are considered to be a minimal approach that could be taken for reducing the weight in the light-weighting process. A more optimal approach would have been a comprehensive, clean sheet design from the ground up to achieve a maximized weight reduction for the Silverado. However, such an approach was beyond the scope of this study.

Baseline FE Vehicle Model

According to NHTSA's aggressivity metric based on the Fatal Analysis Reporting System (FARS) reported fatalities and the General Estimates System (GES) reported crash involvements, the light trucks and vans (LTVs) are over three times more aggressive than passenger cars in all vehicle-to-vehicle crash configurations [45,46]. Blum *et al*. did a study that looked at the aggressivity of the striking vehicle to the driver in the struck vehicle and found that the most important determinant of the risk of injury to a driver in the target vehicle is the weight of the striking vehicle [47]. Since 1990 the average LTV's weight has increased from 1868 kg to 2046 kg in 2000 [46]. So, in the aspects of improving fuel efficiency as well as alleviating aggressivity, an active effort to reduce the weight of LTVs is required.

A 2007 Chevrolet Silverado pickup truck was selected as the baseline vehicle in this study. Figure 1a shows the 2007 Chevrolet Silverado and Figure 1b shows the FE model of this vehicle, which was created by National Crash Analysis Center (NCAC) at the George Washington University (GWU) and is available to the public from the FE model database of NCAC/GWU [48]. The vehicle is a 4-door crew pickup truck (4.8L V8 SFI engine), which is a body-on-frame type vehicle. The vehicle weight is 2307 kg and its size is 5,846 mm (L) × 2,029 mm (W) × 1,917 mm (H). The FE vehicle model consists of about a million elements and 680 parts. The FE vehicle model was validated with test results from front and side crash tests [49] and from suspension tests [50,51]; that is, the FE model is a validated representation of the real vehicle.

The FE vehicle model is divided into assemblies as shown in Figure 2. Since it is a body-on-frame type vehicle, all assemblies are connected to the ladder frame structure. The vehicle mass breakdown is summarized in Figure 3. It shows that the weight of the power-train related and suspension related components accounts for almost 50% of the vehicle weight. The weight of the ladder frame structure is about 13% of the vehicle weight.

(a)

(b)

Figure 1. 2007 Chevrolet Silverado (crew pickup body style); (a) actual vehicle, (b) FE model.

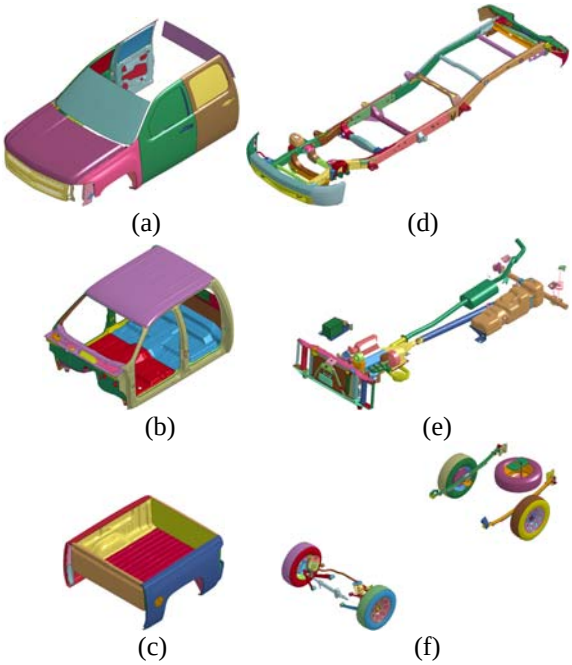

(a) (d) (b) (e) (c) (f)

Figure 2. Assembly of the FE model of Silverado: (a) closures, (b) occupant compartment structure, (c) truck bed structure, (d) ladder frame structure, (e) power-train related, (f) suspension related.

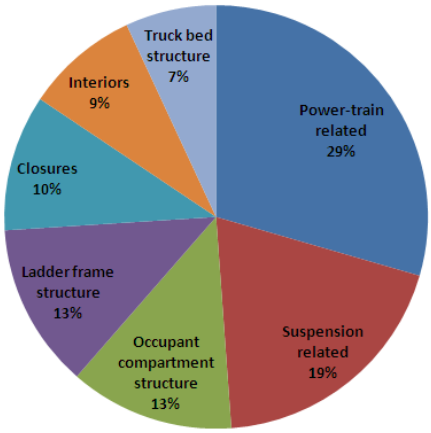

Figure 3. Mass breakdown of the FE model of Silverado.

Light-Weighting Strategies

In order to light-weight the current vehicle model, three strategies were considered: material substitution, component change, and component removal.

Material substitution In order to reduce the vehicle weight, the steel material in the vehicle components was replaced with other lighter-weight materials. In particular, plastics and composites were used as a substitute for the steel material since these materials were primarily the main focus in this study. Plastics and composites have quite different material characteristics than steel. Steel material is isotropic and ductile, while plastics and composites are mostly anisotropic and brittle. So, the ACC-PD and some of its member chemical companies (SABIC, BASF, and Bayer) voluntarily participated in this study to provide information about available components that could be redesigned using plastics and composites. In addition, other available resources were utilized to gather information about the applications of light-weight materials.

When the steel material in the Silverado was replaced by plastics or composites, the components were re-designed by ACC-PD's chemical companies if a design change was deemed necessary. Otherwise, the steel material was simply replaced with the plastics or composites. Note that, in this study, only the frontal NCAP test of the light-weighted vehicle was considered for investigating the effect of weight reduction on the vehicle's crashworthiness. So, if any component was not engaged in the frontal NCAP test, the material substitution was realized by adjusting the weight of the particular component numerically without changing the component design.

It should be noted that plastics and composites are applied not only to non-structural components, but also to structural components in this study. Figure 4 shows the impact energy absorption of components of the Silverado in the frontal NCAP test. Some structural components, such as bumpers, fenders, frontal-end module and ladder frame, are changed to composites. Especially, the ladder frame of the Silverado was determined to be the primary structural member because the ladder frame was observed to absorb over 70% of impact energy in the frontal NCAP test. In addition to being evaluated using NCAP frontal crash test simulations, the new composite structural components are evaluated by component test simulations to prove that these new components provide equivalent structural performance to original components.

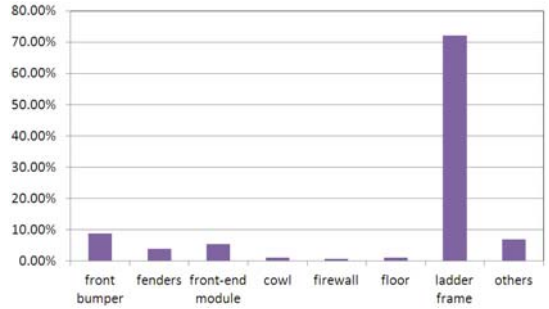

Figure 4. Impact energy absorption of components of the baseline (original) vehicle in NCAP test simulation.

When it was determined that there were no plastics or composites available for a given component but other light-weight materials were available, the original material was replaced with the other lighter-weight materials without undertaking a design change. For example, the steel material of the wheels and rear differential carrier were changed to aluminum and magnesium alloys, respectively.

Component change In the vehicle, there are many finished components, such as the engine, transmission, battery, and so on. It was decided that these existing components could be changed to light-weight ones to reduce the vehicle weight if it was determined that the new components could provide equivalent performance. Since the current vehicle weight was to be reduced, a smaller engine and transmission could be adopted. Additionally, a lighter weight battery could be adopted.

Component removal It was decided that any component which is not directly related to the vehicle operation could be removed to reduce the vehicle weight. Thus, for example, the spare tire and its

carrier in the current vehicle could be removed. This is a practice that already is being utilized by the industry.

RESULTS

Development of a Light-Weight Vehicle

The selected components of the Silverado were light-weighted by following the light-weighted strategies mentioned above. The detail description of each component is explained in the reference [52]. In this paper, several light-weighted components are explained.

Front & rear bumpers SABIC redesigned the front and rear bumpers. The original parts of the front bumper assembly were reduced from nine parts to five parts and those of the rear bumper assembly were reduced from six parts to three parts. The steel material was changed to a blend of semi-crystalline polyester and polycarbonate (i.e., a PBT(or PET)/PC blend) [53] and a polypropylene plastic [54]. The insert support is made of steel. The weights of the front and rear bumpers were reduced to 47% and 39% from their originals, respectively. The light-weighted bumpers are evaluated by component tests which show that their crash performance is equivalent to the baseline bumpers. These materials also are applied to roof and rear window.

Front-end module SABIC redesigned the front-end module. The original parts of the front-end module assembly were reduced from nine parts to one part. The steel material was changed to a long glass fiber reinforced polypropylene [55]. The weight of the front-end module was reduced 58% from its baseline weight.

A- and B-pillar reinforcements Composite inserts were applied to the A- and B-pillars and the thickness of steel pillars was reduced. BASF designed the composite inserts by using a 35% glass reinforced polyamide (PA6) [56]. Both pillars were gauged down 20%. The crash performance of composite inserts in vehicle structure was studied by Park *et al*. [57,58]. The light-weighted A- and B-pillars were evaluated by component tests which show that their crash performance is equivalent to the originals. The 35% glass reinforced polyamide (PA6) is also applied to door beams, transmission crossbeam, and oil pans along with design changes.

Engine and transmission Table 1 shows the specifications of three Silverado models. The Silverado has two kinds of engines: theV6 and V8 engines. Also, the Silverado has two body styles: the extended cab and crew pickups. The FE vehicle model was developed for the crew pickup with the V8 engine. The vehicle size of all three vehicles listed in Table 1 is similar, but there is a weight difference. In the extended cab pickup, there is an 84 kg weight difference depending on which engine is adopted. Basically, this weight difference comes from the change of engine, transmission, and connecting assemblies. In addition, the difference of the gross vehicle weight rating (GVWR) is 182 kg depending on which engine is adopted. This means it would be reasonable to assume that, if the vehicle weight is reduced 183 kg or more, the V8 engine can be replaced by the V6 engine.

In this study, the original V8 engine was replaced by the V6 engine. It was assumed that the engine, transmission, and their assemblies were not changed; but instead the material density was adjusted, although the actual size of V6 and V8 engines are different. Also, it was assumed that even the weight of the V6 engine could be made lighter by using newer technologies and lighter materials, such as aluminum and magnesium. With these assumptions, the substitutions led to a100kg weight saving in the engine and transmission.

Ladder frame Previous studies have shown that fiber-reinforced plastic (FRP) composites offer a means to light-weight vehicle structural components [35-38]. The main advantages of FRP composites over the more conventional isotropic materials are the lower density, very high specific strength, specific stiffness, and specific energy absorption (SAE) that can be achieved. However, introducing the FRP composites into vehicle structural components should be achieved without sacrificing the current

Table 1. Specifications of Silverado

NCAP Test No.	Model	Year	Body Style	Engine Type	GVWR (kg)	Vehicle Weight (kg)	Wheel Base (mm)	Vehicle Length (mm)
6171	SILVERADO	2007	EXTENDED CAB PICKUP	4.3L V6 MPI	2903	2210	3654	5821
6174	SILVERADO	2007	EXTENDED CAB PICKUP	4.8L V8 SFI	3085	2294	3658	5824
6168	SILVERADO	2007	CREW PICKUP	4.8L V8 SFI	3085	2307	3660	5830

performance of crashworthiness and stiffness. Many studies have shown that composite structures deform in a manner different than that of similar structural components made of conventional materials like steel and aluminum [35-37, 59-61]. The micro-failure modes, such as matrix cracking, delamination, fiber breakage, etc., constitute the main failure modes of composite structures. These complex fracture mechanisms make it difficult to analytically and numerically model the collapse behavior of FRP composite structures. This has limited the application of composites for mass production in the automotive industry.

The commonly used FRP composites are unidirectional laminates and textile composites. In general, laminates have good in-plane properties, and textile composites, which include woven, knitted, and braided fabrics, have better dimensional stability, out-of-plane properties, and impact and delamination resistance. Braided composites have some advantages: (1) good impact resistance, (2) better fatigue life and strength, (3) low manufacturing cost, (4) good interlaminar shear properties, and (5) efficient reinforcement for torsional loads [39]. The numerous studies of braided composites have been performed and identified crushing behavior, energy absorption capability, and significant braiding parameters [62-65].

Actually, extensive material experiments of a carbon fiber-thermoset braided composite were performed in this study to identify the crushing behavior, energy absorption capability, and numerical material parameters [52]. Based on the result of material tests and simulations, the steel in side rails was changed to the carbon fiber-thermoset braided composite, which is explained in detail in the references [52,66]. The design of the ladder frame was not changed but the thickness of side rails was increased to twice the thickness of the original design in order to have equivalent stiffness and impact performance to that of the original steel ladder frame. The crashworthiness of the composite ladder frame is evaluated by component tests which show that their crash performance is equivalent to the original. Therefore, the weight of the ladder frame was reduced 32% from that of the original. If the composite material is applied to cross members and mount supporters and optimal design is adopted, the weight of ladder frame could be reduced even more.

Table 2 summarizes all the weight savings of components of the Silverado to develop a light-weighted vehicle. The total saving is 432.76 kg which is about 19% reduction of the original vehicle weight. Thus, the weight of the light-weight vehicle becomes 1,874.24 kg. Today's average U.S. light vehicle contains plastics and composites that account for about 10% of the total vehicle weight [1,21]. Based on this fact, it can be assumed that the weight portion of plastics and composites in the original Silverado is about 10% (i.e., about 187.4 kg). Using this assumption, the total weight of plastics and composites in the light-weighted vehicle can be obtained by summing up the weight of existing plastics and composites (187.4 kg) and the weight of newly added plastics and composites (254.35 kg). In other words, the light-weight vehicle contains about 441.75 kg of plastics and composites, which is about 23.6% of the total light-weight vehicle weight.

Frontal NCAP Test Simulations

The frontal NCAP test was simulated to evaluate the crash performance of the light-weighted vehicle developed above. In the full frontal NCAP test, a vehicle with two dummies in the front seats collides with the rigid barrier in the full overlap configuration at the impact speed of 56 km/h (35mph). In the full frontal NCAP simulation, dummies were considered as added masses. The LS-DYNA hydrocode is utilized for vehicle crash simulations [101].

Three vehicle configurations are considered; (1) the baseline (original) vehicle (2,307 kg), (2) the light-weighted vehicle with the original steel ladder frame referred to as LWV1 (1,949 kg, 16% weight reduction), and (3) the light-weighted vehicle with the composite ladder frame referred to as LWV2 (1,874 kg, 19% weight reduction). Since the ladder frame is the primary energy absorbing structure of the Silverado, its crash performance is of great interest. So, the two different light-weighted vehicles, LWV1 and LWV2, were considered for evaluation to determine if the composite ladder frame could provide equivalent crash performance as the original steel ladder frame. As stated above, the difference between the LWV1 and LWV2 is the material adoption of the composite ladder frame in the LWV2. The LWV2 is the lightest vehicle.

Figure 5 shows vehicle response histories in the frontal NCAP test. Figures 5a and 5b show the acceleration curves. The notable point in the acceleration curve of the baseline vehicle is a big drop at 27 msec, which is induced by the crumple zone deformation of side rails. This big drop in acceleration can be observed in LWV1 and LWV2 as well. Compared to the baseline, the LWV1 has higher peaks at an earlier time, and the LWV2 has a lower peak at an early time, but a higher peak at a later time.

Table 2. Summary of weight savings

components	old material	new material	weight saving (kg)	references
• material substitution with new design (using plastics and composites)				
A- & B-pillars	steel	downgauge, composite inserts	1.32	[56-58]
door beams	steel	composite	4.92 (55%)	[56]
tailgate	steel	plastic, composite	8.66 (44%)	[53,55]
front-end module	steel	composite	7.77 (58%)	[55]
front bumper	steel	plastic, composite	7.61 (47%)	[53,54]
rear bumper	steel	plastic, composite	6.32 (39%)	[53,54]
transmission crossbeam	steel	composite	4.40 (56%)	[56]
• material substitution only (using plastics and composites)				
roof	steel	plastic	8.82 (43%)	[53,54]
front fenders	steel	plastic	3.53 (45%)	[67]
rear fenders	steel	plastic	10.84 (45%)	[68,69]
rear window	glass	plastic	2.73 (42%)	[53,54]
oil pans	steel	composite	3.82 (51%)	[56,69]
stabilizer links	steel	composite	0.14 (40%)	[56]
IP retainer	steel	composite	4.10	[70-74]
truck bed	steel	composite	20.46 (31%)	[75,76]
drive shaft & yokes	steel	composite	3.69 (58%)	[77-80]
front brake disks	steel	composite	14.39 (50%)	[81]
leaf springs	steel	composite	34.73 (70%)	[82-84]
ladder frame	steel	composite	74.80 (32%)	[52,59-66]
• material substitution only (using other materials)				
rear differential carrier	steel	magnesium	8.80 (25%)	[85,86]
wheels	steel	aluminum	20.06 (40%)	[87]
• component change				
front & rear seat			10.00 (20%)	[88-91]
engine & transmission			100.00	[52]
door modules			2.00	[55,92]
battery	lead-acid	lithium-ion	10.76 (60%)	[93-96]
Tires			8.75 (10%)	[97,98]
• component removal				
spare tire & carrier			38.79 (100%)	[99,100]
Vehicle weight (kg)	baseline	2307.00	432.76 (19%)	
	light-weighted	1874.24		

Overall, all three acceleration curves are not much different. Figures 5c and 5d show the velocity curves. All vehicles exhibited a similar rebounding speed and slope. The LWV1 and LWV2 have earlier velocity zero time than the baseline as shown in Figure 5c.

Figures 5e and 5f show the wall force curves. The force curve of the baseline vehicle has five peaks within a certain force range. The LWV1 shows similar wall force to the baseline except the lower peak at the late time, which is because of the lower weight of LWV1. On the other hand, the wall force curve of the LWV2 has just two peaks, which is clearly indicative that the composite ladder frame in the LWV2 makes a big change in the crash mode of the LWV2, compared to the baseline with the original steel ladder frame.

Table 3 summarizes the single response values of vehicles in the frontal NCAP test simulations. In terms of the maximum crush, the LWV1 has a lower crush value than the baseline, but the LWV2 exhibited a similar crush value to the baseline. The weight reduction in the LWV1 possibly leads to lower vehicle crush. However, adopting the composite ladder frame in the LWV2 causes more vehicle crush than the LWV1 although the vehicle weight of the LWV2 is lighter than the LWV1. The vehicle stiffnesses, i.e., the crush-work stiffness (K_W400) [102] and the global energy-equivalent stiffness (K_E) [103], were calculated using the wall force curves in Figure 5f. The LWV1 stiffnesses become softer than the baseline vehicle, which may be the effect of weight reduction. The LWV2 stiffnesses become further softer than the LWV1, which should be the effect of using the composite ladder frame. Thus, using the composite ladder frame leads to the vehicle stiffness being softer but to similar vehicle crush as the baseline. In other words, the composite ladder frame in the LWV2 provides the required crash performance to keep the crashworthiness of the LWV2 equivalent to the baseline.

Figure 6 describes the measurement points of occupant compartment intrusion. The intrusions at

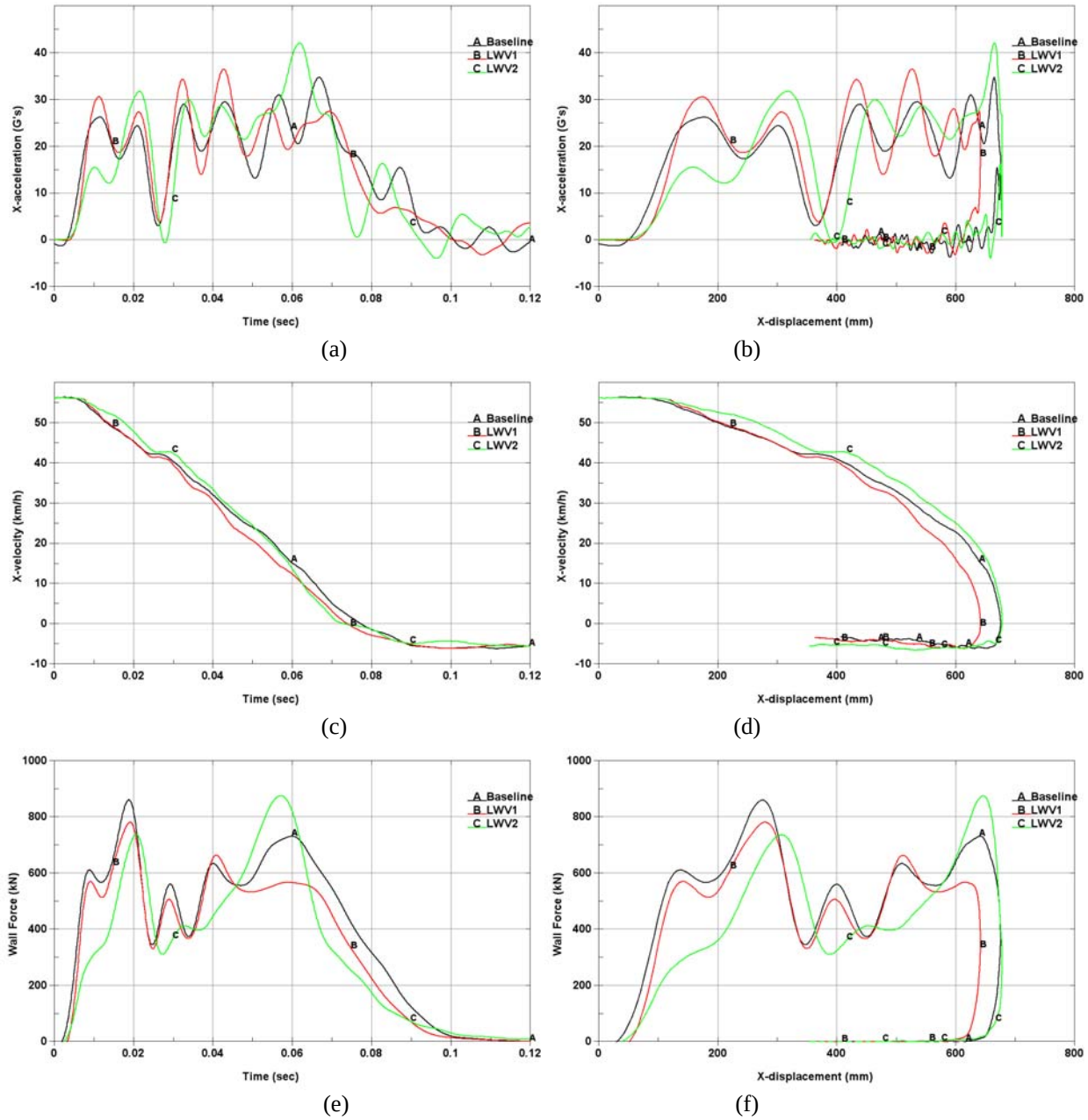

Figure 5. Vehicle response histories in frontal NCAP tests; (a) acceleration in time, (b) acceleration in displacement, (c) velocity in time, (d) velocity in displacement, (e) wall force in time, (f) wall force in displacement.

Table 3. Summary of vehicle responses in frontal NCAP test simulations

Vehicle	baseline	LWV1	LWV2
Maximum X-crush (mm)	675.8	642.1 (-5%)	678.7 (0%)
K_W400 (MPa)	2413.4	2180.8 (-10%)	1768.2 (-27%)
K_E (MPa)	1530.8	1453.2 (-5%)	1255.8 (-18%)

the fifteen cross-points of five Y-lines and three Z-lines were measured at the end of the simulation time. Only the driver-side intrusion was investigated. Z1 was located 100 mm above the vehicle floor. Figure 7 shows the intrusion profiles of the three vehicles.

Both light-weighted vehicles, the LWV1 and the LWV2, show smaller X- and Z-intrusions than the baseline vehicle, which could be attributed to the effect of weight reduction.

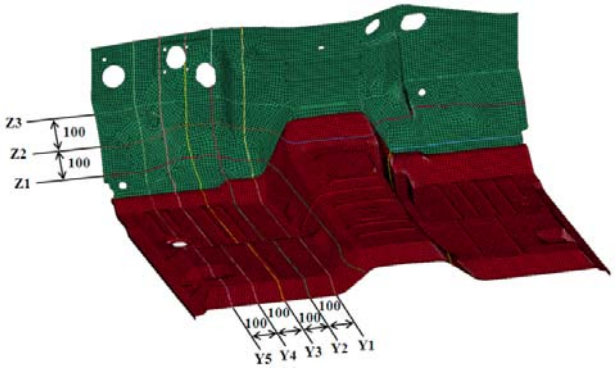

Figure 6. Measurement points of vehicle intrusion (unit: mm).

Figures 8 through 10 show the deformations of three vehicles. The deformation of the baseline vehicle is shown in Figure 8. A folding deformation mode of the steel ladder frame is observed. The deformation of the steel ladder frame reaches a location that is behind the engine as indicated by green arrow in Figure 8a. The deformation of the LWV1 is shown in Figure 9. Since the LWV1 has the original steel ladder frame, the deformation of the LWV1 is similar to that of the baseline. The deformation of the LWV2 is shown in Figure 10. Since the LWV2 has the composite ladder frame, the deformation mode is quite different from the baseline. The brittle fracture mode of the composite ladder frame can be observed. The bending fracture of the composite side rails also occurs at a location around the transmission crossbeam as indicated by the green arrows in Figure 10b.

DISCUSSION

As part of implementing the PCIV safety roadmap of the NHTSA, this study investigates the opportunities

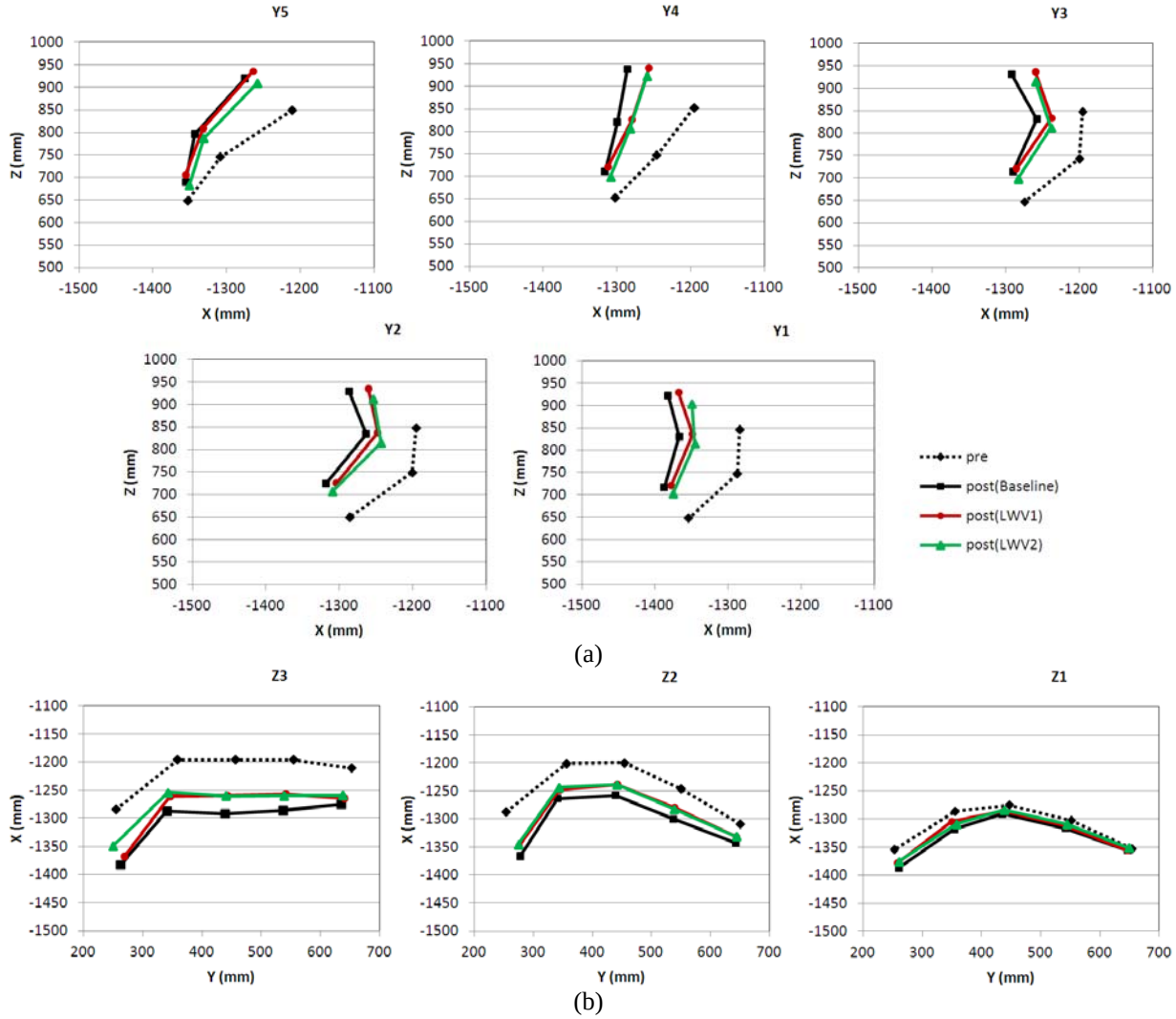

Figure 7. Vehicle intrusions; (a) vertical profile, (b) horizontal profile.

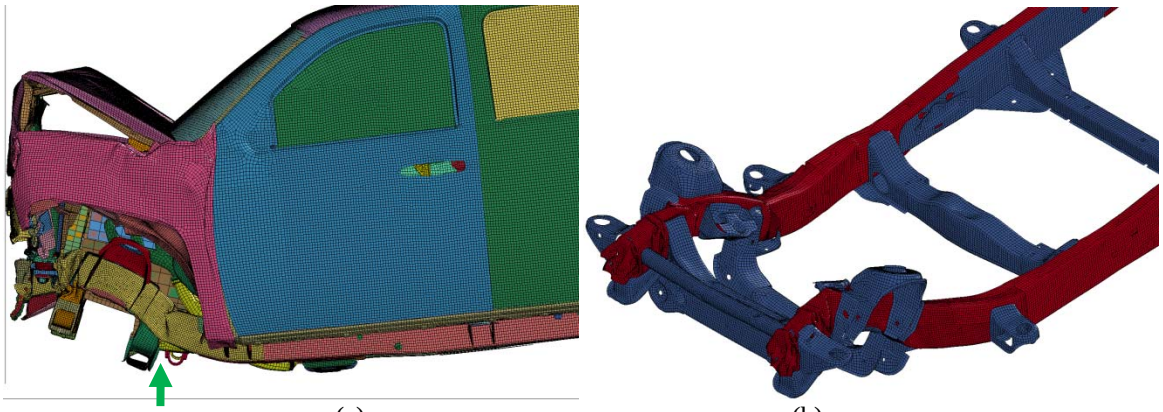

(a) (b)

Figure 8. Deformation of the baseline vehicle; (a) frontal area (wheel hidden), (b) ladder frame.

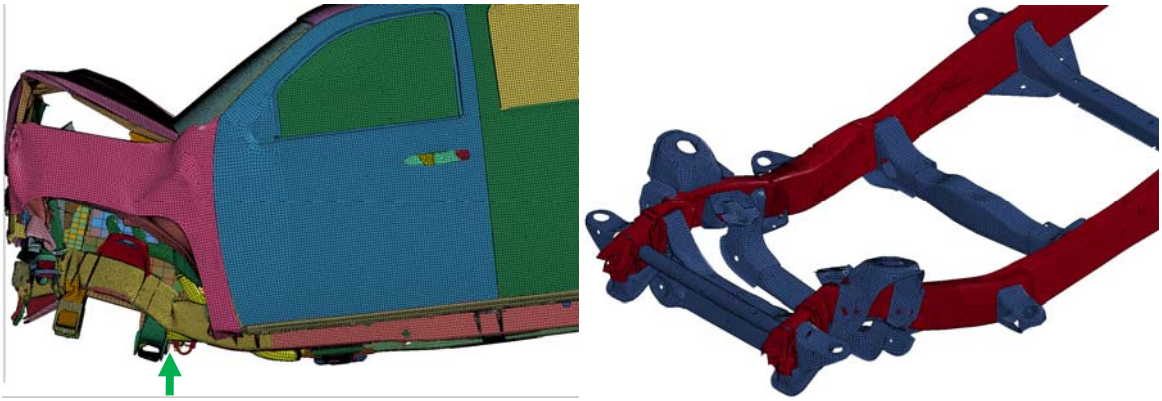

(a) (b)

Figure 9. Deformation of the LWV1 vehicle; (a) frontal area (wheel hidden), (b) ladder frame.

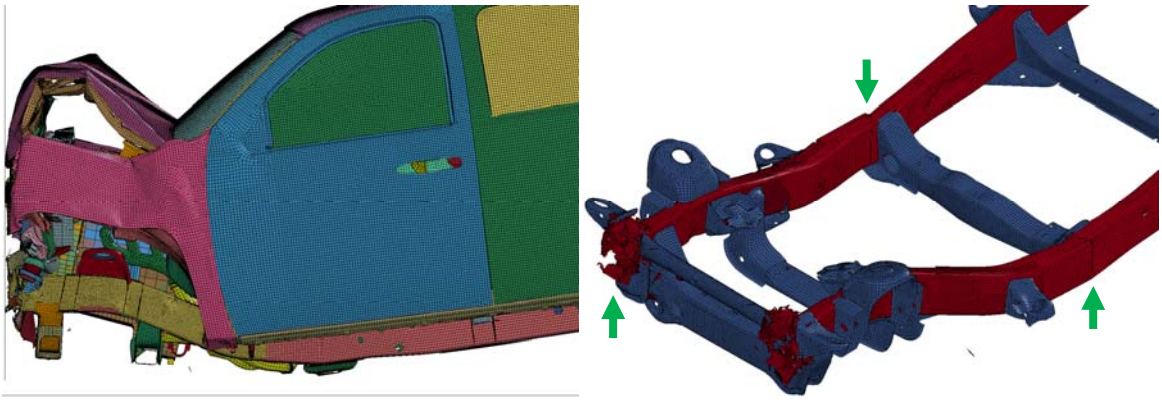

(a) (b)

Figure 10. Deformation of the LWV2 vehicle; (a) frontal area (wheel hidden), (b) ladder frame.

for light-weighting a current body-on-frame type vehicle using advanced plastics and composites. In addition, the safety benefits of structural plastics and composites applications in future lighter vehicles is identified and evaluated by frontal impact simulations.

Over 25 components of the Silverado were light-weighted by using plastics and composites primarily. In consequence, the original vehicle weight, 2,307 kg, was reduced to 1,874 kg, which is about a 19% decrease. The light-weight vehicle contains about 442 kg of plastic and composites, which represents about 23.6% of the total weight of the light-weight vehicle. To reach or exceed a 30% content of plastics and

composites in the development of a PCIV, additional applications of plastics and composites to the vehicle structural components, especially occupant compartment and closures, would be required. Also, adopting optimally sophisticated design can reduce more mass in the light-weighted components. Particularly, the ladder frame can be further reduced if composite material is applied to crossbeams and optimal design is used.

Those light-weighted components include non-structural as well as structural members, such as bumpers, pillar reinforcements, door beams, and ladder frame. Especially, the ladder frame was determined to be the main energy absorbing structure and was changed to a carbon fiber-thermoset braided composite. The crashworthiness of the composite structural members was evaluated by frontal NCAP simulations. Only frontal impact configuration was considered in this study. The simulation results of the light-weighted vehicles show that (1) the vehicle mass reduction contributes to a decrease in the vehicle frontal intrusion, (2) the deceleration of a vehicle was more likely to be dependent on the vehicle stiffness and crash mechanisms, rather than vehicle mass reduction, and (3) overall, the light-weighted vehicles using advanced plastics and composites provide equivalent structural performance (intrusion and crash pulse) to the baseline vehicle in the full frontal impact condition.

In conclusion, this study demonstrates that (1) using plastics and composites can reduce the vehicle weight efficiently, and (2) the light-weighted Silverado using advanced plastics and composites provides equivalent structural performance in the frontal impact condition. Especially, carbon-FRP composites show good structural performance. Also, this study recommends further research, such that (1) undertaking a clean sheet design from the ground up (rather than the less optimal component redesign approach) to provide an maximal approach for light-weighting, (2) the evaluation of the crashworthiness of light-weighted vehicles in other crash configurations (side and rear impacts, roof crush, etc.), (3) the study of cost analysis, and vehicle repair and maintenance issues of plastics and composites components, and (4) the enrichment of material database of plastics and composite.

ACKNOWLEDGEMENTS

This research was sponsored by the National Highway Traffic Safety Administration (NHTSA) under a contract with the Federal Highway Administration (FHWA) of the U.S. Department of Transportation (DOT). Authors gratefully appreciate their financial supports. Prof. Pradeep Mohan in the Channabasaveshwara Institute of Technology in India was appreciated for his early work of this project.

The American Chemistry Council Plastics Division (ACC-PD) industry partners voluntarily participated in this research and provided information and new models of plastics and composite components. Special appreciation is due to James Kolb (ACC-PD), Matthew D. Marks and Dhanendra Nagwanshi (SABIC Innovative Plastics), Scott C. Schlicker and Jeffrey Plott (BASF Corporation), and Don Schomer (Bayer MaterialScience LLC).

REFERENCES

[1] S.C. Davis, S.W. Diegel, and R.G. Boundy, “Transportation energy data book: edition 30”, ORNL-6986, Vehicle Technologies Program, Office of Energy Efficiency and Renewable Energy, U.S. Department of Energy, 2011.
[2] U.S. Environmental Protection Agency, “Inventory of U.S. greenhouse gas emissions and sinks: 1990 – 2010”, EPA-430-R-12-001, 2012.
[3] BBC Research, “Lightweight materials in transportation”, A BCC research advanced materials report, Report ID # AVM056B, 2011.
[4] J.A. Carpenter, “Overview of freedomCAR and its composites crash-energy management work”, The Safety Characterization of Future Plastics and Composite-Intensive Vehicles (PCIVs) Workshop, Cambridge, MA, USA, 2008.
[5] L.W. Cheah, “Cars on a diet: the material and energy impacts of passenger vehicle weight reduction in the U.S.”, Ph.D. Dissertation, Massachusetts Institute of Technology, 2010.
[6] U. Vaidya, “Composites for automotive, truck and mass transit”, DEStech Publications, Inc., Lancaster, PA, USA, 2011.
[7] U.S. Environmental Protection Agency and U.S. Department of Transportation, “Light-duty vehicle greenhouse gas emission standards and corporate average fuel economy standards; final rule”, Federal Register, 2010, 75(88):25324-25728.
[8] U.S. Environmental Protection Agency, “Light-duty automotive technology, carbon dioxide emissions, and fuel economy trends: 1975 through 2011”, EPA-420-R-12-001a, 2012.
[9] A. Burnham, M. Wang, and Y. Wu, “Development and applications of GREET 2.7 - the transportation vehicle-cycle model”, ANL/ESD/06-5, 2006.
[10] G. Keoleian, S. Miller, R.D. Kleine, A. Fang, and J. Mosley, “Life cycle material data update for GREET model”, Report No. CSS12-12, 2012.
[11] A. Bandivadekar, K. Bodek, L. Cheah, C. Evans, T. Groode, J. Heywood, E. Kasseris, M. Kromer, and M. Weiss, “On the road in 2035: reducing transportation’s petroleum consumption and GHG emissions”, Report No.

LFEE 2008-05 RP, Massachusetts Institute of Technology, 2008.
[12] Center for Automotive Research, "Automotive technology: greener products, changing skills – lightweight materials & forming report", 2011.
[13] N.P. Lutsey, "Review of technical literature and trends related to automobile mass-reduction technology", Institute of Transportation Studies, University of California, Davis, Research Report UCD-ITS-RR-10-10, 2010.
[14] H. Singh, "Light-weighting options for vehicle structures for model year 2020", SAE 2012 Government/Industry Meeting, Washington, DC, USA, 2012.
[15] L. Schewel, "Triple safety: lightweighting automobiles to improve occupant, highway, and global safety", SAE Technical Paper # 2008-01-1282, 2008.
[16] K. Chan-Lizardo, A.B. Lovins, L. Schewel, and M. Simpson, "Ultralight vehicles – non-linear correlations between weight and safety", International Crashworthiness Conference, Leesburg, VA, USA, 2011.
[17] National Highway Traffic Safety Administration, "NHTSA workshop on vehicle mass-size-safety", Washington, DC, USA, 2011, http://www.nhtsa.gov/Laws+&+Regulations/CAFE+-+Fuel+Economy/NHTSA+Workshop+on+Vehicle+Mass-Size-Safety, accessed August 2012.
[18] F.J. Tahan, C.K. Park, R.M. Morgan, C. Cui, C.D. Kan, B. Brar, and K. Shanks, "The effect of reduced mass on crashworthiness", International Crashworthiness Conference, # 2012-089, Milan, Italy, 2012.
[19] U.S. Congress, "Committee reports,109th Congress (2005-2006), Senate report 109-293 – transportation, treasury, housing and urban development, the judiciary, and related agencies appropriations bill, 2007", The Library of Congress.
[20] Research and Innovative Technology Administration - U.S. Department of Transportation, "A summary of proceedings for the safety characterization of future plastic and composite intensive vehicles (PCIVs)", 2008, http://ntl.bts.gov/lib/32000/32200/32205/summary_pciv_workshop.pdf.
[21] American Chemistry Council Plastics Division, "Plastic and composite intensive vehicles: an innovation platform for achieving national priorities", 2009, http://www.plastics-car.com/pcivs, accessed August 2012.
[22] A. Brecher, "A safety roadmap for future plastics and composites intensive vehicles (PCIV)", Report No. DOT HS 810 863, Volpe National Transportation Systems Center, 2007.
[23] A. Brecher, J. Brewer, S. Summers, and S. Patel, "Characterizing and enhancing the safety of future plastic and composite intensive vehicles (PCIVs)", The 21st International Technical Conference on the Enhanced Safety of Vehicles (ESV), Stuttgart, Germany, 2009.
[24] G. Barnes, I. Coles, R. Roberts, S.O. Adams, and D.M. Garner, "Crash safety assurance strategies for future plastic and composite intensive vehicles (PCIVs)", Report No. DOT-VNTSC-NHTSA-10-01, Volpe National Transportation Systems Center, 2010.
[25] M. Fisher and B. Cundiff, "APC vision and technology roadmap for the automotive market-defining priority research for plastics in 21st century vehicles", SAE Technical Paper # 2002-01-1890, 2002.
[26] M. Fisher, J. Kolb, and S. Cole, "Enhancing Future Automotive Safety with Plastics", The 20th International Technical Conference on the Enhanced Safety of Vehicles (ESV), Paper # 07-0451, Lyon, France, 2007.
[27] American Chemistry Council Plastics Division (ACC PD), "Plastic in automotive markets technology roadmap – a new vision for the road ahead", 2009, http://www.plastics-car.com/roadmap_fullversion, accessed August 2012.
[28] Automotive Composite Alliance, "History of automotive composites", http://www.autocomposites.org/composites101/history.cfm, accessed August 2012.
[29] B. Tang, "Fiber reinforced polymer composites applications in USA", The First Korea/U.S.A. Road Workshop, 1997, http://www.fhwa.dot.gov/bridge/frp/frp197.cfm, accessed August 2012.
[30] K. Sehanobish, Engineering Plastics and Plastic Composites in Automotive Applications, Warrendale, PA, USA, SAE International, 2009.
[31] S. Das, "The cost of automotive polymer composites: a review and assessment of DOE's lightweight materials composites research", ORNL/TM-2000/283, 2001.
[32] D.R. Cramer and D.F. Taggart, "Design and manufacturing of an affordable advanced-composite automotive body structure", The Proceedings of The 19th International Battery, Hybrid and Fuel Cell Electric Vehicle Symposium & Exhibition, Busan, South Korea, 2002.
[33] N. Tucker and K. Linsey, "An introduction to automotive composites", Rapra Technology Limited, Shawbury, UK, 2002.
[34] H.A. Jahnle, "Feasibility study of plastic automotive structure", Report No. DOT-HS-801-771, U.S. Department of Transportation, 1975.
[35] P. Beardmore and C.F. Johnson, "The potential for composites in structural automotive applications", Composites Science and Technology, 1986, 26:251-281.
[36] P.H. Thornton and R.A. Jeryan, "Crash energy management in composite automotive structures", International Journal of Impact Engineering, 1988, 7(2):167-180.
[37] G.C. Jacob, J.F. Fellers, S.Simunovic, and J.M. Starbuck, "Energy absorption in polymer composites for automotive crashworthiness", Journal of composite materials, 2002, 36:813-850.
[38] E. Mangino, J. Carruthers, and G. Pitarresi, "The future use of structural composite materials in the automotive industry", International Journal of vehicle design, 2007, 44(3/4):211-232.
[39] R.E. Bonnett, H. Kulkarni, G. Lim, P. Beardmore, and R. Knight, "Design and fabrication of automotive components in graphite fiber-reinforced composites", SAE Technical Paper # 790031, 1979.
[40] P. beardmore, J.J Harwood, and E.J. Horton, "Design and fabrication of a GrFRP concept automobile", The 3rd International Conference on Composite Materials, 1980.
[41] R.G. Boeman and N.L. Johnson, "Development of a cost competitive, composite intensive, body-in-white", SAE Technical Paper # 2002-01-1905, 2002.

[42] H. Fuchs, “Design and structural performance assessment of a composite intensive passenger vehicle”, The 6th Annual SPE Automotive Composites Conference, Troy, MI, USA, 2006.
[43] A. Deb, P. Lakshmanan, D.K. Kharat, and S.C. Lakkad, “Composite versus steel rails for vehicle front impact safety”, The IMPLAST 2010 Conference, Providence, RI, USA, 2010.
[44] P. Sklad, “Lightweight SUV frame design development”, Altair Engineering, 2003, http://altairenlighten.com/wp-content/uploads/2011/12/Lightweight-SUV-Frame-Design-Development.pdf.
[45] S.M. Summers, A. Prasad, and W.T. Hollowell, “NHTSA’s research program for vehicle aggressivity and fleet compatibility”, The 17th International Technical Conference on the Enhanced Safety of Vehicles (ESV), Paper # 249, Amsterdam, The Netherlands, 2001.
[46] S.M. Summers, W.T. Hollowell, and A. Prasad, “NHTSA’s research program for vehicle compatibility”, The 18th International Technical Conference on the Enhanced Safety of Vehicles (ESV), Paper # 307, Nagoya, Japan, 2003.
[47] J. Blum, P. Scullion, R.M. Morgan, K. Digges, and C.D. Kan, “Structural attributes of the striking vehicle that control aggressivity toward the struck-vehicle in frontal collisions”, IRCOBI Conference, York, UK, 2009.
[48] National Crash Analysis Center/The George Washington University, “Finite element model archive: vehicle models”, http://www.ncac.gwu.edu/vml/models.html, accessed August 2012.
[49] D. Marzougui, R.R. Samaha, C. Cui, and C-D Kan, “Extended validation of the finite element model for the 2007 Chevrolet Silverado pick-up truck”, NCAC 2012-W-003, National Crash Analysis Center, The George Washington University , 2012, http://www.ncac.gwu.edu/research/pubs/NCAC-2012-W-003.pdf.
[50] P. Mohan, D. Marzougui, E. Arispe, C. Story, “Component and full-scale tests of the 2007 Chevrolet Silverado Suspension System”, NCAC 2009-W-004, National Crash Analysis Center, The George Washington University, 2009, http://www.ncac.gwu.edu/research/pubs/NCAC-2009-R-004.pdf.
[51] P. Mohan, M. Ritter, D. Marzougui, D. Brown, C.D. Kan, K. Opiela, “Modeling, testing, and validation of the 2007 Chevy Silverado finite element model”, NCAC 2009-W-005, National Crash Analysis Center, The George Washington University, 2009, http://www.ncac.gwu.edu/research/pubs/NCAC-2009-W-005.pdf.
[52] C.K. Park, C.D. Kan, W.T. Hollowell, and S.I. Hill, “Investigation of Opportunities for Light-Weighting Vehicles Using Advanced Plastics and Composites”, Report No. DOT HS 811 692, National Highway Traffic Safety Administration, December 2012.
[53] SABIC, “Xenoy resin”, http://www.sabic-ip.com/gep/Plastics/en/ProductsAndServices/ProductLine/xenoy.html, accessed August 2012.
[54] SABIC, “Lexan resin”, http://www.sabic-ip.com/gep/Plastics/en/ProductsAndServices/ProductLine/lexan.html, accessed August 2012.
[55] SABIC, “SABIC innovative plastics” SABIC STAMAX long glass fiber PP helps Hyundai Sonata’s plastic door module win 2010 SPE innovation award”, 2010, http://www.sabic-ip.com/gep/en/NewsRoom/PressReleaseDetail/november_10_2010_sabicinnovativeplasticssabic.html, accessed August 2012.
[56] BASF, “Ultramid® B3ZG7 OSI (Optimized for Stone Impact) PA6 (Polyamide 6)”, http://www2.basf.us/PLASTICSWEB/displayanyfile?id=0901a5e1801631d8, accessed August 2012.
[57] C.K. Park, C.D. Kan, S. Reagan, and B. Deshpande, “Crashworthiness of composite insert in vehicle structure”, International Journal of Crashworthiness, 2012, 17(6): 665-675.
[58] C.K. Park, C.D. Kan, S. Reagan, B. Deshpande, and P. Mohan, “Crashworthiness and numerical analysis of composite inserts in vehicle structure”, SAE International Journal of Passenger Cars- Mechanical Systems, 2012, 5(2): 727-736; SAE Technical Paper # 2012-01-0049.
[59] D. Hull, “A unified approach to progressive crushing of fiber-reinforced composite tubes”, Composites Science and Technology, 1991, 40:377-421.
[60] G.L. Farley and R.M. Jones, “Crushing characteristics of continuous fiber-reinforced composite tubes”, Journal of Composite Materials, 1992, 26:37-50.
[61] A.G. Mamalis, D.E. Manolakos, G.A. Demosthenous, and M.B. Ioannidis, Crashworthiness of Composite Thin-Walled Structural Components, Boca Raton, FL, USA, CRC Press, 1998.
[62] C.H. Chiu, C.K. Lu, and C.M. Wu, “Crushing characteristics of 3-D braided composite square tubes”, Journal of Composite Materials, 1997, 31:2309-2327.
[63] H. Hamada, “Crushing behavior of braided composites”, ASME International Mechanical Engineering Congress and Exposition, AMD-Vol. 250/MD-Vol. 96, pp. 33-40, New York, NY, USA, 2001.
[64] S.J. Beard and F.K. Chang, “Energy absorption of braided composite tubes”, International Journal of Crashworthiness, 2002, 7(2):191-206.
[65] M. Okano, A. Nakai, and H. Hamada, “Axial crushing performance of braided composite tubes”, International Journal of Crashworthiness, 2005, 10(3):287-294.
[66] C.K. Park, C.D. Kan, and W.T. Hollowell, “Evaluation of crashworthiness of composite ladder frame in a body-on-frame vehicle”, International Crashworthiness Conference, #2012-118, Milan, Italy, 2012.
[67] SABIC, “Noryl GTX resin”, http://www.sabic-ip.com/gep/Plastics/en/ProductsAndServices/ProductLine/norylgtx.html, accessed August 2012.
[68] SABIC, “SABIC innovative plastics helps GM create first thermoplastic fenders in a North American truck platform with 2006 HUMMER”, http://kbam.geampod.com/KBAM/Reflection/Assets/9816_5.pdf, accessed August 2012.
[69] Smock D, “Plastic oil pans present major integration opportunity”, Design News, 2009, http://www.designnews.com/document.asp?doc_id=228511, accessed August 2012.

[70] Bayer MaterialScience, "Bayblend® T88 GF-10 and T88 GF-2", http://plastics.bayer.com/plastics/emea/en/library/newpublications/docId-2903947/PCS-3018_en_Bayblend_T88_GF-10_and_T88_GF-20.pdf, accessed August 2012.
[71] Slik G, "Evolution of structural instrumental panels", SAE Paper No. 2002-01-1270, 2002.
[72] Jahn T, Baudouin I, Vatel P, Karnik S, Perez O, Cue JM, Benichou HP, Dittmar H, Sengbusch J, and Kurcz M, "Development of Lightweight, Hybrid Steel / GMT Composite IP Carrier to Meet World Crash Requirements on Passenger Vehicles", The 5th Annual SPE Automotive Composites Conference, Troy MI, USA, 2005.
[73] Marks M, "Long glass fiber-polypropylene light weight instrument panel retainers & door modules", SPE Automotive Composites Conference & Exhibition, Troy MI, USA, 2008.
[74] Melzig J and Lehner M, "Lightweight construction due to thermoplastic foams as exemplified in an instrument-panel support", SAE Paper No. 2006-01-1404, 2006.
[75] Seagrave TD, "Structural RIM choices for today's automotive design", The 3rd Annual SPE Automotive Composites Conference, Troy MI, USA, 2003.
[76] U.S. Department of Energy, "Composite materials production methods developed", Vehicle Technologies Program, 2001, http://www1.eere.energy.gov/vehiclesandfuels/pdfs/success/composite_mtls_mar_2001_2.pdf.
[77] American Chemistry Council, "Composite drive shafts can increase torque and can help prevent injuries", http://www.plastics-car.com/driveshafts, accessed August 2012.
[78] BAC Technology LTD., "Carbon fiber driveshafts", http://www.bactechnologies.com/shafts.htm, accessed August 2012.
[79] Ogando J, "Carbon-fiber drives shaft systems", Design News, 2003, http://www.designnews.com/document.asp?doc_id=222235, accessed August 2012.
[80] Strongwell, "Composite driveshafts", http://www.strongwell.com/selected_markets/comp_driveshaft/, accessed August 2012.
[81] SGL Group, "Carbon-ceramic brake disks", http://www.sglgroup.com/cms/international/products/product-groups/bd/carbon-ceramic-brake-disks/index.html?__locale=en, accessed August 2012.
[82] Hexcel, "New cost optimized axle module for composite leaf springs - from Magna Steyr, composite trends", 2006, http://www.hexcel.com/news/newsletters/letter-20060401.pdf, accessed August 2012.
[83] HYPERCO, "Composite leaf springs", http://www.hypercoils.com/products/hyperco-composite-leaf-springs.aspx, accessed August 2012.
[84] Siddaramanna G, Shankar S, and Vijayarangan S, "Mono composite leaf spring for light weight vehicle – design , end joint analysis and testing", Materials Science, 2006, 12(3):220-225.
[85] Kulekci MK, "Magnesium and its alloys applications in automotive industry", The International Journal of Advanced Manufacturing Technology, 2008, 39(9-10):851-865, DOI: 10.1007/s00170-007-1279-2.
[86] Magnesium Elektron, "Magnesium in automotive", http://www.magnesium-elektron.com/markets-applications.asp?ID=7, accessed August 2012.
[87] Langsdorf J, "Weight savings: steel vs. aluminum wheels", http://www.ehow.com/about_5664238_weight-steel-vs_-aluminum-wheels.html, accessed August 2012.
[88] Hojnacki HE and Taka G, "Lightweight automotive seating system", SAE Paper No. 2011-01-0424, 2011.
[89] Naughton P, Shembekar P, Lokhande A, Kauffman K, Rathod S, and Malunjkar G, "Eco-friendly automotive plastic seat design", SAE Paper No. 2009-26-0087, 2009.
[90] LOTUS engineering, "Vehicle mass reduction opportunities", 2010, http://www.epa.gov/air/caaac/mstrs/oct2010/5_peterson.pdf
[91] Plott J, Personal communication, BASF, June 2011.
[92] Marks MD, Personal communication, SABIC, July 2011.
[93] Energy Efficiency & Technology, 2011, "Lithium technology comes to car batteries", http://eetweb.com/power-supplies/lithium_batteries_3411/
[94] Lithiummoto, "Lithium high performance replacement batteries", 2011, http://www.lithiummoto.com/index.html, accessed August 2012.
[95] Motor Sports Newswire, "Racing batteries USA sparks agreements with the California superbike school & zipty racing", 2011, http://motorsportsnewswire.wordpress.com/tag/lightweight-batteries/, accessed August 2012.
[96] Porsche, "New lightweight battery option for the Porsche 911 GT3, 911 GT3 RS and Boxster Spyder", 2009, http://press.porsche.com/news/release.php?id=510, accessed August 2012.
[97] DuPont, "20% less weight: Revolutionary ultra-lightweight concept tire from Dunlop with DuPont", 2009, http://www2.dupont.com/EMEA_Media/en_GB/newsreleases_2009/article20090303a.html, accessed August 2012.
[98] ExxonMobil, "Exxcore DVA resin", http://www.exxonmobilchemical.com/Chem-English/brands/butyl-rubber-exxcore-dva-resin.aspx?ln=productsservices, accessed August 2012.
[99] AAA, "Vehicles without a spare tire", http://www.aaa.com/AAA/corpcomm/socialmedia/No_Spare-Tires.pdf, accessed August 2012.
[100] Williams D, "GM offering tire inflator kits instead of spare tires on some models", 2011, http://www.everycarlisted.com/blog/2011/05/gm-offering-tire-inflator-kits-instead-of-spare-tires-on-some-models/, accessed August 2012.
[101] Livermore Software Technology Corporation, LS-DYNA Keyword User's Manual, Version 971, 2009.
[102] P. Mohan and D.L. Smith, "Finite element analysis of compatibility metrics in frontal collisions", The 20th International Technical Conference on the Enhanced Safety of Vehicles (ESV), Lyon, France, 2007.
[103] G.S. Nusholtz, L. Xu, Y. Shi, and L.D. Domenico, "Vehicle mass, stiffness and their relationship", The 19th International Technical Conference on the Enhanced Safety of Vehicles (ESV), Washington, DC, USA, 2005.